SYNTHESIS AND CHARACTERIZATION OF NOVEL THIOPHENE-BASED

ELECTROACTIVE POLYMERS

by

Marisa Snapp-Leo, B.S.

A thesis submitted to the Graduate Council of
Texas State University in partial fulfillment
of the requirements for the degree of
Master of Science
with a Major in Chemistry
May 2019

Committee Members:

    Jennifer A. Irvin, Chair

    Tania Betancourt

    Chang Ji

FAIR USE AND AUTHOR'S PERMISSION STATEMENT

Fair Use

Duplication Permission

DEDICATION

To my spouse. Thank you for your love and never-ending patience.

ACKNOWLEDGEMENTS

First and foremost I would like to thank Dr. Jennifer Irvin for her constant support and guidance. She helped me grow as a chemist and constantly challenged me to get out of my comfort zone. I truly could not have asked for a better mentor than her.

I would also like to thank my committee members Dr. Tania Betancourt and Dr. Chang Ji. Dr. Betancourt never hesitated to provide me any insights she could offer, and was very generous by allowing me to use several of her instruments whenever I needed them. Dr. Ji was always more than willing to hear me out when needed and readily accepted to take the time to be in my committee.

I definitely would not have made it far without my wonderful lab mates. The friendship and support you all provided was invaluable. Mariana Ocampo and Kelli Burke in particular, who would both listen to me when I was stressed out and encouraged me to keep going. I will always cherish our lunch outings. I'd also like to thank David Hebert, whom I could always count on to help me figure out my chemistry problems and helped me become a better synthetic chemist.

And lastly, I'd like to thank my family. My mom never doubted my abilities even when I doubted them myself. I'm grateful to my sister, who always had a handy meme or GIF to make me laugh and clear my head. My in-laws, who even though they have only known me for a short period of time never failed to encourage me and believe in me. And of course my spouse, Kelsey. Words cannot begin to express how grateful I am for you. Your unwavering belief in me is what kept me going. Thank you.

TABLE OF CONTENTS

LIST OF TABLES

LIST OF EQUATIONS

Equation	Page

LIST OF FIGURES

ABSTRACT

Electroactive polymers show great promise in a variety of applications, from chemical sensors to energy storage. Their properties such as solubility and band gap can be tailored through the strategic addition of substituents to the monomer. Extended conjugation monomers, which feature a central ring between electroactive moieties, were synthesized via different palladium catalyzed coupling reactions such as Negishi and Stille couplings. These monomers along with thiophene-based non-extended conjugation monomers were then polymerized chemically and electrochemically. Due to the color change these polymers exhibit during different redox states, spectroelectrochemistry was conducted to determine their band gap. Analysis of these compounds elucidated the impact different substituents had on the resulting polymers.

1. INTRODUCTION TO ELECTROACTIVE POLYMERS

1.1 History

The earliest known synthetic polymer was discovered in 1826 by Otto Unverdorben.[1] Known then as aniline black, polyaniline (PANI) was first oxidatively polymerized by Runge in 1834[1] and used to create dyes of different colors. However, it was not until the doping of polyacetylene (PA) in 1974 by Shirakawa, McDiarmid, and Heeger that the first inherently conducting polymer was truly created.[2] Their work was widely lauded, earning them a Nobel Prize in 2000 for "the discovery and development of electrically conductive polymers".[3] Doping polyacetylene provided a means for increasing its conductivity by a factor of millions, as shown in Figure 1.[4]
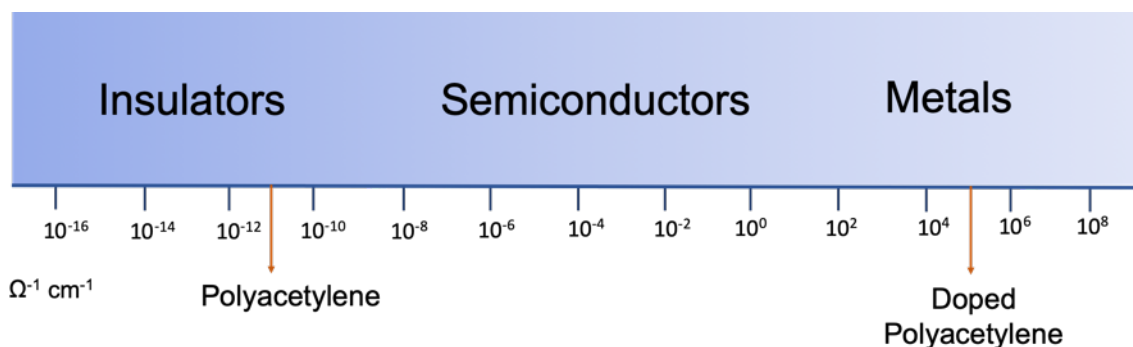
Figure 1. Comparison of polyacetylene vs. doped polyacetylene conductivity

1.2 Electroactive Polymers

Conducting, or electroactive, polymers (EAPs) are defined as highly conjugated systems that can conduct electricity due to the delocalization of π electrons along the polymer chain.[5] Following Shirakawa, McDiarmid, and Heeger's initial work, many other conducting polymers have been synthesized and studied including polythiophene (PT), polypyrrole (PPy), polyaniline (PANI), and poly(3,4-ethylenedioxythiophene) (PEDOT) (Table 1).[6] Of special importance are the polyheterocycles whose heteroatoms (typically O, N, or S) help decrease the oxidation potential, which facilitates polymerization.[7]

Table 1. Common conducting polymers

Polymer	Abbreviation	Common applications
Polyacetylene	PA	None due to stability issues
Polythiophene	PT	Electrochromics, antistatic coatings
Polypyrrole	PPy	Energy storage, sensors, capacitors, antistatic coatings
Polyaniline	PANI	Corrosion protection, electrostatic discharge coatings
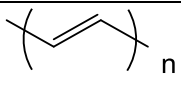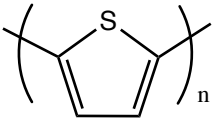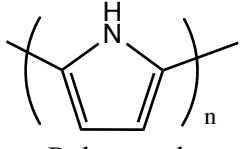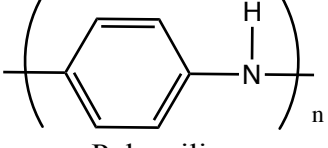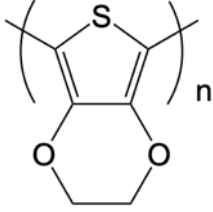
Poly(3,4-ehtylenedioxythiophene)	PEDOT	Corrosion protection, biosensors, capacitors, antistatic coatings, battery electrodes

1.3 Band Gap

What determines whether a material will be a conductor or an insulator is its electronic structure, that is how the electrons are arranged, and the band gap, which is the difference between the highest occupied molecular orbital (HOMO) and the lowest unoccupied molecular orbital (LUMO).[8] A material becomes conductive when the electrons have enough energy to transition from the valence to the conduction band; the energy can be provided by absorption of either light or heat. A small energy gap such as the one found in semiconductors means less energy is required for the electrons to be promoted to the conduction band, which is what allows them to be conductive. In metals the valence and conduction bands overlap, allowing the valence electrons to move freely into the conduction band.[9]

By increasing the amount of conjugation, an insulator can become a semiconductor as shown in Figure 2. As conjugation increases it becomes increasingly easy to promote electrons from the HOMO to the LUMO bands, which is a simple π to π^* transition.
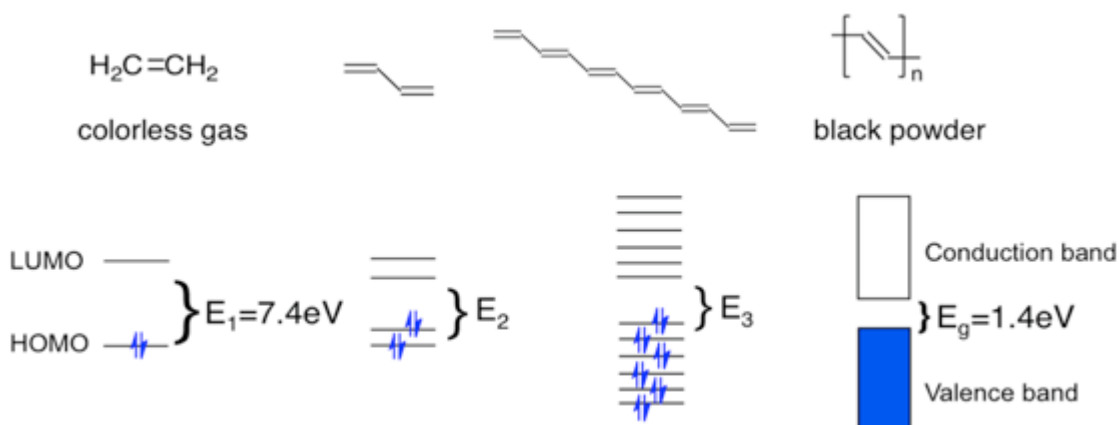
Figure 2. Band gap decreases with increased conjugation [10]

This transition can be easily observed as an absorption in an ultraviolet – visible (UV-vis) spectrum. When a neutral polymer is converted to its oxidized state by removal of electrons, the absorption occurs at higher wavelengths as measured using a UV-vis spectrophotometer; higher wavelengths equate to lower energies according to:

$$Energy\ (eV) = \frac{1240}{\lambda(nm)}$$ Equation 1 [11]

This occurs due to the creation of new intermediate energy levels between the HOMO and the LUMO bands, making the promotion of electrons easier and lowering the band gap. The doping process occurs by either removal (oxidation) or addition (reduction) of electrons along the polymer chain (Figure 3). When a monomer is oxidized it forms a polymer with an overall positive charge, which is said to be in the p-doped state. The p-doped polymer can then be reduced to form the neutral polymer. A second reduction of the system will result in an n-doped polymer with an overall negative

4

charge. In many cases, these oxidation and reduction processes are reversible; reports exist of up to one million reversible oxidation/reduction processes between the neutral and p-doped states.[12]
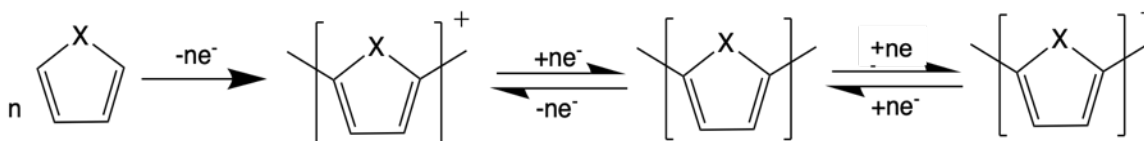
Figure 3. Oxidative polymerization of a heterocycle and doping processes of a polyheterocycle; X is typically NH, O, or S.

Doping changes the oxidation state of the polymer and is accompanied by changes in properties such as color, volume, reactivity, solubility, conductivity, and permeability.[13]

1.4 Conduction

The most widely accepted mechanism explaining the conductive nature of electroactive polymers is depicted in Figure 4. Oxidation of the neutral polymer leaves a resonance-stabilized radical-cation called a polaron.[14,15] Further oxidation of the system results in a dicationic species known as a bipolaron.[16] Unfavorable interactions between the cations are stabilized across three to five heterocycle rings, depending on the specific structure of the polymer. The redox processes between the polaron, bipolaron, and neutral states are reversible and can be achieved by both chemical and electrochemical methods.

5
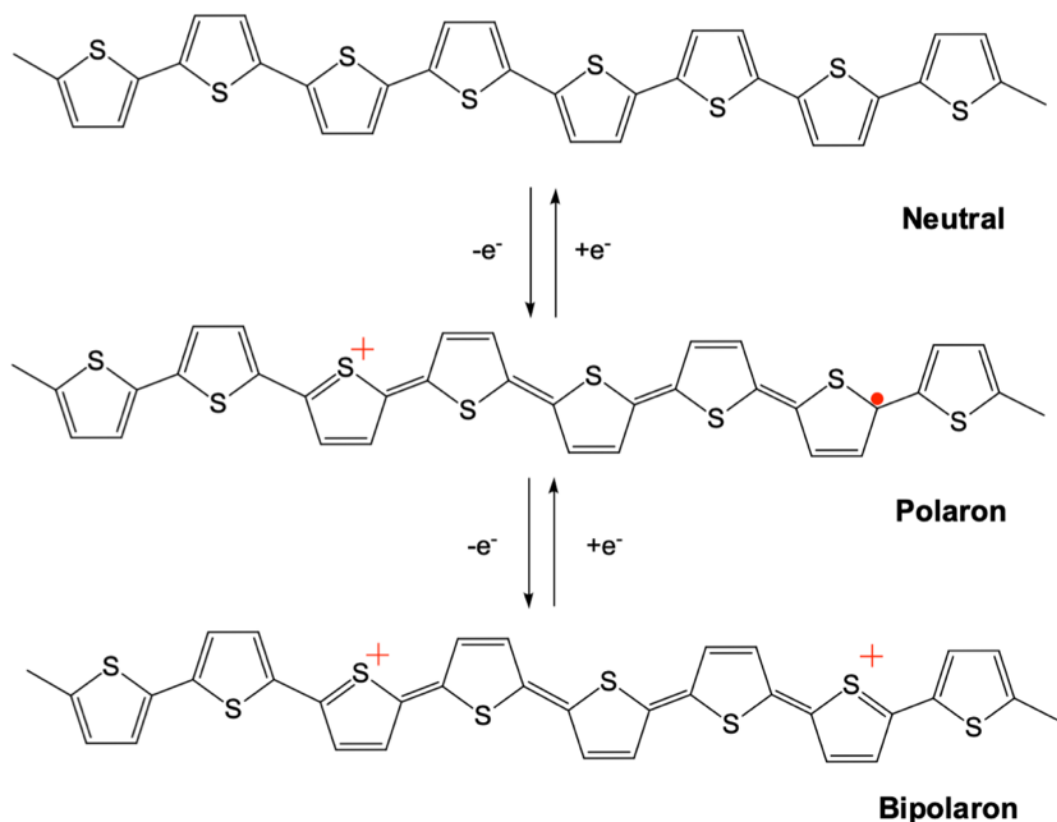
Figure 4. Proposed mechanism of conduction in electroactive polymers [10]

1.5 Substituents and Extended Conjugation Monomers

One way to fine tune the properties of a polymer involves functionalization of the monomer. In polyheterocycles this is typically accomplished by linking the substituent group to the 3-position (particularly for thiophene, furan, and pyrrole) via an alkyl spacer or to the nitrogen in the case of pyrrole.[11] Functional groups commonly used include alkyl and alkoxy chains, which have been known to increase the solubility of a polymer and reduce oxidation potentials. Electron-withdrawing groups such as halides, trihalomethyls, nitro, carbonyl, and nitriles are used to increase n-doping stability by

stabilizing the anions present in fully reduced polymers.[17] On the other hand, electron donating groups such as alkyls, ethers, thioethers, aminos, and alkylaminos stabilize the cations present in the oxidized polymer.[18]

However, despite the relative ease of monomer synthesis, side reactions may occur between the polymer and the substituent as well as regioirregularity of the polymer. [11] As a result, there has been an increasing move towards inserting a functional group such as benzene or pyrimidine between two monomer units, forming an extended conjugation monomer (Figure 5).[11] Putting the substituents on a central ring keeps the benefits of the functional groups while at the same time eliminating steric issues and increasing solubility and processability of the resultant polymer. Perhaps more importantly, extended conjugation provides increased resonance stabilization of both neutral and charged species, reducing oxidation potentials and band gaps.
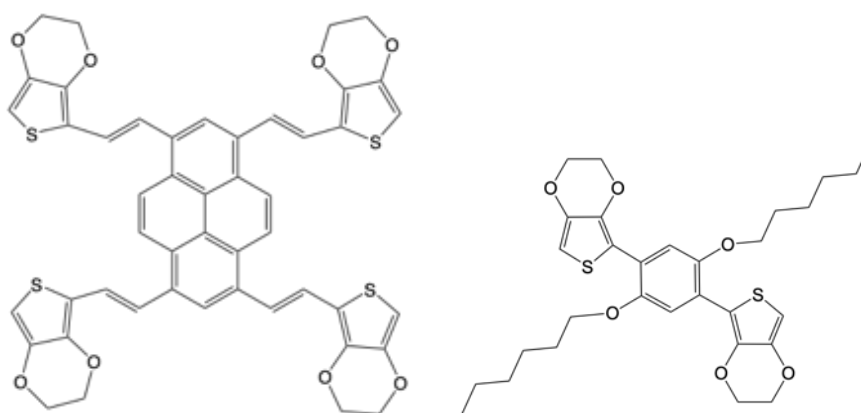
Figure 5. Examples of extended conjugation monomers

1.6 Oxidative Polymerization

Polyheterocycles such as polythiophenes are often synthesized via oxidative polymerization.[19] As shown in Figure 6, removal of one electron (oxidation) creates a radical-cation which is stabilized via resonance. This radical-cation can couple with another molecule of monomer (radical-monomer coupling) to form a radical-cation dimer. Coupling with monomer molecules occurs for n-1 times after which aromaticity is restored and a single electron is introduced, forming the polymer.
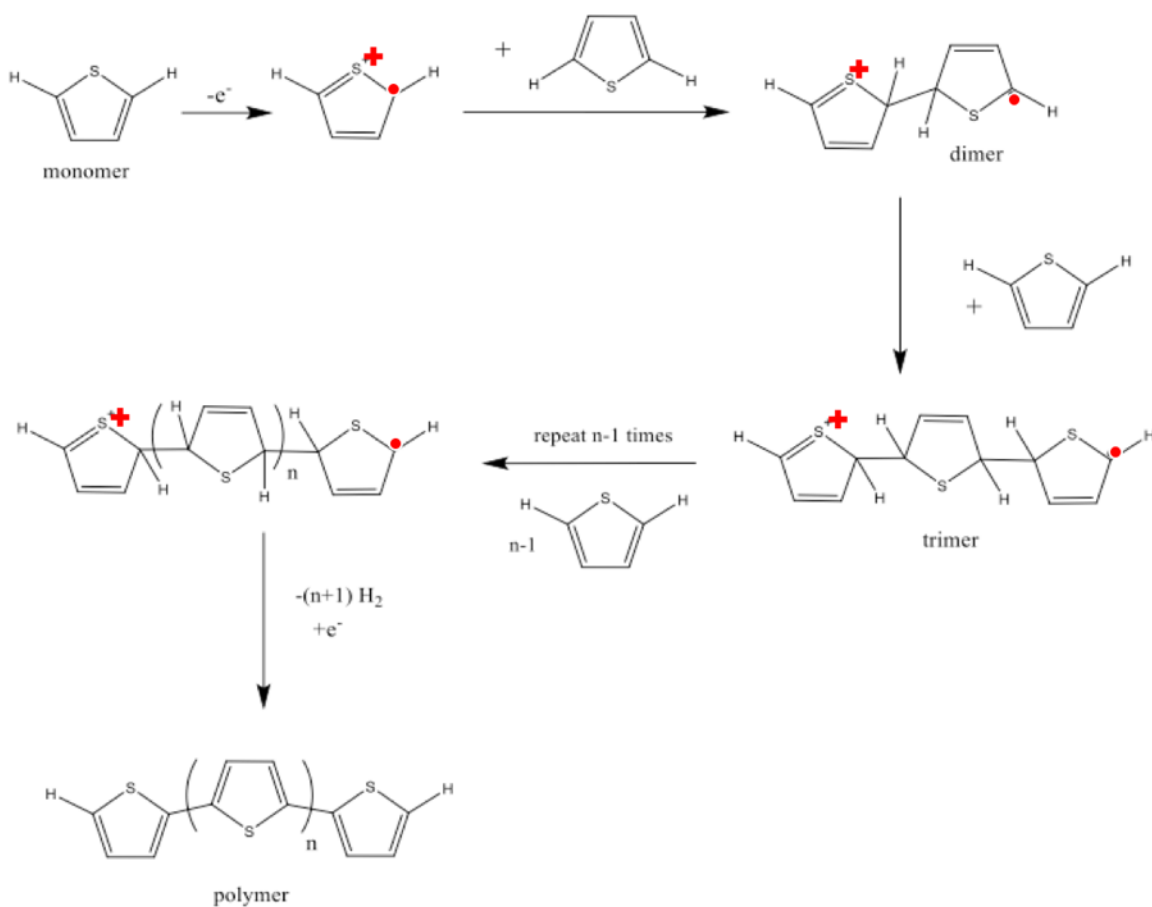
Figure 6. Oxidative polymerization of thiophene

Oxidative polymerization can be achieved by using a chemical oxidant such as ferric chloride or by electrochemical means using a potentiostat. Chemical oxidative polymerizations are fast and simple, and they use relatively mild conditions.[20] However, the resulting polymer is formed in the oxidized state, which is typically less soluble than when in the reduced state, limiting the degree of polymerization by precipitation of the polymer.[21] Another problem associated with chemical oxidative polymerization is the possibility of side reactions, including over-oxidation of the polymer, which results in loss of normal redox behavior and chemical changes to the polymer itself.[22]

1.7 Electrochemistry and Cyclic Voltammetry

As stated above, chemical oxidative polymerizations can present a variety of problems. Electrochemical polymerization not only avoids those issues but also allows for control of the potential and provides additional information that cannot be obtained via traditional chemical means. It is a commonly used method due to its simplicity, cost-effectiveness and the performance of the process in a single section glass cell.[4] In the case of electrochemical polymerization, the monomer is oxidized by the application of an electrical current, and a thin layer of the resulted polymer is deposited on the surface of a conductive electrode.[19]

Polymer growth can be monitored and followed by cyclic voltammetry (CV) by first applying a positive potential and then reversing it in a linear negative sweep and measuring the resulting current response.[23-24] As the potential is increased, monomer molecules at the electrode surface are oxidized, generating a current response and causing

9

an oxidized polymer film to deposit on the electrode. Upon reversal of the potential sweep the oxidized species are reduced. In the data collected, shown in Figure 7, the polymer growth of poly(3,4-ethylenedioxythiophene) can be seen as an increasing reversible peak upon each subsequent scan. The onset of monomer oxidation, $E_{on,m}$, is found in the first sweep and indicates the minimum voltage necessary to oxidize the monomer. The monomer peak $E_{p,m}$ occurs at a higher potential where maximum current response occurs. Upon cycling back to negative potentials, one or more polymer reduction peaks can be observed. Polymer oxidation is also apparent on subsequent oxidation cycles; polymer oxidation always occurs at potentials lower than monomer oxidation, because of increased resonance stabilization of the resultant oxidized polymer. Aside from information on the electrochemical processes, cyclic voltammetry also provides insight into side processes such as pre- and post-electron transfer reactions.[23]
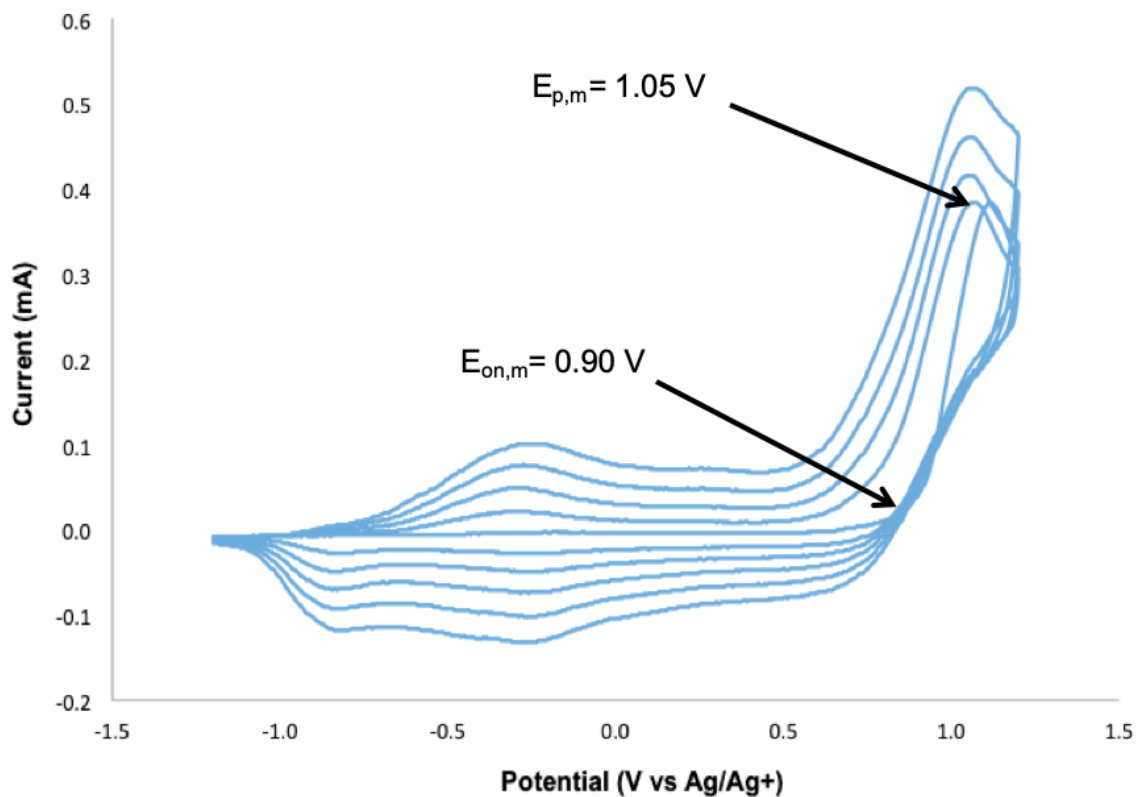
Figure 7. Electrochemical polymerization of 0.01 M 3,4-ethylendioxythiophene (EDOT)/0. 1M tetrabutylammonium perchlorate (TBAP) in acetonitrile (CH$_3$CN) at 100 mV/s*

Once the polymer growth is completed, then a CV of only the polymer is performed at increasing scan rates as shown in Figure 8. This allows for easier identification of polymer oxidation and reduction processes in absence of the monomer. The anodic peak, $E_{a,p}$, and the cathodic peak, $E_{c,p}$, are identified in the 100 mV/s scan and labeled.
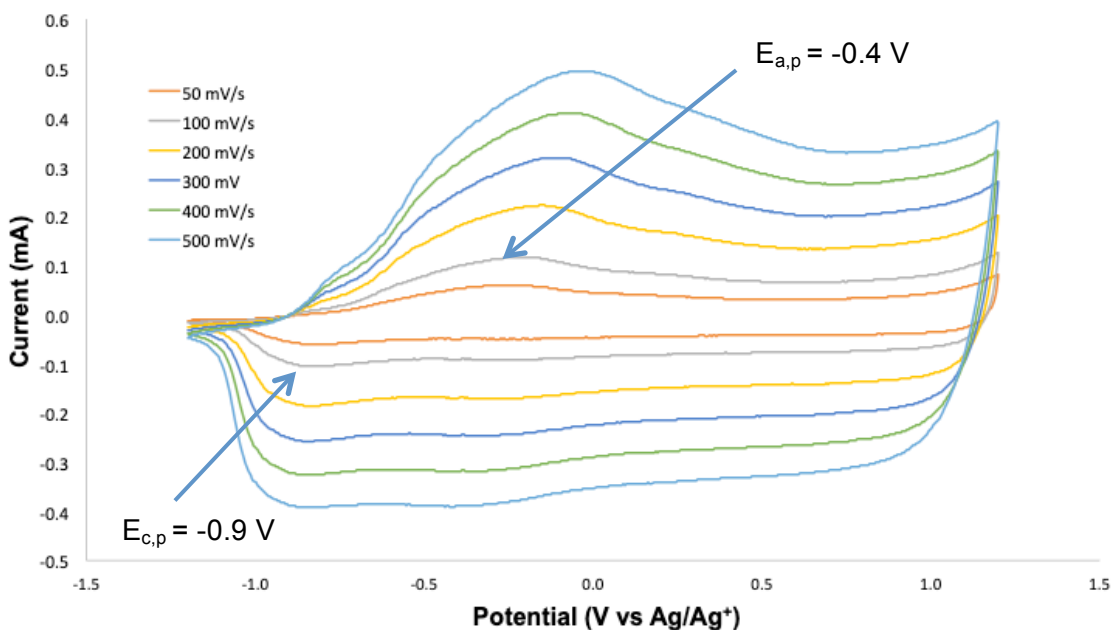
Figure 8. Cyclic voltammetry of PEDOT film (growth shown in Figure 7) in 0.1 M

---

* Experiment performed using materials and conditions described in sections 2.2.1 and 2.2.3, respectively

TBAP in CH_3CN at 50, 100, 200, 300, 400, and 500 mV/s[†]

In most electrochemical systems the redox species can be found freely diffusing

between the surface of the working electrode and the electrolyte system depending on its

redox state. These systems are described by the Randles-Sevick equation:

$$i_p = (2.69 \times 10^5)n^{3/2} AD^{1/2} C^b v^{1/2}$$
   Equation 2

Where i_p is the peak current, n is the number of transferred electrons, A is the

electrodes surface area (cm^2), D is the diffusion constant (cm^2 s^{-1}), C^b is the bulk

concentration (mol cm^{-3}) and v is the scan rate (V s^{-1}).[25] In these systems the peak current

is directly proportional to the *square root* of the scan rate.

However, the electrochemistry of electroactive polymers is slightly different. An

irreversible oxidation is observed upon monomer polymerization, and the polymer

becomes immobilized onto the working electrode as a film. As such the system is no

longer a freely diffusing species, so the Randles-Sevick equation is not applicable.

Instead the theory for surface immobilized redox centers applies in these cases:

$$i_p = \frac{n^2 F^2 \Gamma^2 v}{4RT}$$
   Equation 3

Where i_p is the peak current, n is the number of transferred electrons, F is

Faraday constant (96,485.3365 C/mol), and Γ is the amount of reactant initially present at

---

[†] Experiment performed using materials and conditions described in sections 2.2.1 and 2.2.3, respectively.

the electrode surface.[23] In these systems the relationship between the scan rate and peak current is *linearly dependent* rather than being proportional to the square root of the scan rate. So, if an electroactive film is shown to have a linear dependence between its scan rate and peak current, then that indicates that the film is well-adhered onto the surface of the working electrode (Figure 9). It is for this reason that polymer cyclic voltammetry is conducted at a variety of scan rates as shown in Figure 8.

$$i_p = \frac{n^2 F^2 \Gamma^2 v}{4RT}$$

y = 0.001x + 0.0201
R² = 0.99811

y = -0.0007x - 0.0179
R² = 0.99892
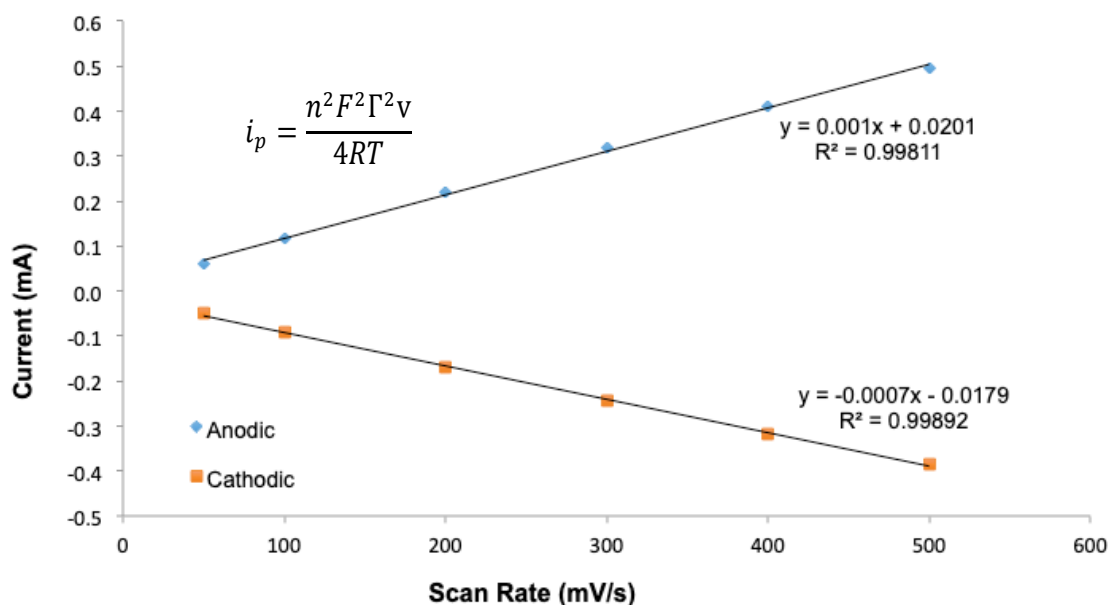
Figure 9. Linear dependence of PEDOT current response[‡]

A three-electrode system consisting of a working electrode (WE), counter electrode (CE), and a reference electrode (RE) provides the most useful information (Figure 10). A working electrode is typically a conductive surface such as platinum, gold,

---

[‡] Data for PEDOT electrochemistry shown in Figure 8

carbon, or indium tin oxide (ITO) and is where the polymer deposition takes place. [26] The

counter electrode is a piece of conductive metal that serves as an electron source and

sink. The reference electrode consists of a well-controlled redox system with known

oxidation and reduction potentials. Commonly used reference electrodes include Ag/Ag^+,

Ag/AgCl, and standard hydrogen electrode (SHE).[23] In some cases a pseudo-reference

electrode like silver wire, which has a less-controlled electrochemistry, may be used as

long as the system is calibrated with a well- behaved redox couple, such as the

ferrocene/ferrocinium couple, after the experiment. [27] The inclusion of a reference

electrode allows for accurate comparison of electrochemical data obtained in separate

experiments.
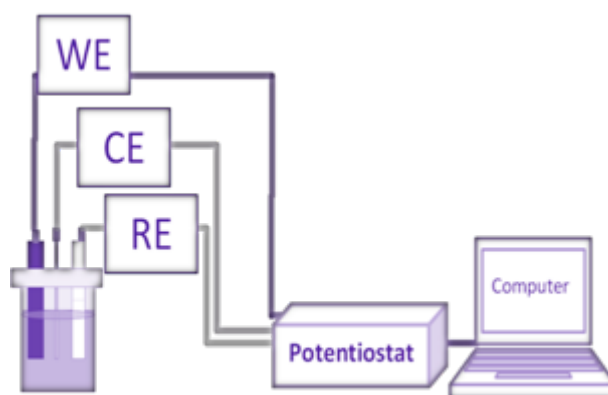
Figure 10. Electrochemistry with a three-cell electrode system[28]

An electrolyte solution is used to conduct current and balance charges during the

electropolymerization and during polymer electrochemistry. [19] Tetraalkylammonium salts

such tetrabutylammonium perchlorate and tetraethylammonium tetrafluoroborate are

commonly used as electrolytes due to their high solubility in organic solvents.

Electroactive polymers can be used in many applications, including chemical sensors[29], energy storage[30], electrochromics[23], actuators[31], and static dissipation.[29] A chemical sensor is a device that transforms chemical information, ranging from the concentration of a specific sample component to total composition analysis, into an analytically useful signal (Figure 11).[29] The chemical information may originate from a chemical reaction of the analyte or from a physical property of the system investigated. Chemical sensors can be prepared from EAPs by analyzing changes in oxidation/reduction potentials or other properties resulting from exposure of the EAP to an appropriate analyte.
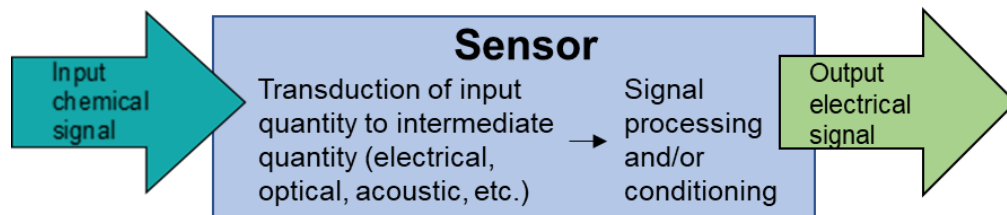
Figure 11. Process of a chemical sensor

EAPs can be used for energy storage, either as battery electrodes or electrochemical capacitors (also known as supercapacitors), due to the reduction and oxidation (redox) processes they undergo. While metals, metal oxides, and carbonaceous materials are typically used in these devices, EAPs have the potential for reduced cost, weight, and environmental impact.[32] EAPs can be tailored to control conductivity, voltage window, storage capacity, and chemical and environmental stability.[33] When

used as battery electrodes, EAPs have shown mixed electronic and ionic conductivity during charge and discharge, and can exhibit high conductivities, flexible morphologies, ease of manufacturing, and low cost.[34] Some of the polymers investigated for use in energy storage include polyacetylene, polyaniline, polypyrrole, and polythiophene. [34]

1.9 Motivation for Research

The increasing prevalence of chemical sensors in our daily lives has highlighted the necessity of further research to improve current systems. Electroactive polymers show great promise in this area due to their reduced cost and ability to be easily tailored for different needs. Elucidating the impact of different functional groups on the overall polymer's electrochemical properties would greatly advance the corresponding research.

1.10 Thesis of This Work

Novel thiophene-based monomers were synthesized and then chemically or electrochemically polymerized along with monomers synthesized by other members of the Irvin Research Group. Polymer electrochemistry was performed to determine polymer oxidation and reduction potentials. Spectroelectrochemistry was used to examine the effect of oxidation potential on polymer band gaps and elucidate the impact of different functional groups on the polymer's properties.

2. SYNTHESIS AND ELECTROCHEMICAL POLYMERIZATION OF P-DOPING EXTENDED CONJUGATION MONOMERS

2.1 Background

2.1.1 Cross-Coupling Reactions

In order to synthesize the extended conjugation monomers discussed in Chapter 1 the molecule must be built step by step. A common approach to synthesizing complex compounds involves attaching new aromatic rings successively to a preformed heterocycle. [35] A carbon-carbon bond must be formed to join the new ring to the heterocycle, using a special set of reactions called cross-coupling reactions.

These reactions (shown in Figure 12 [36]) involve three distinct steps. In the oxidative addition step, a transition metal catalyst (typically nickel, iron, copper, or palladium) with nucleophilic ligands (ML_n), reacts with an organic electrophile such as an alkyl halide (R-X).[35, 37, 38] The alkyl halide bonds with the catalyst, forming ML_2RX. Transmetallation then occurs, where the halogen on the catalyst is replaced by the alkyl in an organometallic reagent (R′M′X′), forming ML_2RR' and the byproduct M′X′X. Finally, in reductive elimination the metal catalyst is reformed and kicks off the coupled product (R-R'). The compatibility of the reagents involved is of the utmost importance as are the conditions required. As a result, a variety of different reactions have been created, each with their own distinct advantages and disadvantages. The most common cross-coupling reactions are briefly described below and summarized in Table 2.
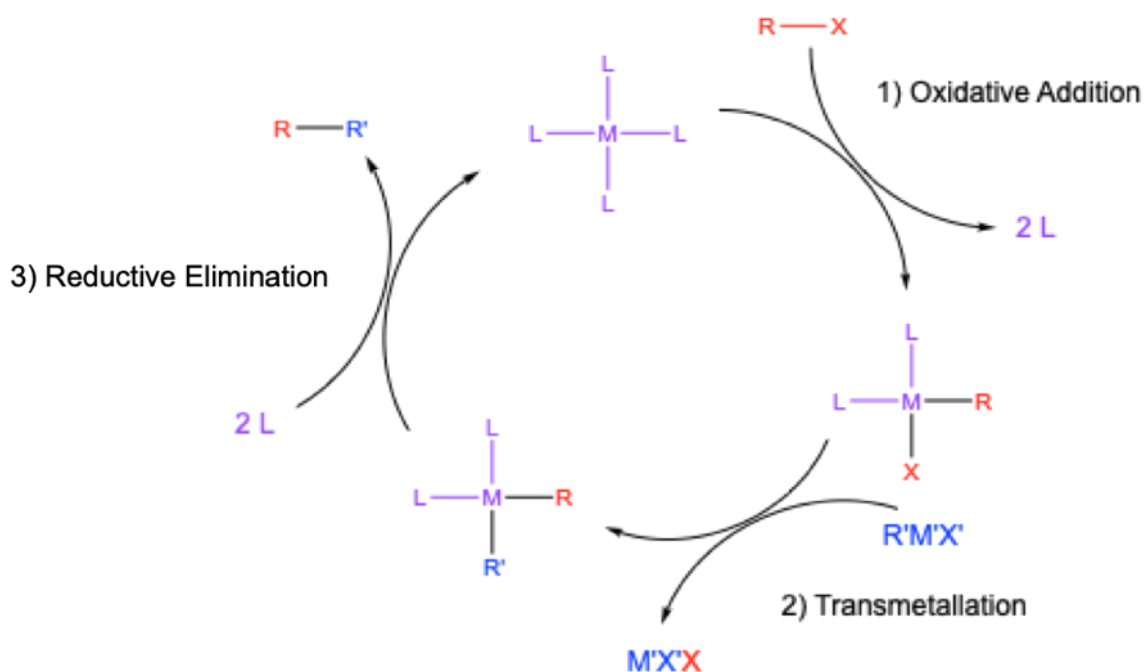
Figure 12. General cross-coupling reaction mechanism

2.1.1.1 Kumada-Tamao cross-coupling

Discovered independently by Kumada and Tamao, this cross-coupling involves the reaction of organomagnesium compounds with aryl halides. [35, 39] It employs a nickel or palladium catalyst, typically dichloro[1,3-bis(diphenylphosphino)-propane] nickel(II) (NiCl$_2$(dppp)) or tetrakis(triphenylphosphine)palladium(0) (Pd(PPh$_3$)$_4$) in diethyl ether. [35, 37] The advantage of this reaction is that it proceeds readily, even at low temperatures, however the limited functional group compatibility of the Grignard reagents is a notable disadvantage. [35]

2.1.1.2 Negishi cross-coupling

First published in 1977, Negishi cross-coupling uses a palladium or nickel catalyst

with an organozinc reagent and a heteroaryl or aryl halide. [38] The reaction is usually

carried out in tetrahydrofuran (THF) or diethyl ether. An advantage of this reaction is the

high functional group tolerance of zinc, however organozincs are not stable at high

temperatures, so the reaction temperature must be closely monitored. [35]

2.1.1.3 Suzuki cross-coupling

The palladium-catalyzed reaction between an organoboron with an aryl halide is a

Suzuki coupling. It occurs in a benzene or toluene solvent mixed with water. The key to

this reaction is the addition of a base, which activates the borane for the transmetallation

step. [35] Some the advantages of Suzuki coupling are that it is unaffected by the presence

of water, it is tolerable of a variety of functional groups, the organometallic reagents used

are unusually stable, and the reaction yields nontoxic byproducts. [40] However, Suzuki

coupling requires high reaction temperatures of 80 – 110 °C, which may not be

suitable/desired for certain reactions. [35]

2.1.1.4 Stille cross-coupling

Stille coupling is the reaction between an organostannane with an aryl halide or

another electrophile. [41] It is palladium catalyzed and typically occurs in DMF, THF, or

toluene. [35] A main advantage of this reaction is the stability of the organostannane, even

in air. [41] However the reaction requires high temperatures, and organostannes are highly

toxic.

2.1.1.5 Sarandeses cross-coupling

Triorganoindium compounds are coupled with aryl or benzyl halides in the presence of a palladium catalyst. [42] The reaction is typically done in refluxing THF. The ability to transfer multiple substituents attached to the metal is a notable advantage of Sarandeses cross-coupling. [43]

Table 2. Common cross coupling reactions

Reaction	Common Reagents	Metal Catalyst	Solvent	Important Notes
Kumada	Organomagnesium halide and aryl halides	Ni or Pd	Diethyl ether	Limited compatibility of organomagnesium
Negishi	Organozinc halide and aryl halides	Ni or Pd	Diethyl ether or THF	Organozincs not stable at high temperatures
Suzuki	Organoboron and aryl or hetaryl halides	Pd	Benzene/H_2O or Toluene/H_2O	Requires high reaction temperature
Stille	Organostannane and aryl halides or other electrophiles	Pd	THF, Toluene, or DMF	Organostannanes are very toxic
Sarandeses	Triorganoindium and aryl or benzyl halides	Pd	THF	Requires high reaction temperature

2.1.2 Extended conjugation monomers

As discussed in Chapter 1, attaching alkyl or alkoxy substituents to the central ring helps to increase solubility and processability of the resultant polymer without introducing significant steric effects. [10] However, substituent chain length and type have been proven to have a significant effect on solubility and oxidation potential. [44] The chain must be long enough to successfully increase solubility and therefore processability; however, long/branched chains containing over 9 carbons prevent π-π overlap between

adjacent chains. Similarly, substituent chains must be equal to or greater than four

carbons long to increase conductivity and solubility significantly.[44-46] Irvin and Reynolds

synthesized and electrochemically polymerized several alkoxy substituted bisEDOT

benzenes to create low oxidation potential electroactive polymers.[6] While they

synthesized monomers with varying alkyl chain lengths, a monomer with hexyl groups

was not synthesized. Therefore, a dihexyloxy bisEDOT benzene (BEB-(OHex)$_2$, Figure

13 left) was synthesized by another group member, polymerized, and studied

electrochemically to determine if any of its properties were significantly affected

compared to the alkoxy substituted bisEDOT benzenes synthesized by Irvin et al.[22, 47]

For comparison purposes, another extended conjugation monomer similar to the

dihexyloxy benzene but with an ester group in the alkyl chain was synthesized (BEB-

(OEs)$_2$, Figure 13, right). The addition of an ester group, which is an electron

withdrawing group, should result in a higher oxidation potential and band gap but should

improve solubility in polar organic solvents. Additionally, the ester moiety should

provide an opportunity for post-polymerization functionalization with other species, such

as those useful for electrochemical sensing applications. This particular monomer has

been synthesized previously for photothermal therapy applications;[48-49] however, its

electrochemical characterization was carried out with a different electrochemical cell and

necessitated further study.

21
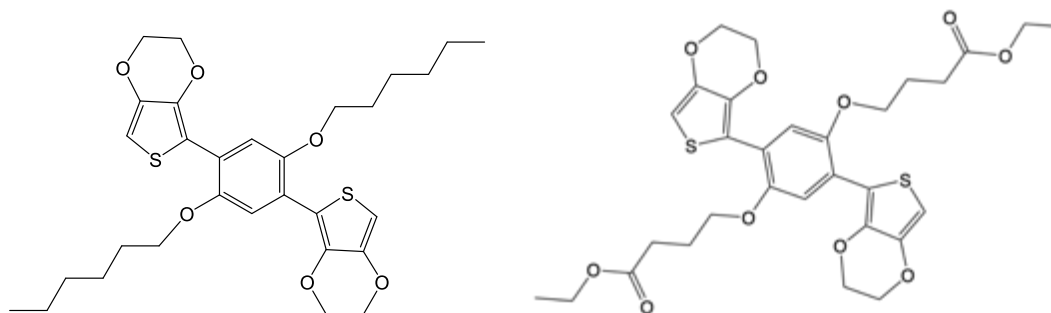
Figure 13. Extended conjugation monomers BEB-(OHex)$_2$ (left) and BEB-(OEs)$_2$ (right)

An alternative to the alkoxysubstituted bisEDOT benzenes involves using fused aromatic rings conjugated to multiple polymerizable moieties. Such a hyperconjugated system would provide a variety of pathways for the electrons to travel through, minimizing chain-hopping and improving conductivity, but at the expense of solubility. An extended conjugation monomer with a hexabenzocoronene core (HBC) (Figure 14, left) is of interest, but due to solubility and processability issues, smaller hyperconjugated central molecules would be easier to work with. Due to this, a smaller hyperconjugated core based on pyrene has been prepared. This molecule, 1,3,6,8-tetrakis[(E)-2-(3,4-ethylenedioxythien-2-yl)vinyl]pyrene (PyVEDOT, Figure 14 right) [50] was expected to provide multiple conjugation pathways to lower the resulting conductivity but with reduced solubility issues.
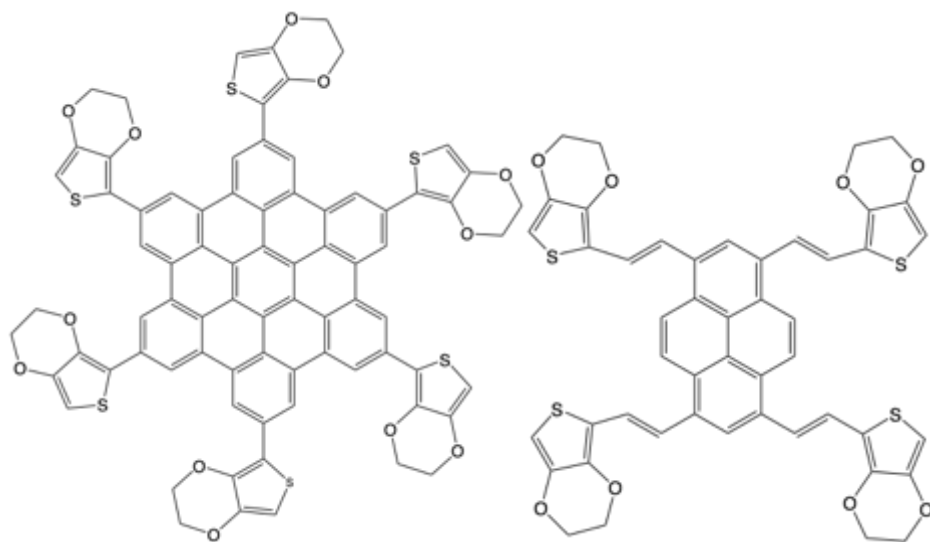
Figure 14. Extended conjugation monomers HBC-EDOT (left) and PyVEDOT (right)

In this chapter, both alkoxy bisEDOT benzene monomers were synthesized, characterized, polymerized, and studied using electrochemistry and spectroelectrochemistry. They were also chemically polymerized, and their average molecular weight determined via gel permeation chromatography (GPC). Electrochemical polymerization was attempted on PyVEDOT to figure out band gap and further study the feasibility of an extended conjugation monomer with a pyrene core.

2.2 Experimental

2.2.1 Materials

Acetonitrile (CH$_3$CN, anhydrous 99.8%) was purchased from Sigma Aldrich and refluxed for 2 days over CaH before distilling for use. Tetrabutylammonium perchlorate (TBAP) was purchased from Alfa Aesar, recrystallized from ethyl acetate, and dried in a vacuum oven for 24 hours prior to use. Dichloromethane (DCM) was purchased from VWR and used as received. Hydroquinone and magnesium sulfate were purchased from

Fisher Scientific and used as received. Hydrazine (anhydrous), iron (III) chloride ($FeCl_3$), and methanol were purchased from Sigma Aldrich and used as received. Bromine, 1-bromohexane, tetrahydrofuran (THF), and zinc chloride were purchased as a 1.0 M solution in THF were purchased from Acros Organics and used as received. Trimethyl tin chloride was purchased as a 1.0 M solution in THF from Acros Organics and used as received. n-Butyllithium was purchased as a 2.5 M solution from Acros Organics and was titrated prior to use to determine actual concentration. [51]

Tetrakis(triphenylphosphine)palladium(0) was purchased from Frontier Scientific and used as received. Ethanol was purchased from Pharmaco-Aarper and used as received. Potassium hydroxide was purchased from Macron and used as received. Sodium sulfite was purchased from Amresco and used as received.

BEB-(OHex)$_2$ was synthesized as described below by Steven Gralinski. PyVEDOT was synthesized by Xu Wang as described in his thesis.[50] The precursor to BEB-(OEs)$_2$, diethyl 4,4'-[(2,5- dibromo-1,4-phenylene)bis(oxy)]dibutanoate (DBDEBE), was prepared according to a procedure reported by Travis Cantu.[52]

2.2.2 Synthesis

2.2.2.1 Synthesis of 1,4-dihexyloxybenzene

1,4-Dihexyloxybenzene was prepared using a method adapted from a procedure reported by Ko *et al.*[53] A 3-neck round bottom flask was equipped with two gas inlet adapters, a high efficiency condenser, and a stir bar, flame dried, and left under argon. Hydroquinone (0.0454 mol, 5 g) and THF (30 mL) were added to the flask. In a Schlenk flask a mixture of KOH in ethanol (0.100 mol, 5.603 g) was prepared and added slowly via syringe into the round bottom flask. 1-Bromohexane (0.0816 mol, 15.9 mL) was then

added to the reaction mixture and refluxed to 60 °C for 24 hours. The reaction was poured into water (125 mL), extracted using DCM (125 mL), and washed three times with deionized water (ca. 100 mL), yielding a yellow-tan organic layer. The organic extract was then dried over magnesium sulfate, filtered through a short silica plug, and concentrated under reduced pressure to yield a tan solid. The compound was then recrystallized from methanol to yield white crystals. MP: 45-46 °C. (lit: 45-46 °C) Yield 4.6 g, 36.4% (lit: 63.7%). ^{1}H NMR (CDCl$_3$, 6.82 (s), 3.90 (t), 1.75-1.65 (q), 1.45-1.33 (m), 0.91 (t) ppm)] (lit. Ko et al.[53] ^{1}H NMR (CDCl$_3$, 6.82 (s), 3.90 (t), 1.80-1.73 (q), 1.47-1.30 (m), 0.90 (t) ppm).

2.2.2.2 Synthesis of 1,4-dibromo-2,5-dihexyloxybenzene

1,4-Dibromo-2,5-dihexyloxybenzene was prepared using a method adapted from a procedure reported by Umezawa et al.[54] 1,4-Dihexyloxybenzene (0.018 mol, 4.92 g) and DCM (30mL) were added to a flame dried 3-neck round bottom flask equipped with two gas inlet adapters and a stir bar. The mixture was kept under argon and cooled at 0 °C for 10 minutes while stirring. Br$_2$ (0.05 mol, 2.49 mL) was then added slowly drop wise with a syringe. The reaction was warmed up to room temperature and left stirring under argon for 24 hours. The reaction was then quenched using a 10% Na$_2$SO$_3$ solution (12 g in 112 mL H$_2$O) leaving a white organic layer. The product was then dissolved in DCM and washed with deionized water three times. The organic layer was then dried over MgSO$_4$ and filtered through a silica short plug yielding a clear solution, which was then concentrated under reduced pressure. The compound was then recrystallized from ethanol yielding a white solid. MP: 61-63 °C. (lit: 51-53 °C) Yield 6.0601g, 79.01%. (lit: 90.5%) ^{1}H NMR (CDCl$_3$, 7.08 (s), 3.94 (t), 1.81 (q), 1.50-1.46 (m), 1.36-1.34 (m), 0.91

(t) ppm): [lit. (Umezewa *et al.*[54]) ^{1}H NMR (CDCl$_3$, 7.09 (s), 3.95 (t), 1.80 (q), 1.51-1.46 (m), 1.37-1.32 (m), 0.90 (t) ppm)]

2.2.2.3 Synthesis of 1,4-bis[2-(3,4-ethylenedioxy)thienyl]-2,5-dihexyloxybenzene (BEB-(OHex)$_2$)

BEB-(OHex)$_2$ was prepared according to a procedure reported previously for an analogous compound. [6] 3,4-Ethylenedioxythiophene (EDOT, 0.0102 mol, 1.1 mL) and THF (30 mL) were added to a flame dried 3-neck round bottom flask equipped with two gas inlet adapters, a condenser, and a stir bar. The flask was chilled to -78 °C in a dry ice/acetone bath and allowed to equilibrate for 10 minutes under flowing argon. Once the reaction was chilled, n-butyllithium (2.5 M, 5.2 mL) was slowly added via syringe to the reaction and allowed to react for one hour while stirring. The reaction was then warmed up to 0 °C in an ice bath and zinc chloride (1.0 M, 10.6 mL) was added to the reaction. After one hour the ice bath was removed and 1,4-dibromo-2,5-dihexyloxybenzene (0.018 mol, 2 g) was added to the reaction along with 0.05 g of tetrakis(triphenylphosphine)palladium(0). The reaction was then heated to reflux and allowed to react for five days; reaction progression was monitored using thin layer chromatography (TLC). The organic layer was then dried over MgSO$_4$, filtered and concentrated under reduced pressure to yield a yellow solid. The solid was purified via column chromatography using a neutral alumina column with 10% ethyl acetate/90% hexane mobile phase. The fractions containing product were then collected and evaporated under reduced pressure to yield a pale yellow powder (15 % yield). MP 116-118 °C. ^{1}H NMR (C$_6$D$_6$) δ 8.07 (s, 2H) 6.33 (s, 2H), 4.02 (t, 4H), 3.5 (dd, 8H), 1.81 (m,

4H), 1.45 – 1.24 (m, 12H), 0.86 (t, 6H). ^{13}C NMR (CDCl$_3$) δ (113.6, 99.6, 92.76, 69.9, 64.9, 64.4, 31.7, 29.3, 26.1, 22.4, 14.6 ppm)

2.2.2.4 Chemical oxidative polymerization of BEB-(OHex)$_2$ to form PBEB-(OHex)$_2$

BEB-(OHex)$_2$ (100 mg) was added to a round bottom flask with chloroform (20 mL) and stirred under flowing argon for ten minutes. FeCl$_3$ (0.0538 mol, 100 mg) was added slowly to the flask and the reaction was stirred for 24 hours under argon. Upon addition of FeCl$_3$ the reaction mixture immediately turned blue. The reaction was poured into a flask containing rapidly stirring methanol (50 mL), after which the polymer was collected via vacuum filtration and rinsed with additional methanol (5 mL). The solids were then resuspended in chloroform (10 mL), and two drops of hydrazine were added to reduce the polymer. The reaction was stirred for another 24 hours in the dark, and the now red reaction mixture was filtered via vacuum filtration to yield a bright red solid (90% yield). An aliquot was taken from the solution and filtered through a 0.2 μm PTFE filter prior to injection into the GPC.

2.2.2.5 2-Trimethylstannyl-3,4-ethylenedioxythiophene (EDOT-SnMe$_3$)

Synthesis was conducted as reported by Wang *et al*.[55] EDOT (0.035 mol, 5 g) was mixed with dry THF (50 mL) in a flame dried three neck round bottom flask under argon fitted with 2 gas inlet adapters and a stir bar. The mixture was cooled to -78 °C for 10 minutes, after which n-BuLi (1.6 M in hexanes) (0.035 mol, 21.98 mL) was added drop wise by syringe. After stirring for one hour, 1 M Sn(CH$_3$)$_3$Cl (0.035 mol, 35 mL) was added slowly with a syringe. The reaction was warmed to room temperature and left

stirring for one day. Thin layer chromatography (TLC) was used to monitor the reaction. The mixture was evaporated under reduced pressure to yield an opaque dark brown liquid. The crude product was then diluted tenfold with dry THF, dried over $CaCO_3$, filtered, and evaporated under reduced pressure leaving a viscous dark brown compound (70% yield). ^{1}H NMR (THF-d_8) δ 6.53 (s, 1H), 4.18 (d, 9H), 0.30 (s, 9H).

2.2.2.6 Synthesis of BEB-(OEs)$_2$

Synthesis was adapted from a procedure reported by Wang *et al.*[55] EDOT-Sn(CH$_3$)$_3$ (0.023 mol, 0.7 g) was mixed with Pd(PPh$_3$)$_2$Cl$_2$ (0.03 g) and DBDEBE (0.001 mol, 0.5 g) with anhydrous THF (20 mL) in a flame dried 3-neck flask fitted with a gas inlet adapter, a high efficiency condenser, and a stir bar. The mixture was kept under argon and heated to 110 °C and stirred for 5 days. The crude product was washed with 1 M HCl (5 mL), chloroform (5 mL) and 1 M NaOH (5 mL). The organic layer was then dried over MgSO$_4$, filtered and concentrated under reduced pressure to yield a dark brown solid. The solid was purified via column chromatography using a neutral alumina column with 25% ethyl acetate/75% hexane mobile phase. The fractions containing product were then collected and evaporated under reduced pressure to yield brown crystals (0.30 g, 30%). ^{1}H NMR (C$_6$D$_6$) δ 7.93 (s, 2H), 6.53 (s, 2H), 4.18 (d, 9H), 0.30 (s, 9H).

2.2.3 Instrumentation

A Ag/Ag$^+$ reference electrode system was prepared following BASi ® procedure. A glass body with a CoralPor ® porous frit was filled with 0.1 M TBAP/CH$_3$CN

electrolyte solution and placed into a vial filled with electrolyte solution. After an hour, the electrolyte solvent was removed, and the glass body filled with ~3 mL of 0.01 M $AgNO_3$ in 0.1 M TBAP/ CH_3CN. A Teflon ™ cap with silver wire was placed into the glass body.

All electrochemical experiments were accomplished using a Pine WaveNow potentiostat. Unless otherwise noted, electrochemistry was performed in a solution of 0.01 M monomer in 0.1 M TBAP in CH_3CN/DCM (1:1) and 0.01 M monomer in 0.1 M TBAP in CH_3CN only. The working electrode was a platinum button (Bioanalytical Systems, Inc., part number MF-2013; 1.6mm diameter), a glassy carbon button (Bioanalytical Systems Inc. MF-2012, 3.0mm diameter) or an ITO-coated glass slide (7 x 50 x 0.7 mm, Rs = 4 – 8 Ω, Delta Technologies). The counter (CE) and reference (RE) electrodes were a platinum flag and a Ag/Ag^+ system, respectively. Cycling of the polymer films occurred in monomer-free solution of 0.1 M TBAP in CH_3CN.

2.2.4 Characterization

For spectroelectrochemistry, ITO slides coated with polymer films that were reduced with hydrazine were used as the working electrodes. The counter electrode used was a clean ITO-coated glass slide, and a silver wire was the pseudo-reference electrode. The electrolyte solution was 0.1 M TBAP in CH_3CN. ITO-coated glass slides were rinsed three times with deionized water, wiped with an acetone dampened low lint paper wipe (KIMWIPE ®), dipped into 1 M hydrochloric acid (HCl) and rinsed three more times with deionized water prior to use.[28]

UV-Vis spectroelectrochemistry was carried out using a Perkin Elmer Lambda

365 UV-Visible spectrophotometer with quartz cuvettes (VWR, 10 mm light path).

Characterization analysis was performed using a Bruker Avance 400 MHz NMR. ^{1}H NMR analysis was performed using either deuterated chloroform or dichloromethane for 16 scans. ^{13}C NMR was performed in deuterated chloroform for 720 scans.

Molecular weight analysis was accomplished using a Viskotek GPC with a Viskotek 270 dual detector (Right-Angle Light Scattering (RALS) and Low-Angle Light Scattering (LALS)) and a VE 3580 Refractive Index (RI) detector. All molecular weights are relative to polystyrene standards prepared in HPLC grade CHCl$_3$, passed through a 0.2 µm Acrodisc ® Pall PTFE filter, and injected through a VE 1122 solvent delivery system followed by a T3000 organic GPC/SEC column at a flow rate of 1 mL/min. Retention times were calibrated against polystyrene standards (5 mg/mL) of molecular weights: 5,200, 13,000, 25,000, 30,000, 50,000, and 65,000 g/mol. Polydispersities (M$_w$/M$_n$) of the all the polymer standards used was 1.06.

2.3 Results and Discussion

2.3.1 Synthesis of BEB-(OHex)$_2$ and BEB-(OEs)$_2$

Many alkoxy substituted bisEDOT benzenes have been synthesized via Negishi coupling, a palladium catalyzed reaction with an aryl zinc halide.[38, 56] The Negishi method was chosen due to the zinc compound's relatively high functional group tolerance and low toxicity [35], making it useful for a wide variety of reactions. As shown in Figure 15, hydroquinone underwent etherification with 1-bromohexane followed by bromination to create 1,4-dibromo-2,5-dihexyloxybenzene. This was then coupled with EDOT-ZnCl in a 1:2 ratio in the presence of palladium catalyst Pd(PPh$_3$)$_4$ to synthesize the product

BEB-(OHex)₂.
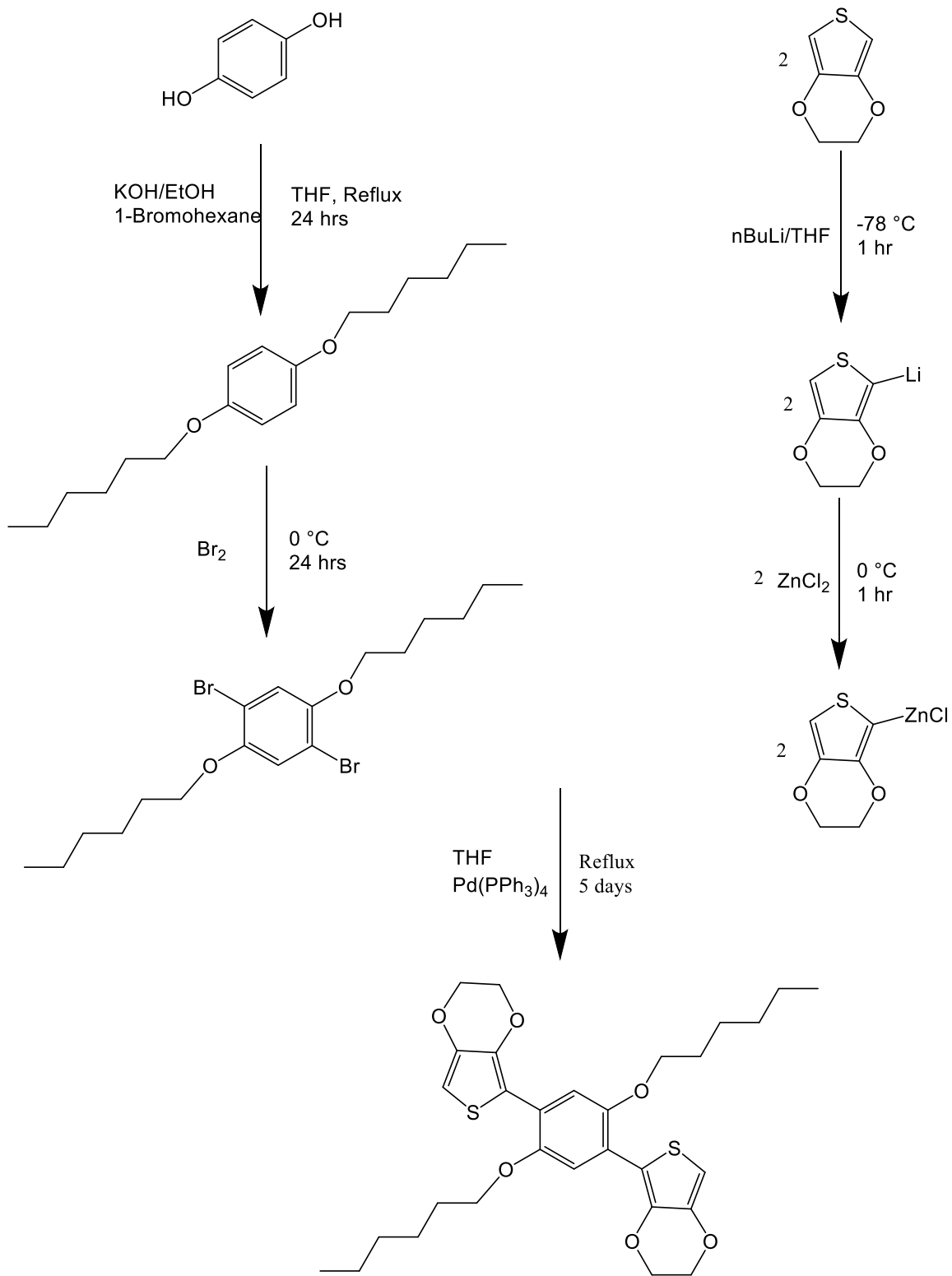
Figure 15. Synthesis of BEB-(OHex)$_2$ via Negishi coupling

      While the synthesis of BEB-(OEs)$_2$ has been accomplished in our group previously using Negishi coupling, [52] the method proved unreliable for this molecule. The ester group is likely to blame, either interfering with the coupling reaction or undergoing hydrolysis during workup. Instead, an improved route to BEB-(OEs)$_2$ was developed using the Stille coupling reaction (Figure 16). Stille coupling is known to be tolerant of a wide range of functional groups, including esters.[35] As discussed in section 2.1.1.4, while Stille coupling is also palladium catalyzed, it instead uses an aryl trialkylstannyl compound as the organometallic substance. Unfortunately, organostannyl compounds are highly toxic, so Stille coupling should only be used when other methods are unsuccessful.
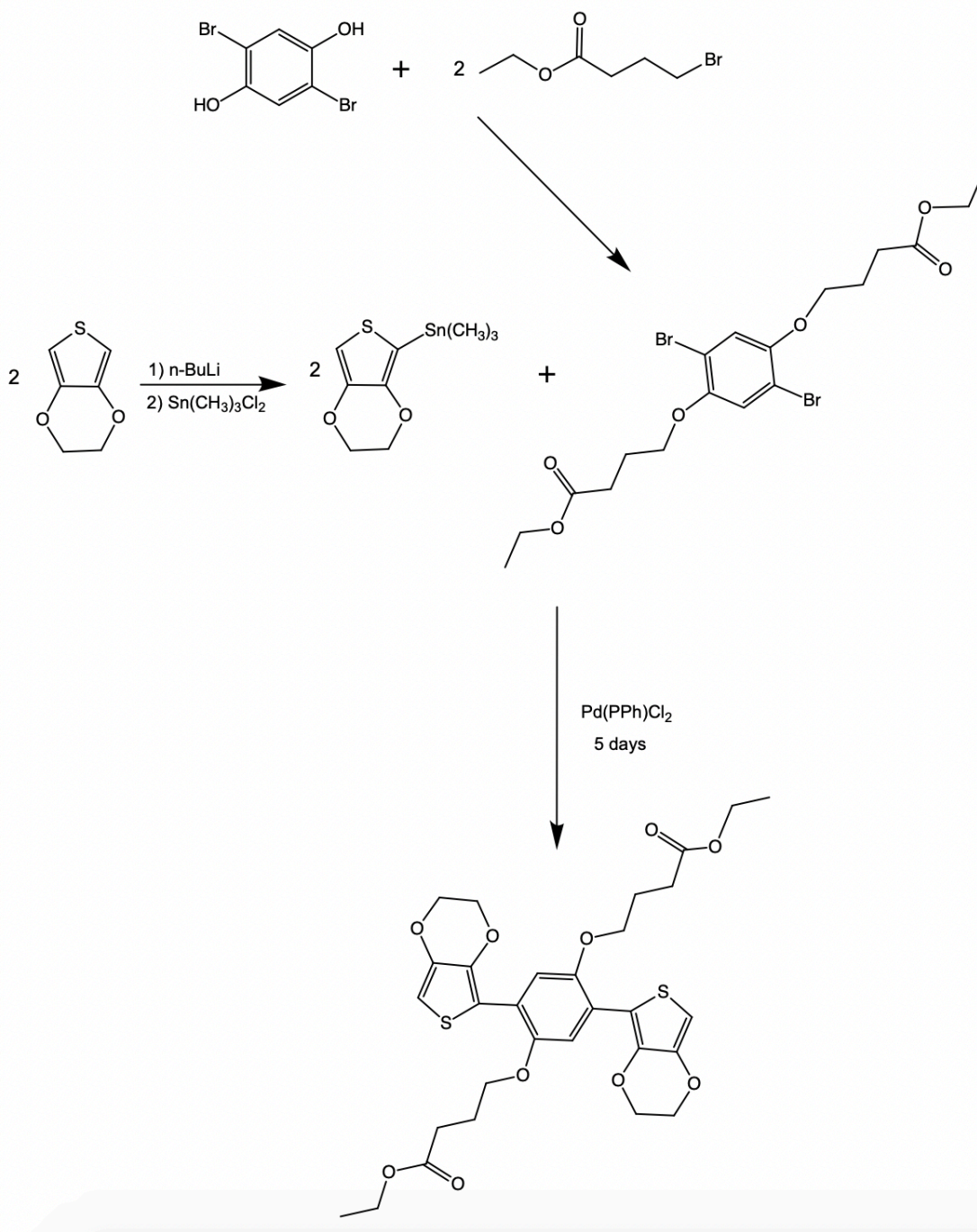
Figure 16. Synthetic scheme for the Stille cross-coupling of DBDEBE with EDOT-Sn(CH$_3$)$_3$ to prepare BEB-(OEs)$_2$

DBDEBE was prepared according to a procedure from Cantu *et al.*[49] A synthetic

method adapted from Wang *et al.*[50] was followed for the stannylation of EDOT as well as

the Stille coupling of DBDEBE with EDOT-Sn(CH$_3$)$_3$. The crude product was purified

via column chromatography. The NMR showed successful coupling of DBDEBE with

EDOT-Sn(CH$_3$)$_3$ as evidenced by the 1:1 ratio of the phenyl proton (δ 7.79) and the

EDOT proton (δ 6.24) (Figure 17).
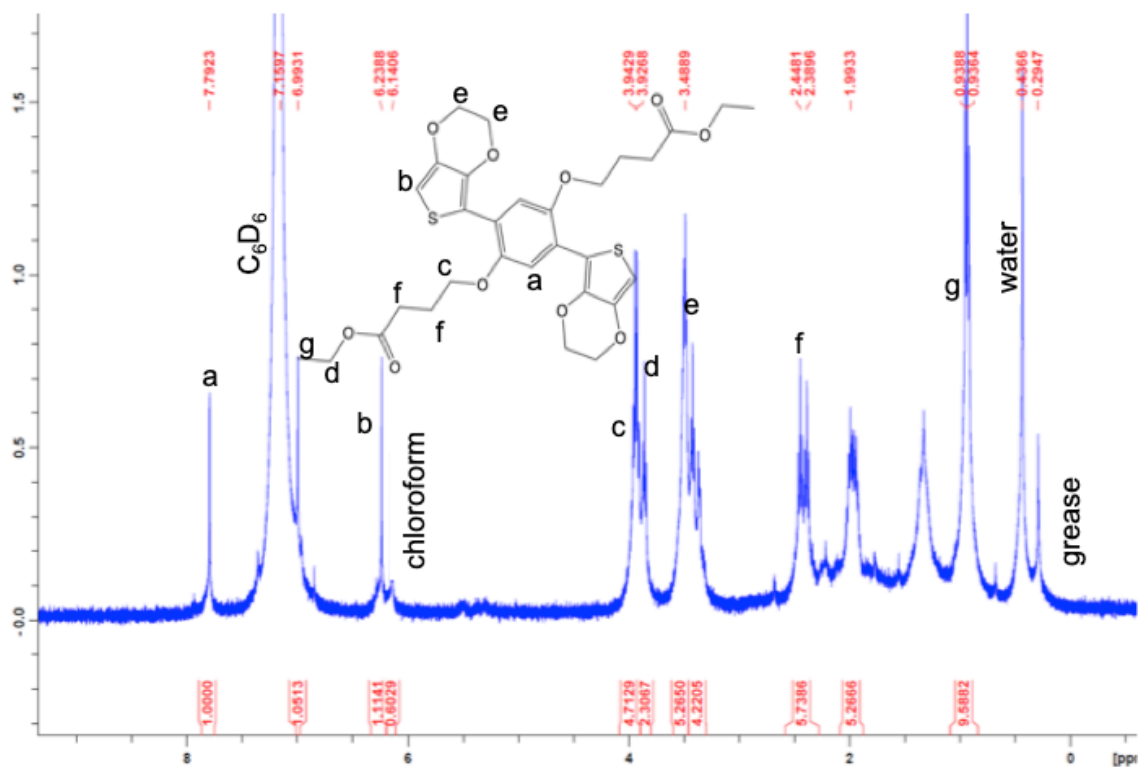
Figure 17. NMR spectrum of BEB-(OEs)$_2$, the 1:1 ratio of the phenyl proton to the

EDOT proton indicates compound was successfully coupled

2.3.2 BEB-(OHex)$_2$ Monomer and Polymer Electrochemistry

To study the electrochemistry of the monomer BEB-(OHex)$_2$, it was attempted to

create a 0.01 M monomer solution in 0.1 M TBAP/CH$_3$CN electrolyte solution. However,

it was observed that the monomer would not dissolve in the electrolyte solution despite extensive stirring, which indicated that the solution in CH_3CN (dielectric constant (ε) =36.64) [57] was too polar to dissolve the monomer. The electrolyte solution was then concentrated under reduced pressure to half of its original volume, and the less polar solvent DCM (ε=8.93) [57] was added to the solution at a 1:1 CH_3CN:DCM. Irvin *et al.* reported similar solubility issues with other alkoxysubstituted bisEDOT benzenes.[56]

Electrochemical polymerization of BEB-(OHex)$_2$ was then accomplished using a 0.01 M monomer solution in 0.1 M TBAP in CH_3CN /DCM at 100 mV/s. The monomer was cycled between -1.0 V and +0.7 V vs Ag/Ag$^+$ for five full cycles on a platinum button working electrode. Onset of monomer oxidation ($E_{on,m}$) was observed (Figure 18) at 0.38 V with a peak ($E_{p,m}$) at 0.56 V. With each subsequent scan the current response increased, indicating the amount of polymer on the electrode was increasing.
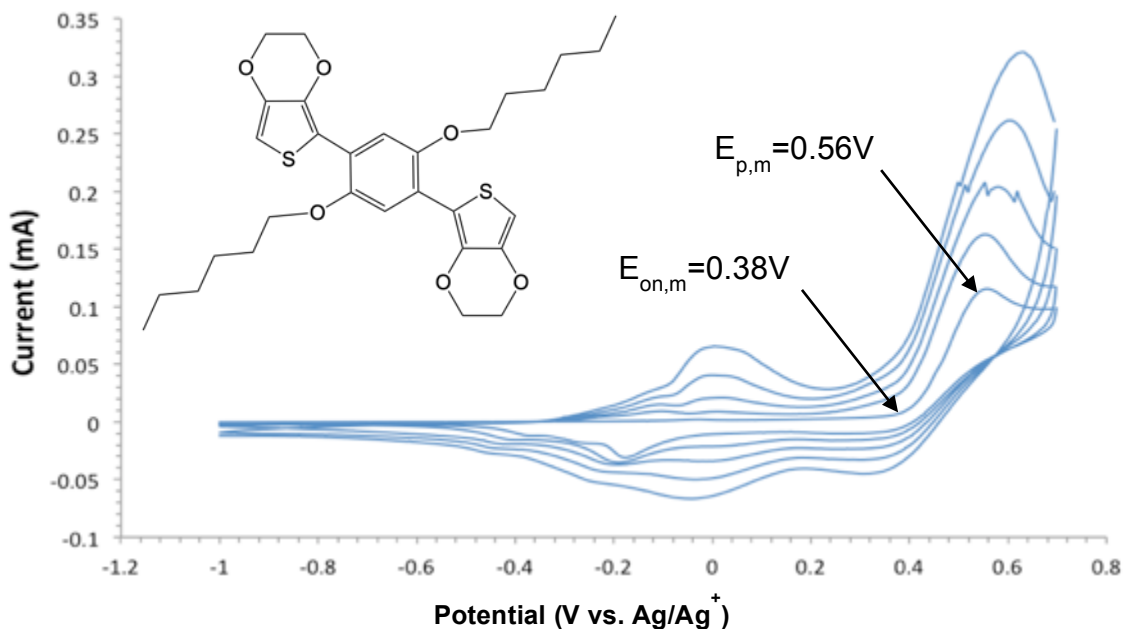
Figure 18. Electrochemical polymerization of 0.01 M BEB-(OHex)$_2$ in 0.1M TBAP in

CH₃CN/DCM at 100 mV/s for 5 cycles between -1.0 and +0.7 V. WE: Pt button

The polymer was then rinsed with electrolyte solution and transferred to a monomer-free solution of 0.1 M TBAP in CH$_3$CN/DCM to study its electrochemistry as a function of scan rate. The polymer was first cycled four times to ensure that no monomer remained on the WE. It was then cycled at 50, 100, 200, 300, 400, and 500 mV/s from -1.0 to +0.7 V (Figure 19). The nonlinear increase of the peak current as a function of scan rate (Figure 20) indicates that the polymer was not well adhered to the electrode. This is most likely due to the solubility of the polymer in DCM.
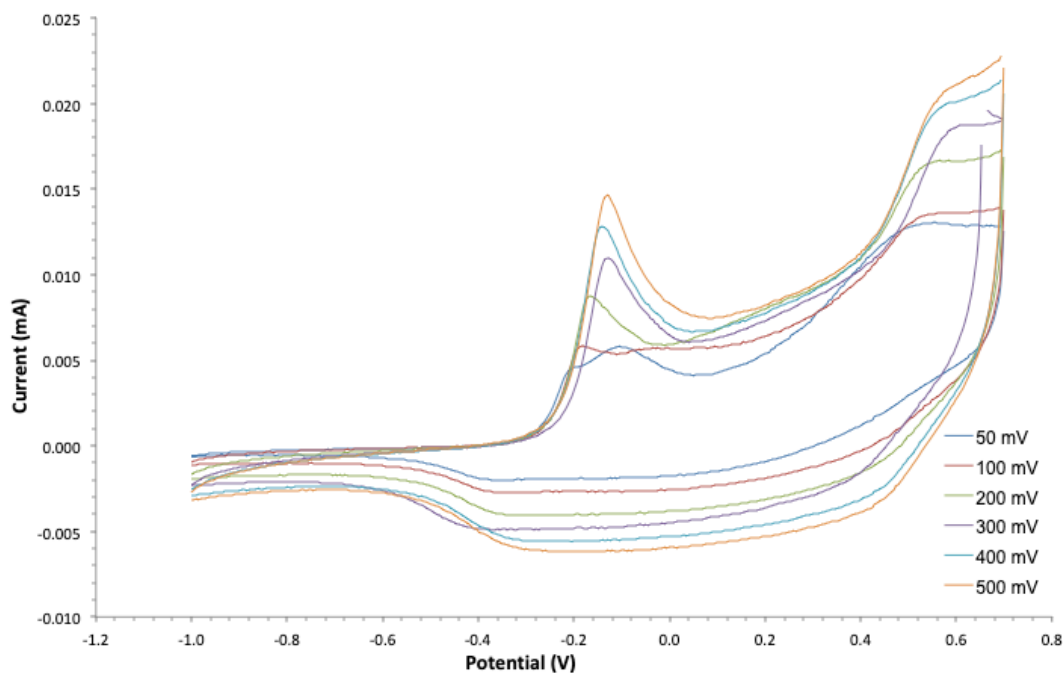
Figure 19. Cyclic voltammetry of PBEB-(OHex)$_2$ in 0.1 M TBAP CH$_3$CN/DCM at 50, 100, 200, 300, 400, 500 mV/s from -1.0 to +0.7 V. WE: Pt button
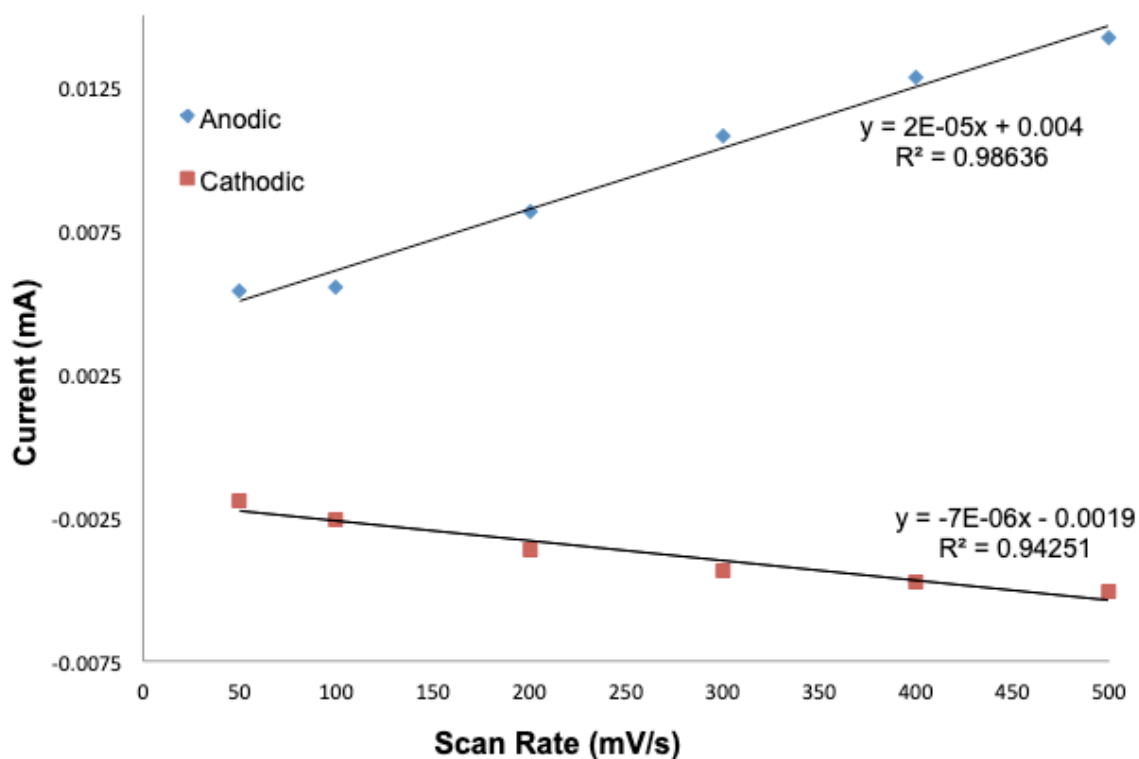
Figure 20. Peak current versus scan rate dependence of PBEB-(OHex)$_2$ in 0.1 M TBAP in CH$_3$CN/DCM

The electrochemical polymerization of BEB-(OHex)$_2$ was then repeated exactly as above, and then the polymer electrochemistry was studied in a 0.1 M TBAP/CH$_3$CN electrolyte solution. As can be observed in Figure 21, the scan rate dependence is remarkably different from the previous attempt. Not only is the peak current at each scan rate much higher, but it is also much more even throughout the cycle with no other redox processes occurring. The linear dependence on scan rate is also changed, with a much more linear response in both the cathodic and anodic peaks (Figure 22 insert). The initial anodic data points that deviate from linearity are evidence of residual dissolved polymer from the monomer electrolyte solution. With the new solvent system, the polymer film is

not soluble and is adhered to the working electrode.
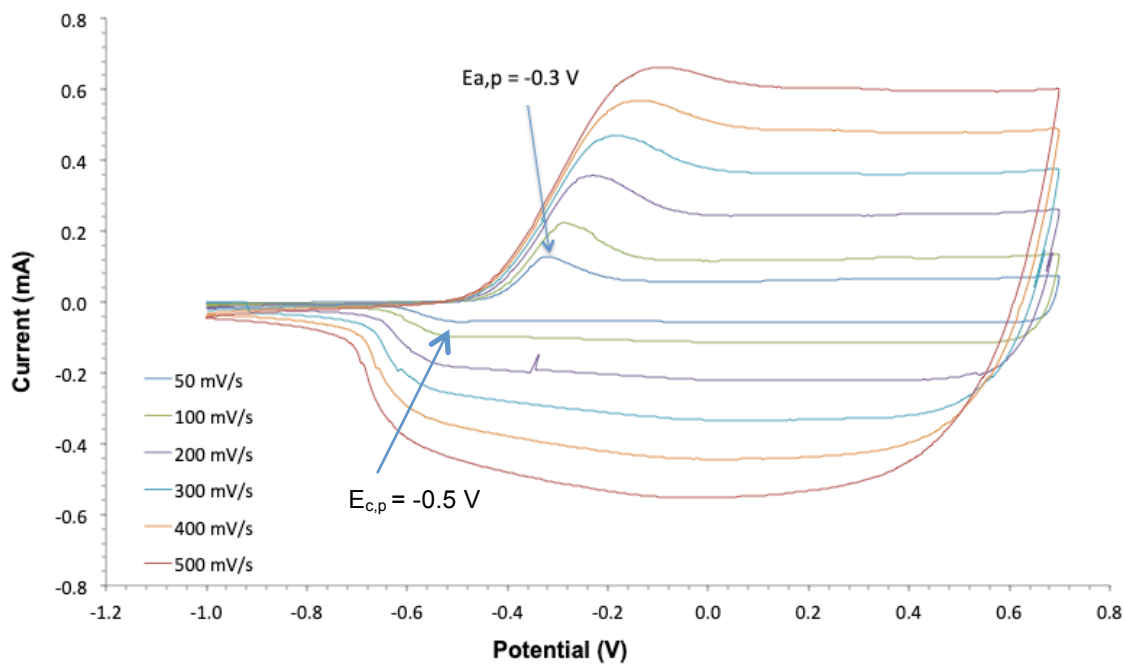
Figure 21. Cyclic voltammetry of PBEB-(OHex)$_2$ in 0.1 M TBAP in CH$_3$CN at 50, 100, 200, 300, 400, 500 mV/s from -1.0 to +0.7 V. WE: Pt button
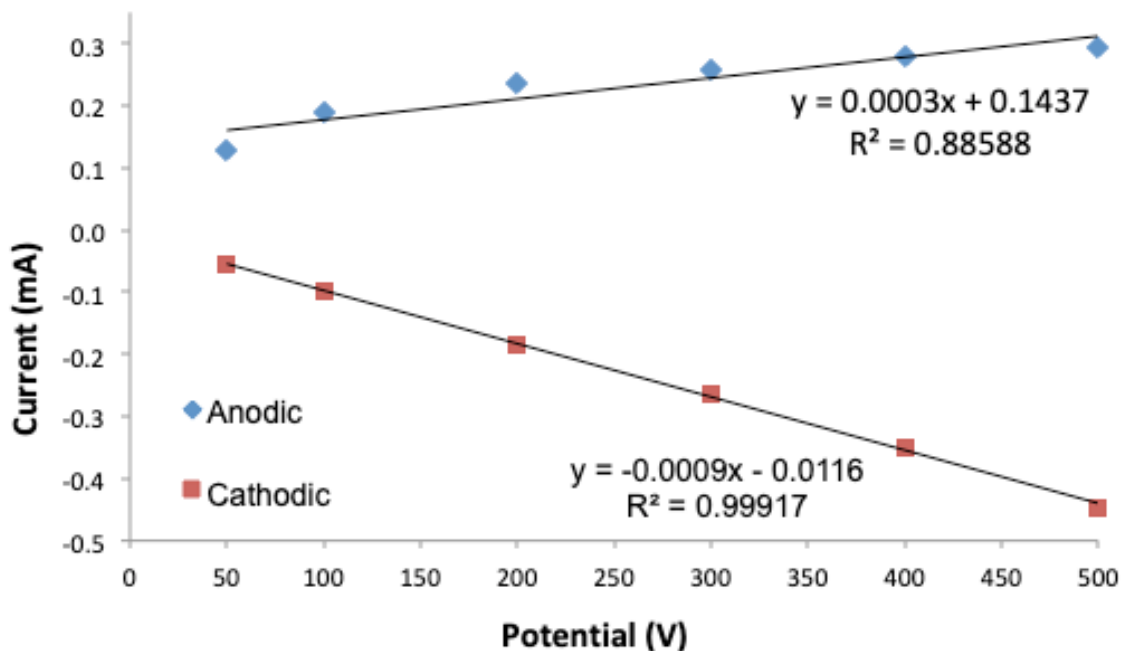
Figure 22. Peak current versus scan rate dependence of PBEB-(OHex)$_2$ in 0.1 M TBAP in CH$_3$CN

2.3.3 BEB-(OHex)$_2$ Spectroelectrochemistry

The polymer undergoes a color change from red to blue when changing between the reduced to the oxidized states. Spectroelectrochemistry can be used to determine the exact potential at which the polymer undergoes a redox change. The absorption spectrum of the reduced polymer film reveals the polymer band gap (E$_g$) as the onset of the π to $\pi*$ transition (band gap). Acquiring spectra at a series of increasing potentials shows how the electronic state of the polymer changes during oxidation and reveals the development of intermediate energy levels as the polymer is doped.

Prior to conducting the spectroelectrochemical experiments, polymer films were first deposited onto ITO-coated glass slides, which functioned as the working electrodes.

An ITO-coated glass slide represents an optimum WE alternative for absorbance

measurements, as it is highly conductive and is greater than 75% transmissive from ca.

400 nm to 1000 nm.[58] Deposition of the polymer film was achieved using the same set-up

as with the electrochemistry, with the exception of the ITO-coated glass slide being used

as the working electrode. The polymer was cycled four times to ensure formation of a

film and was left in the reduced state. The slides were then rinsed several times and

placed into separate vials containing electrolyte solution and a drop of hydrazine to

prevent any further oxidation.

For the spectroelectrochemistry the counter electrode was replaced by an ITO

slide, and a silver wire was used as a pseudo-reference electrode. The working, counter,

and pseudo-reference electrodes were placed inside a quartz cuvette, which was then

filled with electrolyte solution. A piece of Teflon™ spacer was used to ensure that the

counter and working electrodes did not touch each other. It was attempted to conduct

spectroelectrochemistry on the polymer films; however, as shown in Figure 23, there was

very little space to maneuver the leads for the electrodes. Attempts at cycling the polymer

films resulted in them disintegrating due to the leads moving and touching each other.
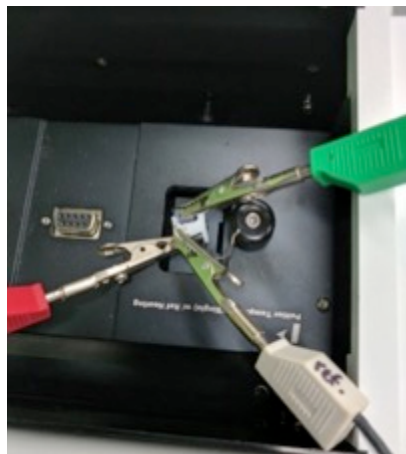
Figure 23. Electrochemistry setup in a cuvette with non-modified ITO coated glass slide electrodes

The ITO slides were then modified by attaching a piece of bent silver wire (a) and secured in place with copper tape (b) and electrical tape (c) prior to the electrochemical polymerization of the monomer as shown in Figure 24. This allowed for greater maneuverability and ease for the spectroelectrochemistry experiment (Figure 25), while simultaneously reducing electrical resistance at the lead-slide interface.
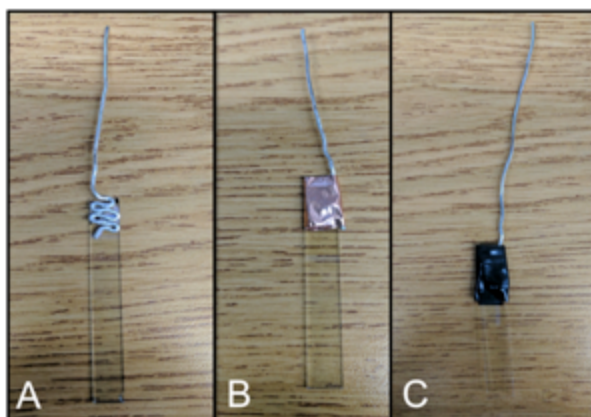
Figure 24. Steps for modifying ITO-coated glass slides for spectroelectrochemistry

Figure 25. Electrochemistry in a cuvette with modified ITO slides

Spectroelectrochemistry with the modified slides proved to be successful. The resulting absorption spectra are displayed (Figure 26), where it is apparent that the red-pink neutral polymer absorbs between 450 and 625 nm with a λ_{max} at ca 550 nm. There is a distinct change in the absorbance from 0.3 V to 0.4 V, where the absorption shifts to higher wavelengths (lower energies), which is characteristic of a polymer in the oxidized state. The blue-purple oxidized polymer absorbs between 600 and 900 nm with a λ_{max} at ca. 735 nm.
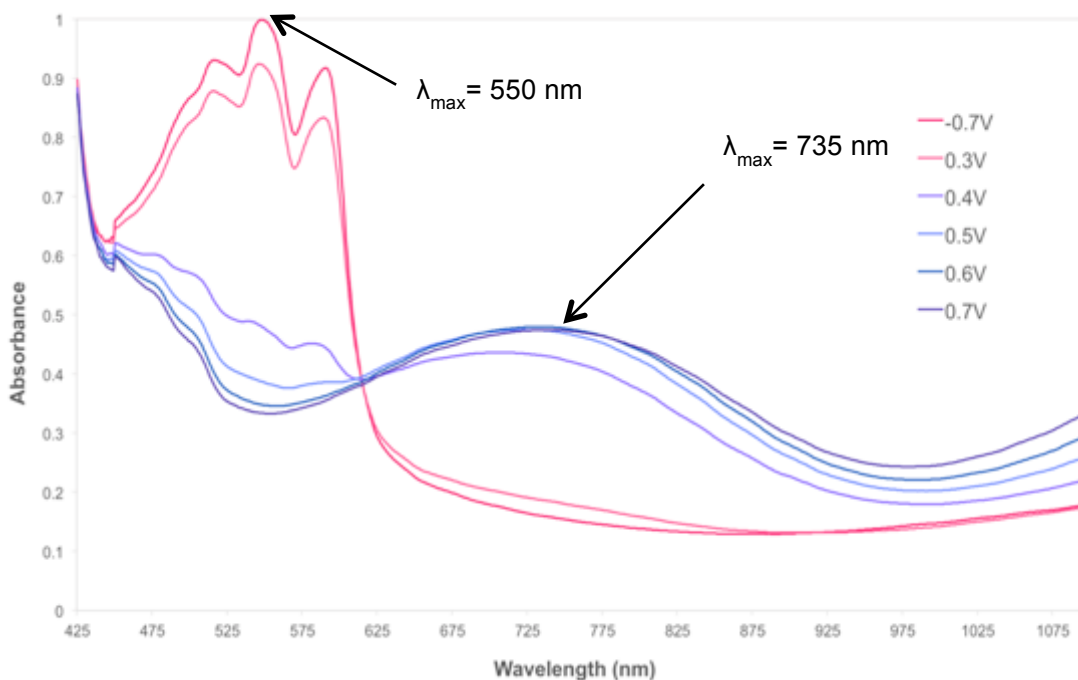
Figure 26. PBEB-(OHex)$_2$ absorption spectra as a function of oxidation potential, plotted in wavelength, for a polymer film electrochemically deposited onto an ITO working electrode in 0.1 M TBAP in CH$_3$CN

In order to more easily view the polymer band gap, the absorption spectra are also plotted in electron volts (eV, converted as per Equation 1). As can be seen in Figure 27, the onset of the π-π* transition, which defines the polymer band gap, can be seen at 1.9 eV. This is consistent with other dialkoxy-substituted BEB derivatives, which have band gaps between 1.8 and 2.0 eV. [6, 56]
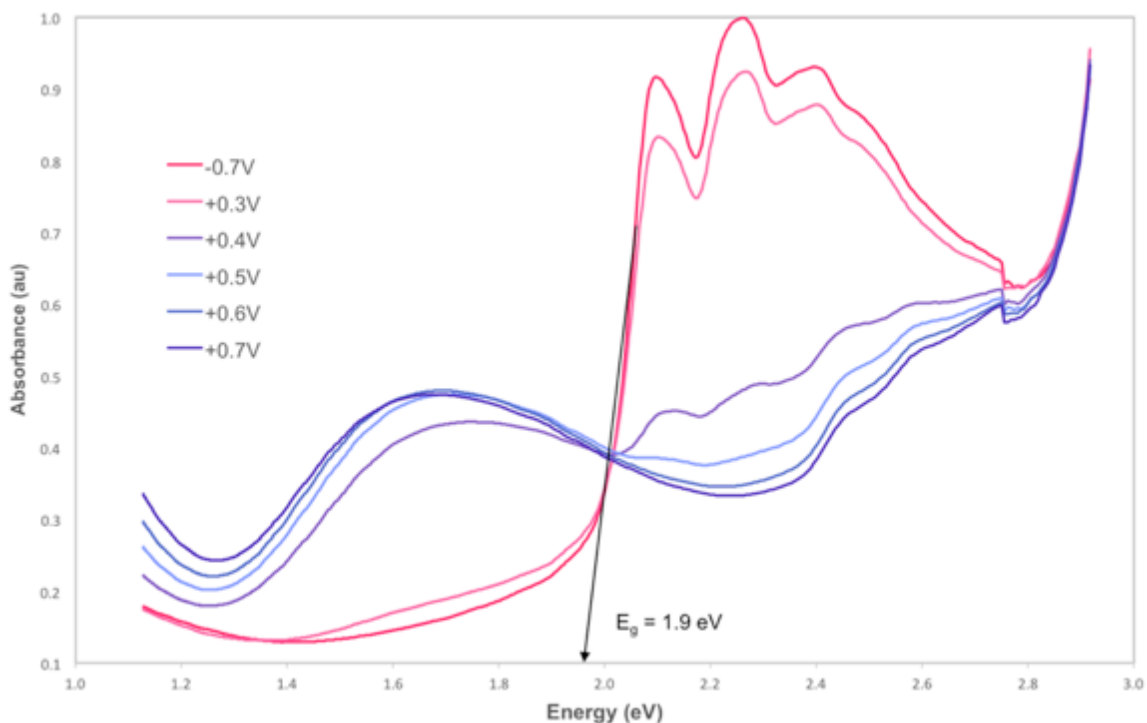
Figure 27. PBEB-(OHex)$_2$ absorption spectra as a function of oxidation potential, plotted in electron volts, for a polymer film electrochemically deposited onto an ITO working electrode in 0.1 M TBAP in CH$_3$CN

2.3.3 Chemically Polymerized of PBEB-(OHex)$_2$

BEB-(OHex)$_2$ was chemically polymerized in chloroform using iron (III) chloride

as the oxidant. The radical polymerization (Figure 6) proceeds until the polymer chain

reaches its solubility limit, at which point it precipitates in its oxidized form. The

oxidized polymer was resuspended in CHCl$_3$ and reduced using hydrazine. The average

molecular weight of PBEB-(OHex)$_2$ was investigated using GPC. As shown below in

Figure 28, the polymer eluted at 9.5 minutes It bears to note that the Refractive Index

(RI) detector was offline, therefore no polymer peaks were observed. As such, the

calibration curve was calibrated with respect to the Right-Angle Light Scattering (RALS)

detector, giving an average molecular weight of 1765 g/mol, which translates to about

three repeat units per polymer chain. The calibration standards used though were of

higher MW (lowest was 5.2 K) than that of PBEB-(OHex)$_2$, therefore the molecular

weights measured for this polymer and others in the rest of this thesis are not exact.
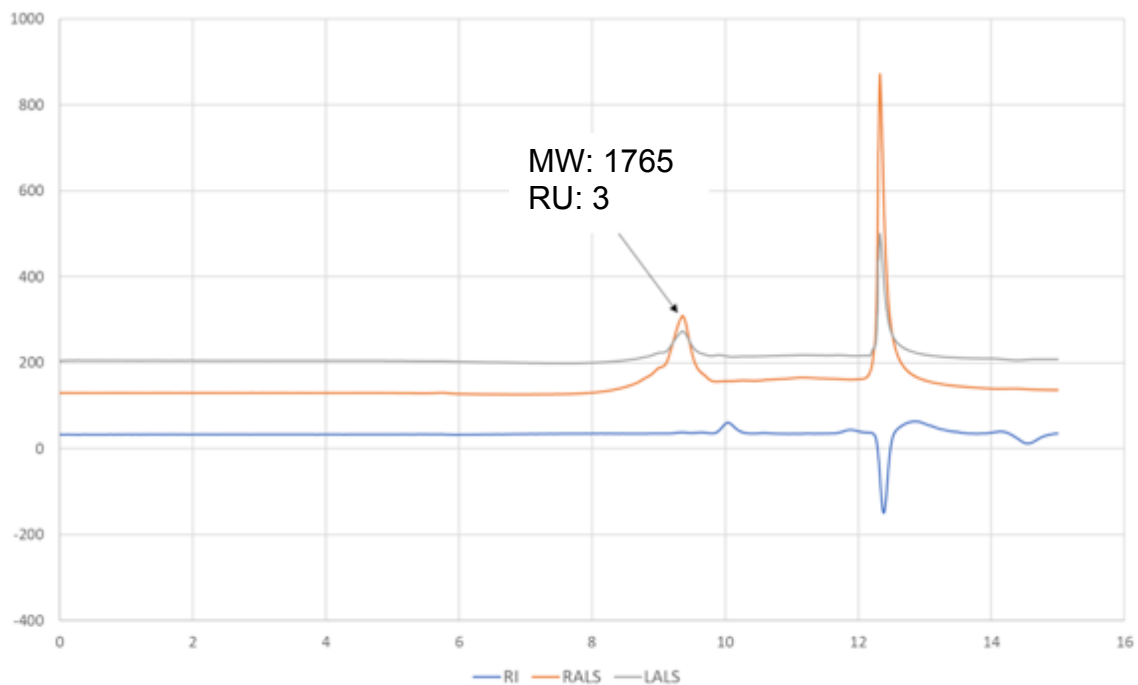
Figure 28. Gel permeation chromatogram of PBEB-(OHex)$_2$ in chloroform

While these numbers may be particularly low, it must be remembered that this accounts only for the chloroform-soluble fraction that was able to pass through the PTFE filter. Prior to filtration the polymer solution was a bright, opaque red with visible particulates; filtration caused it to become a pale, transparent orange.

Another aliquot was taken from the fully reduced polymer solution and drop-cast onto an ITO glass slide. After allowing it to air dry, a UV-Vis spectrum was taken as shown in Figure 29 (top) and converted into energy (bottom). The band gap was determined to be ca. 2.1 eV, which is very close to the value determined using spectroelectrochemistry for electrochemically prepared polymer (1.9 eV).
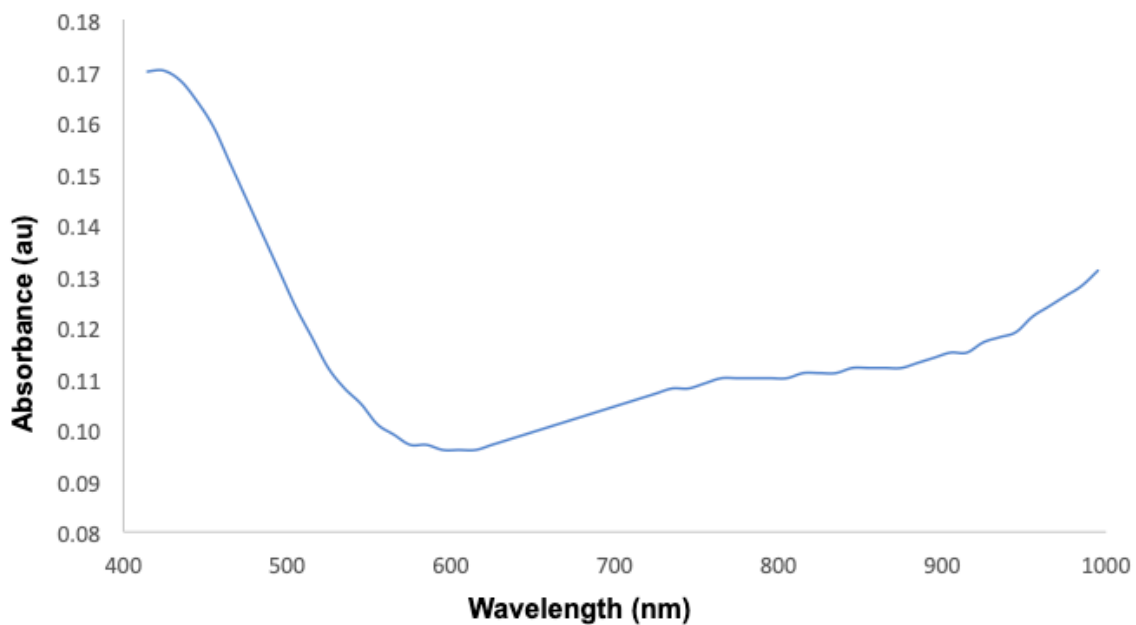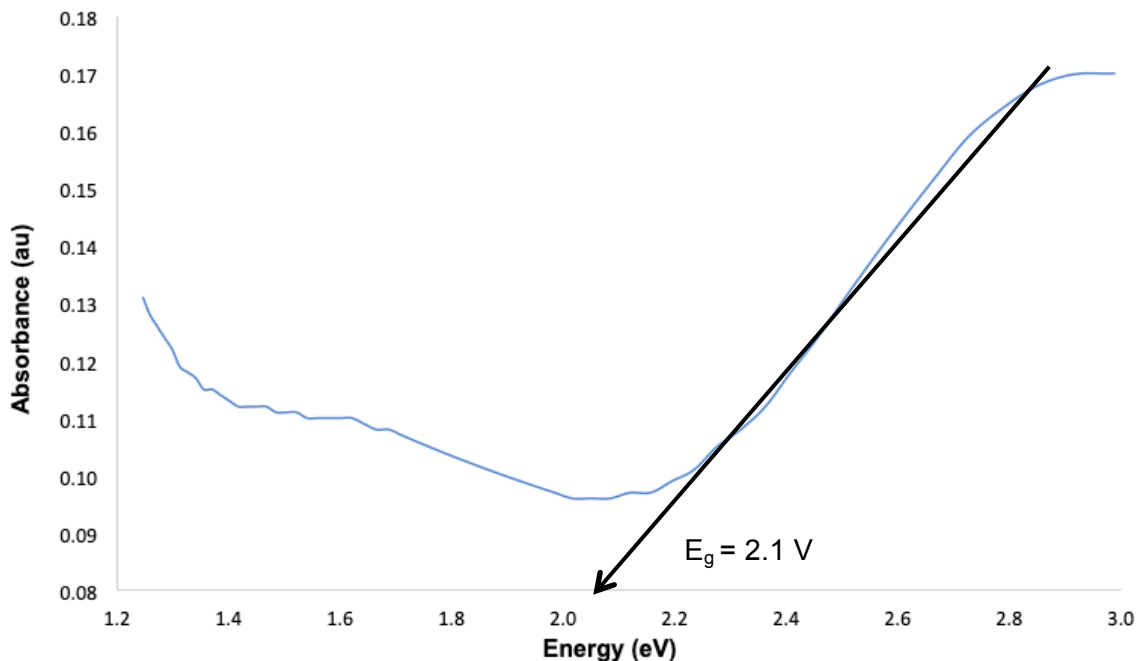
Figure 29. UV-vis of dropcast chemically prepared PBEB-(OHex)$_2$ in wavelength (top) and in energy (bottom)

2.3.4 BEB-(OEs)$_2$ Monomer and Polymer Electrochemistry

To study the electrochemistry of the monomer BEB-(OEs)$_2$, a 0.01 M monomer solution in 0.1 M TBAP/CH$_3$CN electrolyte solution was prepared. Electrochemical polymerization of BEB-(OEs)$_2$ was then accomplished using a 0.01 M monomer solution in 0.1 M TBAP in CH$_3$CN at 100 mV/s for 5 cycles. The monomer was cycled from -1.25 V to +0.90 V vs Ag/Ag$^+$ on a platinum button working electrode. Onset of monomer oxidation (E$_{on,m}$) was observed at 0.4 V with a peak (E$_{p,m}$) at 0.8 V as shown in Figure 30. With each subsequent scan the current response increased, indicating the amount of polymer on the electrode was increasing.
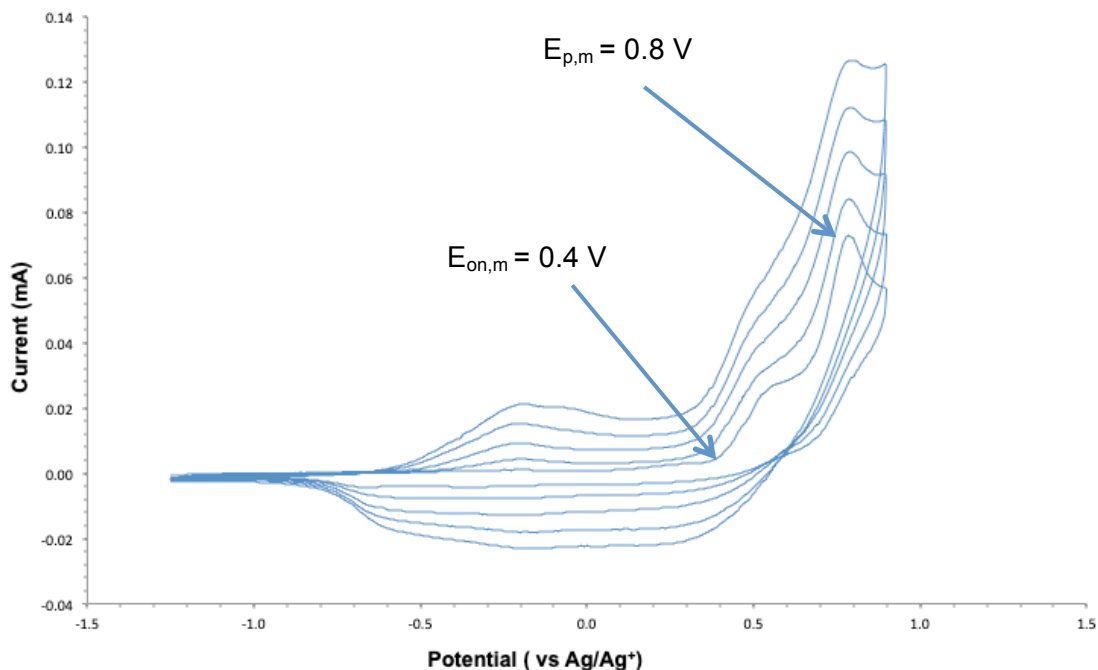
Figure 30. Electrochemical polymerization of 0.01 M BEB-(OEs)$_2$ in 0.1M TBAP in CH$_3$CN at 100 mV/s for 5 cycles from -1.25 to +0.90 V. WE: Pt button

The polymer was then rinsed with electrolyte solution and transferred to a monomer-free solution of 0.1 M TBAP in CH$_3$CN to study the electrochemistry as a function of scan rate. The polymer was first cycled two times to ensure that there was only polymer left on the WE. It was then cycled at 50, 100, 200, 300, 400, and 500 mV/s from -1.15 to +0.90 V (Figure 31). As shown on Figure 32 there is a linear relationship between the peak current and scan rate, indicating that the polymer is well adhered to the electrode.
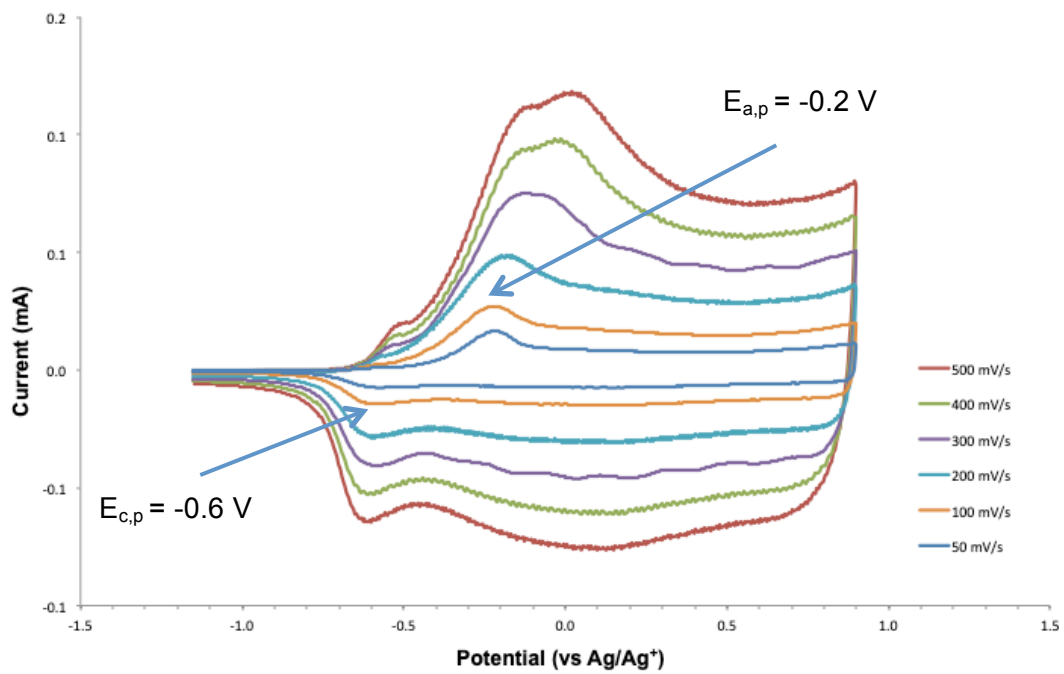
Figure 31. Cyclic voltammetry of PBEB-(OEs)$_2$ in 0.1 M TBAP in CH$_3$CN at 50, 100, 200, 300, 400, 500 mV/s from -1.25 to +0.90 V. WE: Pt button
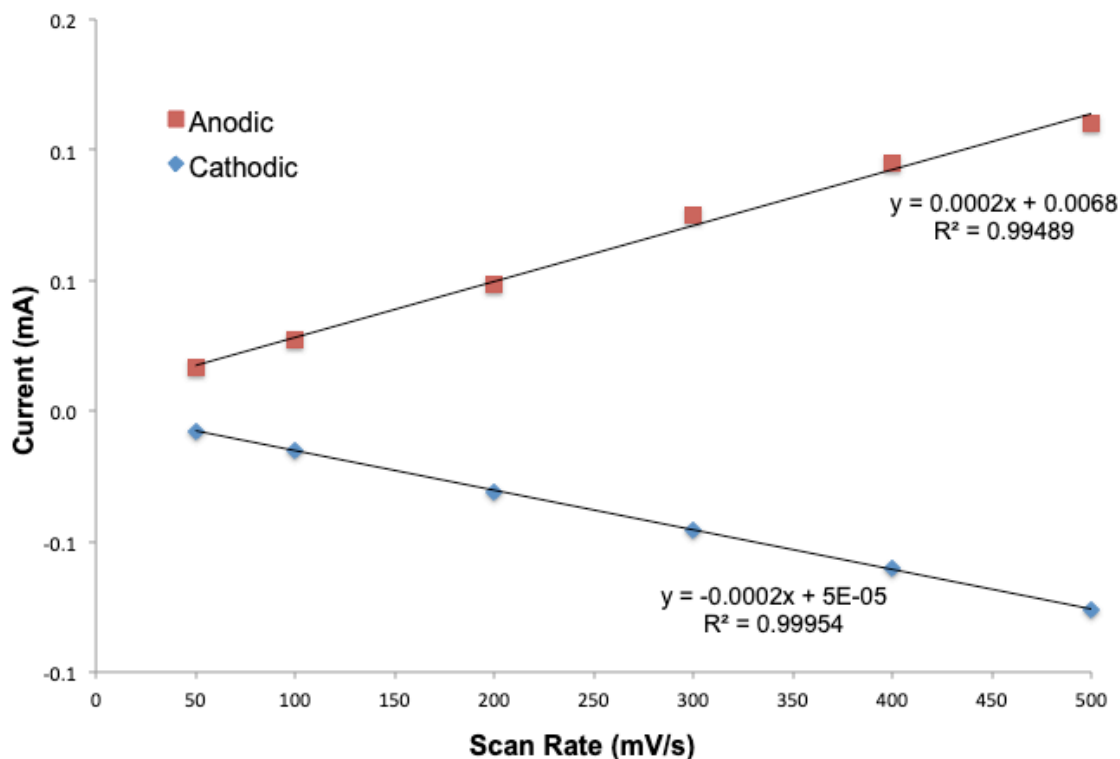
Figure 32. Peak current versus scan rate dependence of PBEB-(OEs)$_2$ in 0.1 M TBAP in CH$_3$CN

Lamentably the electrochemistry of BEB-(OEs)$_2$ depleted all of our stores of the compound preventing any further experiments including spectroelectrochemistry. However, the band gap of PBEB-(OEs)$_2$ has been previously determined. [52]

2.3.5 Analysis

As discussed in Section 1.5, the oxidation potential of extended conjugation monomers can be manipulated through the use of substituents. As shown in Table 3, 1,4-bis[2-thienyl]-benzene (BTB), first reported by Reynolds *et al.* [59], has an E$_{on,m}$ of +1.7 V. Meanwhile the EDOT derivative, 1,4-bis[2-(3,4-ethylenedioxy)thienyl]-benzene (BEB), reported by Sotzing *et al.* [60], has an E$_{on,m}$ of +0.61 V and an E$_{p,m}$ of +0.65 V. This

49

demonstrates that the inclusion of the ethylenedioxy moiety drastically decreases the oxidation potential of the overall system, proving that substituent changes in the backbone will greatly alter the polymer's properties. Addition of strong electron-withdrawing pendant groups like fluorine (BEB-F$_2$) [47] will result in a higher oxidation potential as shown below. Irvin *et al.* [6] synthesized several BEB-alkoxy derivatives, including 1,4-bis[2-(3,4-ethylenedioxy)thienyl]-2,5-heptyloxybenzene (BEB-(OHept)$_2$). With an E$_{on,m}$ of +0.3 V and an E$_{p,m}$ of +0.5 V, its oxidation potential is lower than that of BEB-F$_2$ but has the same band gap of 1.9 eV.

For the novel monomers/polymers, the onset of monomer polymerization for BEB-(OHex)$_2$ was very close to that of its ester counterpart BEB-(OEs)$_2$, 0.42 V and 0.38 V respectively. The peak monomer oxidation on the other hand was somewhat lower, 0.56 V compared to 0.8 V. The difference between the anodic peaks (E$_{a,p}$) for BEB-(OHex)$_2$ and BEB-(OEs)$_2$ was minimal, -0.3 V vs. -0.2 V as was that between the cathodic peaks (E$_{c,p}$), -0.5 V vs. -0.6 V. Any differences between the electrochemistry of the two compounds can be attributed to the presence of the ester moiety in the pendant group, as the two compounds are virtually identical otherwise. Spectroelectrochemistry was not carried out for BEB-(OEs)$_2$ due to insufficient quantity of monomer, but the band gap previously reported by Cantu *et al.* [49] is similar to that of BEB-(OHex)$_2$ at 1.8 eV. Compared to BEB-(OHept)$_2$, the differences are also negligible.

Table 3. Comparison of electrochemical properties of different substituents (V vs. Ag/Ag$^+$)

Monomer	$E_{on,m}$	$E_{p,m}$	$E_{a,p}$	$E_{c,p}$	E_g (eV)
BTB [59]	+1.2	+0.9	>1.0	+0.8	2.2
BEB [60]	+0.6	+0.7	N/A	N/A	1.8
BEB-F$_2$ [47]	+0.8	+0.9	+0.7	+0.5	1.9
	+0.3	+0.5	-0.3	-0.4	1.9
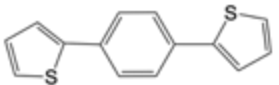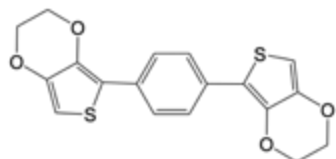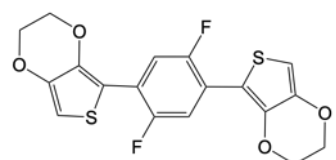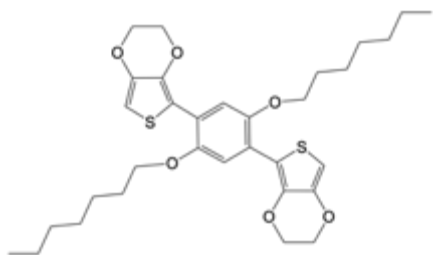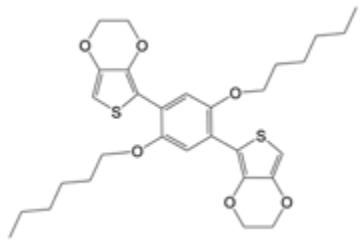
BEB-(OHept)$_2$ [6]					
BEB-(OHex)$_2$	+0.4	+0.6	-0.3	-0.5	1.9
BEB-(OEs)$_2$	+0.4	+0.8	-0.2	-0.6	1.8 [52]
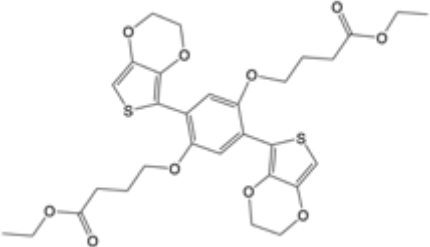
2.3.6 Electrochemical Polymerization of 1,3,6,8-tetrakis[(E)-2-(3,4-ethylenedioxythien-2-yl)vinyl]pyrene (PyVEDOT)

Electrochemical analysis was attempted to study PyVEDOT and determine its potential as a low band gap material. While a 0.01 M monomer in 0.1 M electrolyte solution is typically made for electrochemical studies, the poor solubility of PyVEDOT required a lower concentration. Due to its poor solubility, PyVEDOT was not expected to fully dissolve in any solvent but was predicted it could form a suspension with a compatible solvent. Solvent studies with acetonitrile during synthesis proved it to be a suitable enough solvent for the suspension. The solution was sonicated for 10 minutes to

promote suspension, a significant amount of unsuspended monomer remained (Figure 33).

Figure 33. A partially suspended 0.005 M PyVEDOT solution in 0.1 M TBAP in CH$_3$CN electrolyte solution

The electrochemistry experiment was set up as shown in Figure 10, with a platinum button as the reference electrode, a platinum flag as the counter electrode, and an Ag/Ag$^+$ reference electrode. Experiment parameters were set similar to those used for BEB-(OHex)$_2$, cycling from -1.2 V to +1.2 V for 5 cycles (Figure 34). While the small bump seen at ca 0.5 V seemed to indicate onset of oxidation, no polymer deposition was observed on the working electrode, probably due to poor monomer solubility. In an effort to encourage deposition, monomer electrochemistry was performed at slower scan rates over an extended number of cycles.
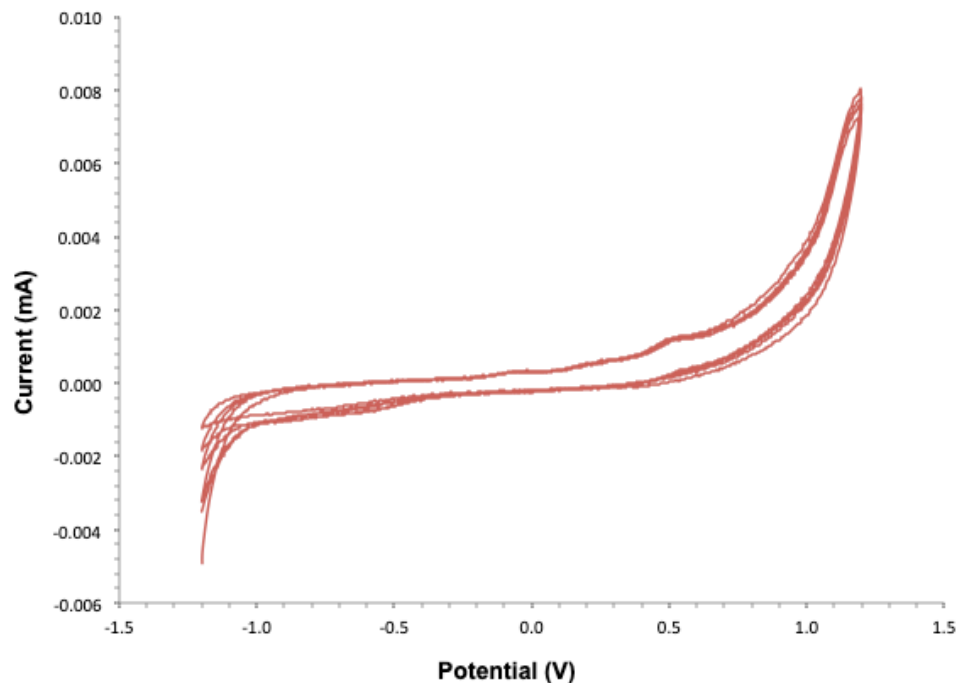
Figure 34. Electrochemical polymerization attempt of 0.005 M PyVEDOT in 0.1 M TBAP in CH$_3$CN at 10 mV/s for 10 cycles from -1.2 to +1.2 V. WE: Pt button

The monomer system was run for 500 cycles at a scan rate of 10 mV/s from -1.2 V to +1.2 V (Figure 35). Due to the time length of the experiment, the system was monitored several times a day to replenish any solvent that may have evaporated. The outlier peak seen at about +0.9 V likely occurred during the addition of extra solvent, which may have interfered with the scan. The sharp peak seen at ca. -1.2 V increased with each successive scan, denoting an irreversible reduction. Meanwhile at ca. 0.45 V a small bump can be observed, which may indicate the onset of monomer oxidation. However, there was no polymer deposition observed on the working electrode, which may have been due to poor solubility or the polymer structure being incompatible with the platinum working electrode. To determine if the working electrode material was the

issue, polymerization was next attempted using a carbon working electrode (Figure 36).
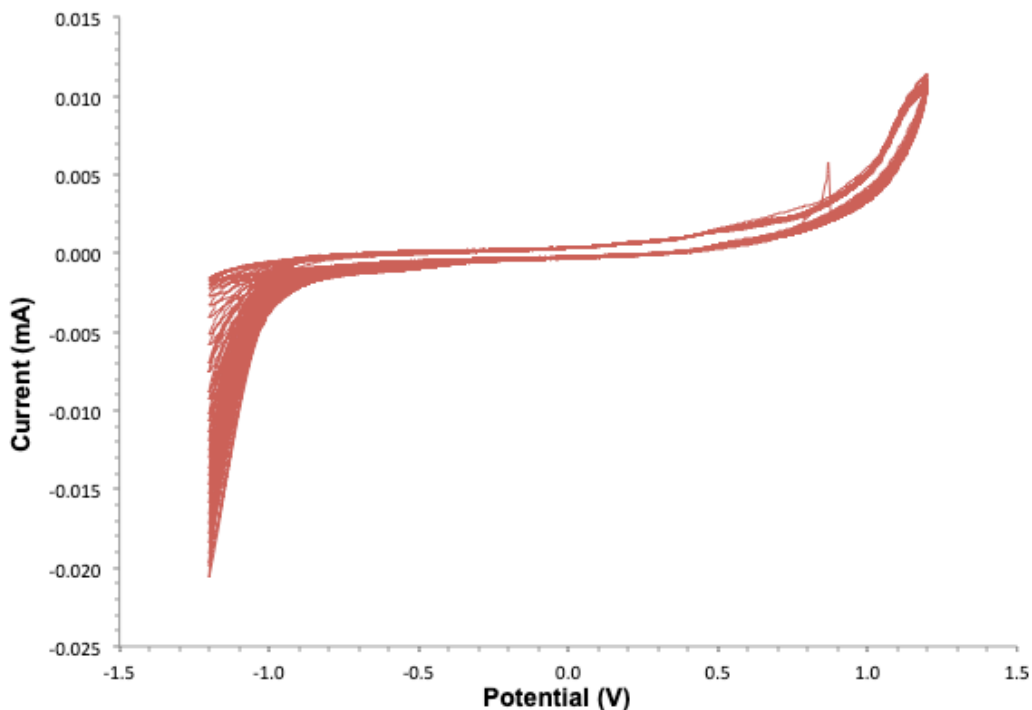
Figure 35. Electrochemical polymerization attempt of 0.005 M PyVEDOT in 0.1 M
TBAP in CH$_3$CN at 10 mV/s for 500 cycles from -1.2 to +1.2 V. WE: Pt button

The parameters for this next experiment were unchanged, with the exception of

the carbon electrode as the working electrode instead of the platinum electrode (Figure

33). After 500 cycles ran for over 2 days, no polymer deposition was observed on the

working electrode. Analysis of the cyclic voltammetry shows that the current peaked

early on in the experiment, after which it just kept on decreasing. It is unclear there was

ever any monomer oxidation, likely due to poor solubility. However, it is suspected that

the process seen above is that of n-doping, that is the reversible reduction of the neutral

polymer. It is hypothesized that the reduced polymer reacted with the ambient water and

air, resulting in degradation. Performing the electrochemistry in an inert atmosphere such as in a glove box would prevent this. Unfortunately, these experiments depleted our stores of PyVEDOT and additional experiments were not possible.
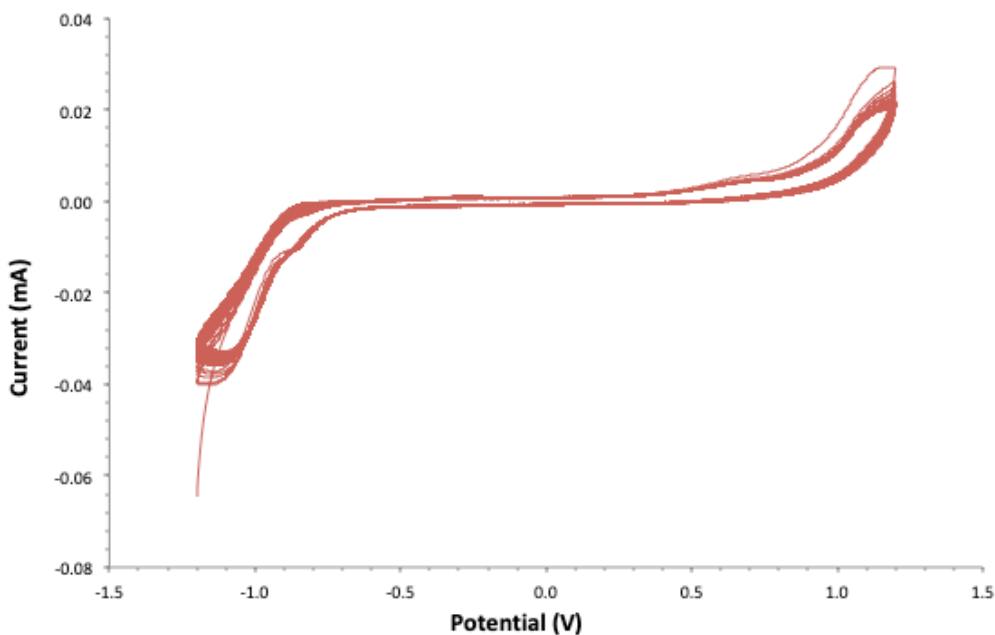
Figure 36. Electrochemical polymerization attempt of 0.05 M PyVEDOT in 0.1 M TBAP in CH$_3$CN at 10 mV/s for 500 cycles from -1.2 to +1.2 V. WE: Carbon button

2.4 Conclusions

Two similar compounds, BEB-(OHex)$_2$ and BEB-(OEs)$_2$ were synthesized in order to study the impact of a small modification on the alkyl substituent. While BEB-(OHex)$_2$ was synthesized via Negishi coupling, this same method proved unreliable for the synthesis of BEB-(OEs)$_2$. Stille coupling on the other hand was a successful path in

producing the monomer. Electrochemically the ester group had a small impact on the electrochemistry, with the biggest difference in the peak monomer oxidation (BEB-(OHex)$_2$ 0.56 V vs. BEB-(OEs)$_2$ 0.8 V). While there was not enough BEB-(OEs)$_2$ monomer left to conduct spectroelectrochemical experiments, literature[49] showed the band gap to be marginally lower than that of BEB-(OHex)$_2$ (1.8 eV vs 1.9 eV respectively). The addition of the ester group significantly affected the polymer's solubility, showing an increased compatibility with CH$_3$CN. Multiple attempts to electrochemically polymerize PyVEDOT proved unfruitful despite decreasing the monomer concentration and running the experiment for several days.

3. NON-EXTENDED CONJUGATION MONOMERS

3.1 Background

As discussed in Chapter 1, electroactive polymers have attracted attention not only due to their conductivity, but also because of the relative ease with which they can be modified. If a monomer is adequately functionalized (either with good leaving groups or click chemistry compatible groups), then a variety of reactions can be performed to modify the monomer. A prime example is 3,3-bis(bromomethyl)-3,4-dihydro-2*H*-thieno[3,4-*b*][1,4]dioxepine, (ProDOT-Br$_2$), which is synthesized via Williamson transetherification of 3,4-dimethoxythiophene with the dibromo diol in the presence o p=toluene sulfonic acid as a catalyst, as shown in Figure 37. Godeau *et al.*[61] used ProDOT-Br$_2$ as a basis for the synthesis of various monomers with distinct properties. Even though the monomer has been used extensively as a step to create other monomers, its electrochemical polymerization has not been reported previously. If ProDOT-Br$_2$ could be polymerized, subsequent chemical modifications of the polymer film could be performed, resulting in a modified polymer film that could then be used for a variety of applications such as sensors.
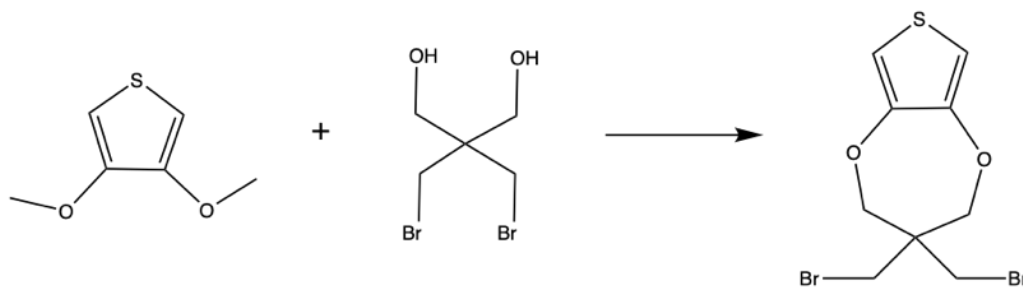
Figure 37. Synthesis of ProDOT-Br$_2$ via Williamson transetherification

As discussed in Ch. 1, PEDOT has been studied widely as an electroactive polymer due to its relatively low band gap and its commercial availability. However, an issue often encountered with these kinds of systems is solubility. Solubility becomes an important parameter when considering processability and scalability of the systems. Attaching a functional group that increases solubility without adversely affecting band gap or other electrochemical properties would result in polymers that could be used in a wide range of applications. Therefore, a dodecyl-functionalized EDOT (EDOT-C_{12}) was synthesized and polymerized electrochemically to determine the effects on solubility and band gap by an alkyl chain on the polymer's backbone. EDOT-C_{12} was chosen because 1,2-tetradecanediol is one of the few long chain commercially available 1,2-alkanediols, allowing the monomer to be prepared in only one step (Figure 38).
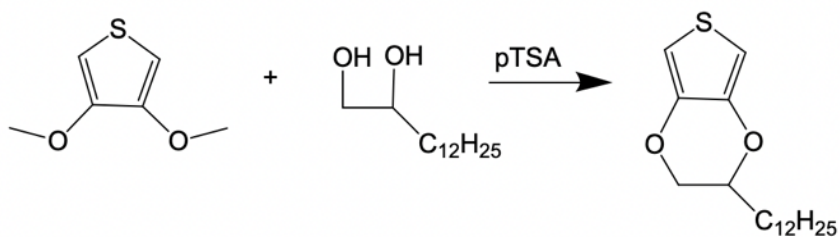
Figure 38. Synthesis of EDOT-C_{12} via Williamson transetherification

3.2 Experimental

3.2.1 Materials

Acetonitrile (CH_3CN, anhydrous 99.8%) was purchased from Sigma Aldrich and refluxed for 2 days. Tetrabutylammonium perchlorate (TBAP) was purchased from Alfa

Aesar, recrystallized from ethyl acetate and dried in a vacuum oven for 24 hours prior to use. Tetraethylammonium tetrafluoroborate (TEABF$_4$) was purchased from TCI and recrystallized from methanol prior to use. Dichloromethane (DCM) was purchased from VWR and used as received. 1,3-Tetradecanediol was purchased from Aldrich and used as received. p-Toluenesulfonic acid was purchased from Acros. Toluene and pentane were purchased from Fisher Scientific and used as received. 3,4-Dimethoxythiophene was purchased from Ark Pharm and used as received.

ProDOT-(CH$_2$Br)$_2$ was synthesized by Kelli Burke according to procedures reported by Reeves et al. [62]

3.2.2 Synthesis of EDOT-C$_{12}$

EDOT-C$_{12}$ was prepared using a method adapted from a procedure reported by Reeves et al. [62] A 3-neck round bottom flask was equipped with two gas inlet adapters, a high efficiency condenser, and a stir bar. The reaction set up was flame dried under vacuum and backfilled with argon. 1,2-Tetradecanediol (4.39 g, 0.019 mol) and p-toluenesulfonic acid (PTSA, 0.329 g, 0.001733 mol) were added to the round bottom flask. Toluene (115 mL) was transferred into the flask using a cannula and was left stirring for one and a half hours while blanketed under argon. 3,4-Dimethoxythiophene (2.07 mL, 0.01733 mol) was added via syringe. The reaction was heated to 120 °C, covered in glass wool, and monitored using TLC. Upon completion (72 hours) the reaction was then washed with ultrapure water (18 MΩ), and the organic layer was extracted with DCM and dried over magnesium sulfate. After vacuum filtration the filtrate was concentrated under reduced pressure. The viscous dark brown liquid was purified via a silica gel column with pentane as the eluent. The last 35 fractions were

collected and concentrated under reduced pressure and dried in a vacuum oven for 24 hours (56% yield) to yield a yellow-orange solid. MP 34 – 36 °C. ^{1}H NMR (CD$_2$Cl$_2$) δ 6.29 (s, 2 H), 4.1 (d, 2H), 3.8 (d, 1H), 1.26 (s, 11H), 0.86 (t, 1H). ^{13}C NMR (CD$_2$Cl$_2$) δ 142.97 (1 C), 142.48 (1 C), 99.59 (1 C), 74.49 (1 C), 69.11 (1 C), 32.51 (1 C), 30.21 (8 C), 25.55 (1 C), 23.27 (1 C), 14.46 (1 C).

3.2.3 Instrumentation

All cyclic voltammetry experiments were accomplished using a Pine WaveNow potentiostat. All chronoamperometry experiments were performed using a Gamry Reference 600 ™ potentiostat. Electrochemistry was performed in a solution of 0.01 M monomer in 0.1 M TBAP in CH$_3$CN or in 0.1M TEABF$_4$ in ultrapure water. The working electrode was either a platinum button (Bioanalytical Systems, Inc., part number MF-2013; 1.6mm diameter), a glassy carbon button (Bioanalytical Systems Inc. MF-2012, 3.0mm diameter) or an ITO coated glass slide. The counter (CE) and reference (RE) electrodes were a platinum flag and a Ag/Ag$^+$ system, respectively. Cycling of the polymer films occurred in monomer free solution of 0.1 M TBAP in CH$_3$CN or in 0.1M TEABF$_4$ in ultrapure water.

For spectroelectrochemistry, ITO slides coated with polymer films were placed in a DI water solution with FeCl$_3$. Following absorbance measurements, the films were then reduced with hydrazine.

UV-Vis spectroelectrochemistry was carried out using a BioTek Synergy H4 Hybrid Reader.

Characterization analysis was performed using a Bruker Avance 400 MHz NMR.

^{1}H NMR analyses were performed using either deuterated chloroform or dichloromethane for 16 scans.

Molecular weight analysis was accomplished using a Viskotek GPC with a triple detector (RALS, LALS, and RI).

3.2.4 Characterization

A Ag/Ag$^+$ reference electrode system was prepared following BASi procedure. A glass body with a CoralPor ® tip was filled with 0.1 M TBAP/CH$_3$CN electrolyte solution and placed into a vial filled with electrolyte solution. After an hour the electrolyte solvent was removed, and the glass body filled with ~3 mL of 0.01 M AgNO$_3$ in 0.1 M TBAP/ CH$_3$CN. A Teflon ™ cap with silver wire was placed into the glass body.

3.3 Results and Discussion

3.3.1 ProDOT-Br$_2$

3.3.1.1 Monomer and Polymer Electrochemistry

Electropolymerization was first accomplished using a 0.01 M ProDOT-Br$_2$ monomer solution in 0.1 M TBAP/CH$_3$CN solution. Unlike BEB-(OHex)$_2$ from Chapter 2, ProDOT-Br$_2$ readily dissolved in the electrolyte solution without the use of DCM. Onset of monomer oxidation (E$_{on,m}$) can be observed at 1.05 V with an oxidation peak at 1.5 V (Figure 39). The polymer was deposited for five cycles to ensure an adequate polymer film formed. The unusual appearance of the monomer oxidation peaks is due to them not being allowed to fully form. Ideally the window would have been extended to

1.6 V or 1.7 V, but the electrolyte solution showed current responses beyond 1.5 V,

limiting the available window. During the growth process it was observed that the

polymer film was partly soluble in the solvent. This was evidenced by pieces of film

separating from the ITO slide and dissolving in the solution.
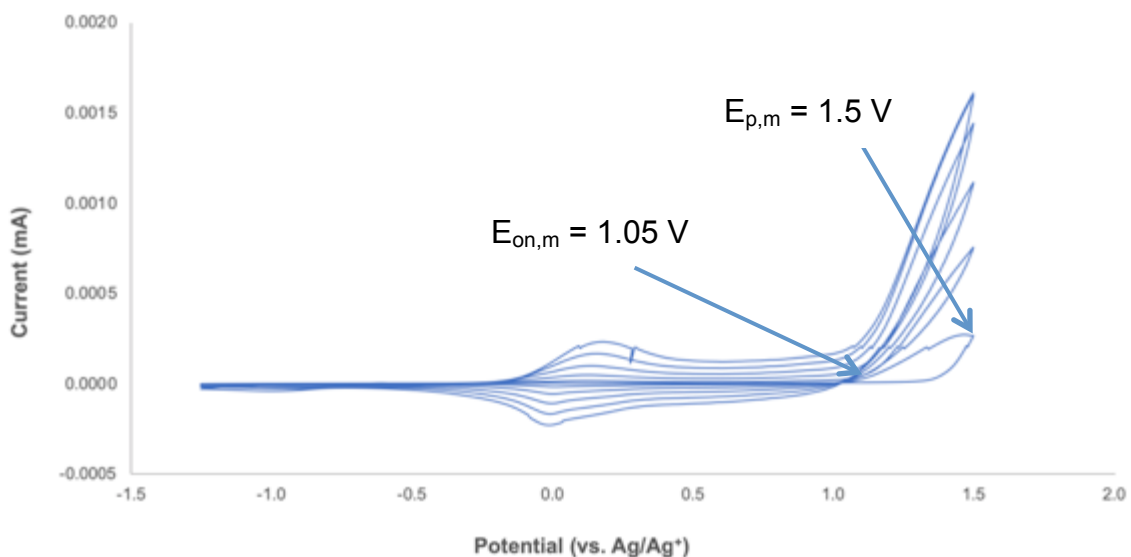
Figure 39. Electrochemical polymerization of 0.01 M ProDOT-Br$_2$ in 0.1 M TBAP in
CH$_3$CN at 100 mV/s for 5 cycles from -1.25 to +1.5 V. WE: Pt button

After the electrochemical polymerization, the polymer film was rinsed with

electrolyte solution and placed into a monomer-free electrolyte solution of 0.1 M TBAP/

CH$_3$CN. The polymer electrochemistry was then studied as a function of scan rate at rates

of 50, 100, 200, 300, 400, and 500 mV/s (Figure 40). Analysis of the peak current vs.

scan rate (Figure 36 insert) showed the relationship was not linear, indicating that the

polymer film was freely diffusing into the electrolyte solution. At the end of the scan rate

dependence experiment, it was noted that the polymer film on the working electrode was

no longer visible, supporting the conclusion that the polymer film was soluble in the

electrolyte solution. As the likelihood of an organic polymer being soluble in an aqueous

solution is low, aqueous electrochemistry was attempted next.
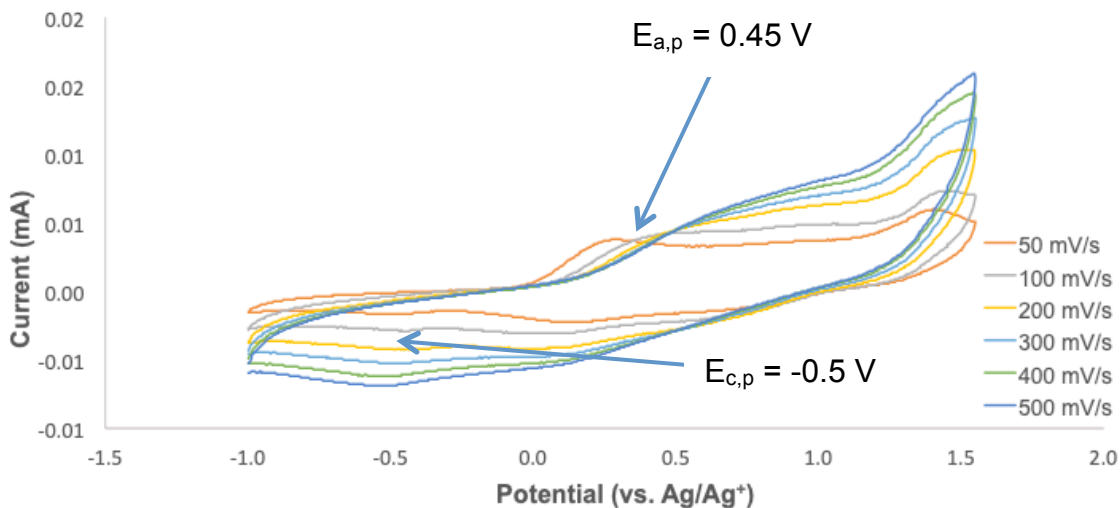
Figure 40. Cyclic voltammetry of 0.01 M PProDOT-Br$_2$ in 0.1 M TBAP in CH$_3$CN at 50,

100, 200, 300, 400, 500 mV/s from -1.0 to +1.5 V. WE: Pt button.
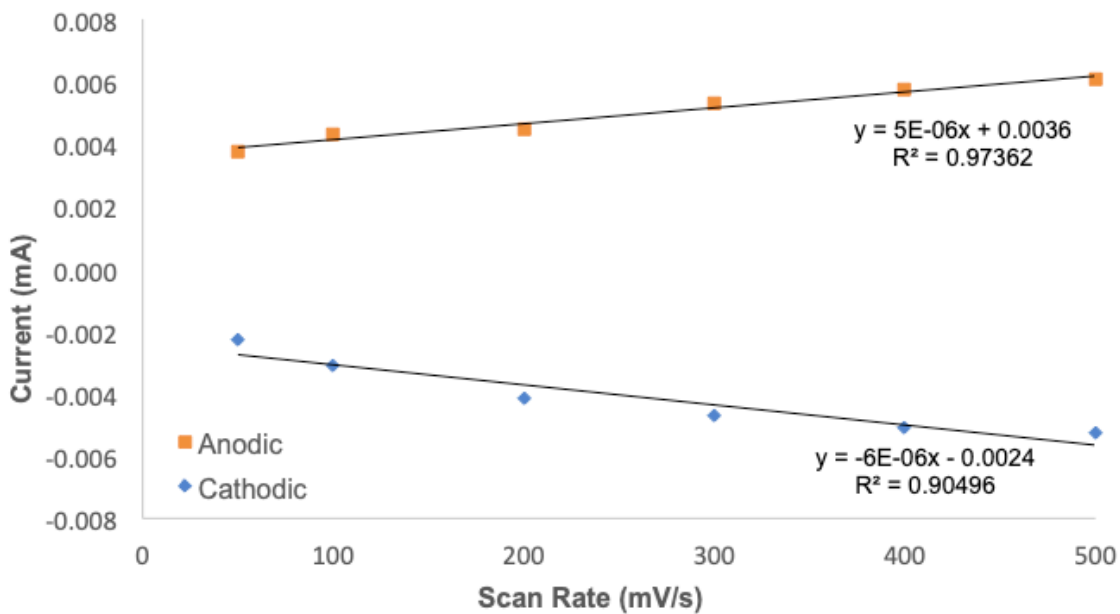
Figure 41. Peak current versus scan rate dependence of 0.01 M PProDOT-Br$_2$ in 0.1 M TBAP in CH$_3$CN

A possible complication with the electropolymerization of PProDOT-Br$_2$ was the bromine groups reacting during the process. If the bromine groups were unaffected by the polymerization then this could open up the possibility for post-electrochemistry modification of the polymer film by performing chemical reactions on the film's surface. Infrared spectroscopy (IR) was used to analyze the two solvent solutions used during electrochemistry. In theory the monomer solution used should show bromine groups in the IR (500 – 600 nm) but the monomer-free electrolyte solution (MFES) both pre- and post-electrochemistry should not if there are no side reactions the bromine participates in that are solvent soluble. As shown on Figure 42 however, there is no appreciable difference between the solutions, possibly a result of the low concentration of bromine in solution.
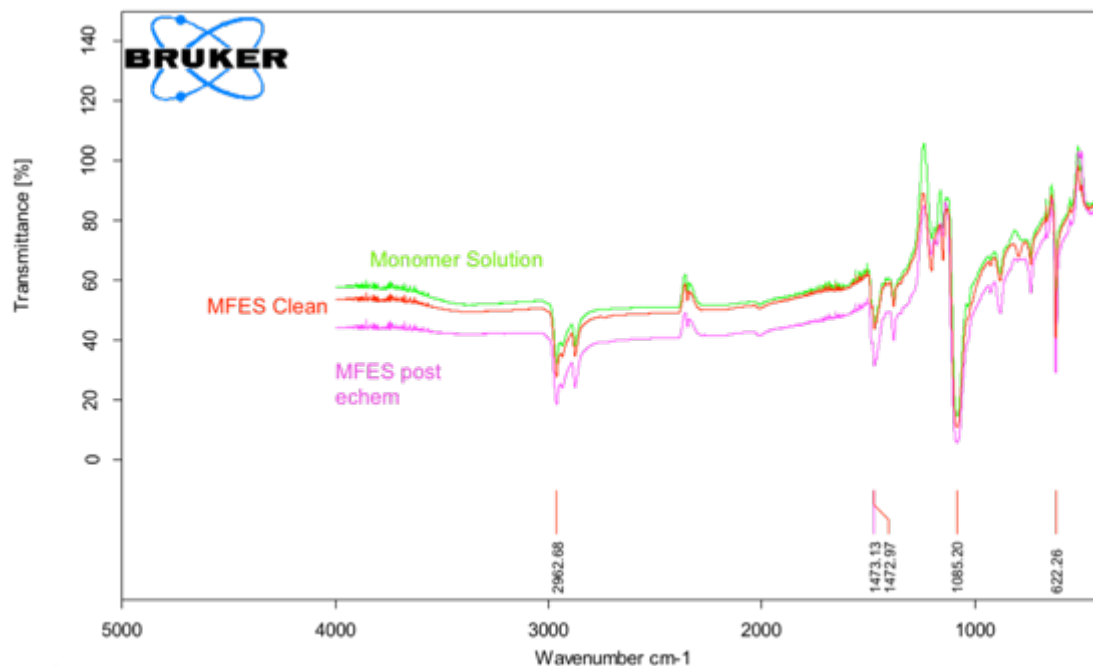
Figure 42. Infrared spectroscopy of monomer/electrolyte solution ("Monomer Solution"), pristine monomer free electrolyte solution ("MFES Clean") and monomer free electrolyte solution post electrochemistry ("MFES post echem")

For the electrochemistry the next step was to confirm that the polymer had a greater affinity for the solvent than the electrode. This was done by performing a cyclic voltammogram using a clean, bare working electrode in the same monomer-free solution that had been used previously for the scan rate dependence experiment (Figure 43). From the CV it seems appears that there is no polymer migrating to the electrode surface from the lack of change in current, which might be due to too low a concentration of the polymer in the solvent. Lamentably the solution could not be concentrated under reduced pressure due to the instability of the polymer in air. Therefore, an alternative solvent system had to be found where the polymer film would not dissolve.
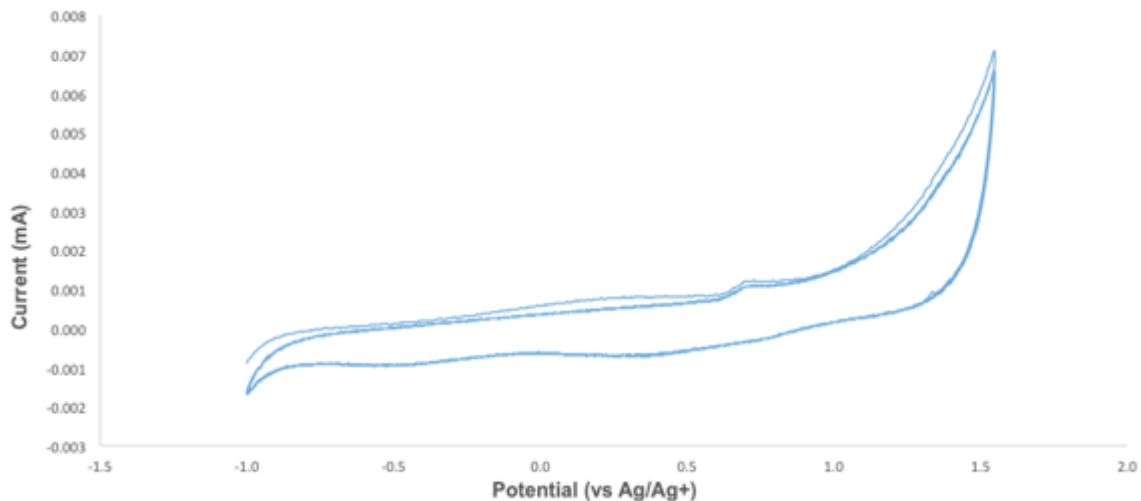
Figure 43. Bare electrode cyclic voltammetry to determine whether PProDOT-Br$_2$ had dissolved during polymerization in 0.1 M TBAP in CH$_3$CN from -1.0 to +1.55 V at 100 mV/s. Response is typical of a monomer-free electrolyte solution.

3.3.1.2 ProDOT-Br$_2$ Monomer and Polymer Aqueous Electrochemistry

Since most organic polymers are not readily soluble in water, aqueous electrochemistry was attempted for the polymerization of ProDOT-Br$_2$ using a 0.01 M monomer solution in 0.1 M TEABF$_4$/Ultrapure water. During the preparation of the solution it was noted that the monomer had low solubility in the aqueous electrolyte solution, requiring 10 minutes of sonicating to fully dissolve. Electrochemistry was first performed in the monomer-free electrolyte solution (MFES) 0.1 M TEABF$_4$/Ultrapure water to determine the voltage window. Cyclic voltammetry was performed over a wide window (-1.5 V to +1.5 V). The current response was then analyzed. The window chosen (-1.2 V to +1.0 V) showed current responses less than or equal to 30 µA. Electrochemistry was then performed to the full extent of the window, -1.2 V to +1.0 V but lamentably no redox processes were observed. This may be due to the narrow

window available in the aqueous electrolyte solvent, which is too small to initiate

polymerization.

3.3.1.3 ProDOT-Br$_2$ Chronocoulometry

Due to the difficulties in growing a film of PProDOT-Br$_2$, alternative

electrochemical polymerization methods were investigated. Chronocoulometry involves

measurement of the charge that flows through the electrode when the potential is changed

from a value in which there is no current flow to a value where a faradaic current does

flow.[63] It is a measurement of charge evolved as a function of time.[64] First, an induction

period is set for a brief period of time to allow the cell time to equilibrate. A forward step

period then begins, during which the working electrode is stepped to a predetermined

potential for a set amount of time to allow for polymer deposition. Lastly a relaxation

period where the potential of the working electrode is held at the initial potential for a

brief moment of time. In a Cottrell plot, where charge is plotted as a function of time,

charge will increase linearly as time progresses if polymer growth is occurring. As more

polymer adheres to the electrode, a greater amount of charge will flow through the

system.

Electropolymerization was accomplished using the same setup as for cyclic

voltammetry. A 5 second induction period was used followed by a 300 second forward

step period and a 15 second relaxation period. Figure 44 shows that as time progressed

the charge increased in a linear fashion, indicating polymer deposition on the platinum

button working electrode was occurring.
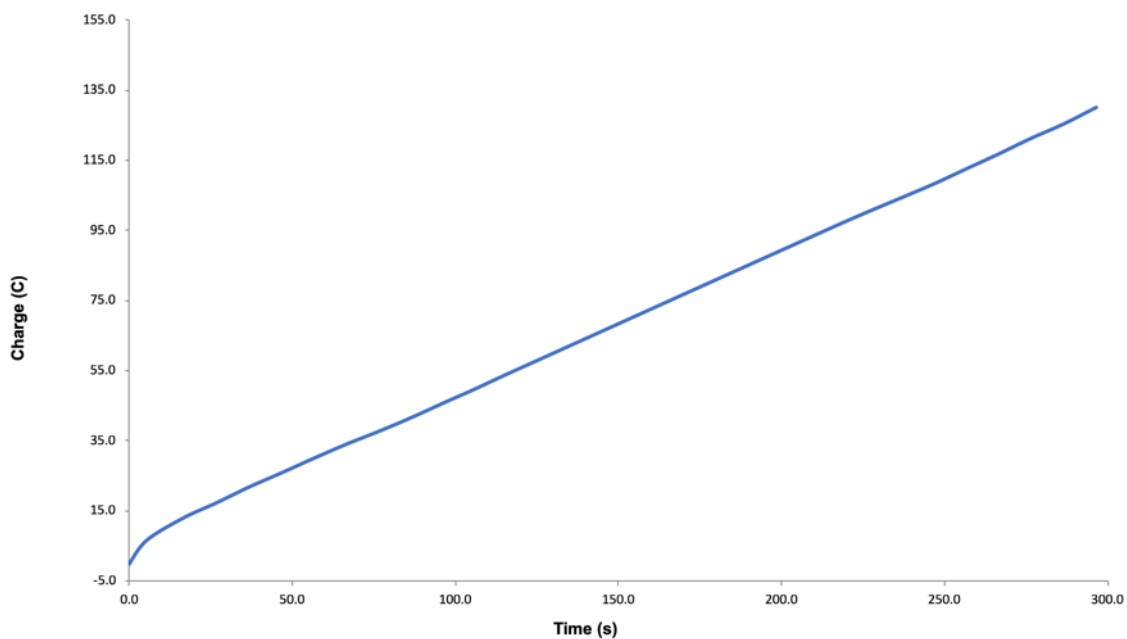
Figure 44. Cottrell plot for PProDOT-Br$_2$. Parameters: induction period: 0 V for 5 seconds, forward step period: 1.5 V for 300 seconds, relaxation period: 15 seconds.

The experiment with the same parameters was the repeated, but this time an ITO slide was used instead as the working electrode. If a PProDOT-Br$_2$ film could be deposited on the ITO slide without it dissolving back into solution, then chronocoulometry could prove a reliable way to produce easily modifiable polymer films. However, even growth at constant potential resulted in some of the polymer diffusing into the solution as seen on Figure 45.

Figure 45. PProDOT-Br$_2$ can be seen diffusing into electrolyte solution during chronocoulometry.

3.3.1.4 Chemical Oxidative Polymerization of ProDOT-Br$_2$

The average molecular weight of PProDOT-Br$_2$ was investigated using gel permeation chromatography (GPC) similar to PBEB-(OHex)$_2$ from Chapter 2. ProDOT-Br$_2$ was chemically polymerized in chloroform using iron (III) chloride as the oxidant. The precipitated, oxidized polymer was re-suspended in solution and reduced with hydrazine. An aliquot was taken from the solution and filtered through a 0.2 μm PTFE filter prior to injection into the GPC. As shown below in Figure 46, the polymer eluted out at two distinct times at minutes 8 and 10. The two different elution times might be due to left over polymer from previous runs. The calibration curve was then created using the Right-Angle Light Scattering (RALS) detector, which provided average molecular weights ranging from 6506 g/mol, which corresponds to 19 repeat units, to 625 g/mol, which is approximately 1.8 repeat units. This indicates that some residual monomer and dimer remained trapped in the polymer despite the purification process. Once again, the polymer is minimally soluble in chloroform, as such these data accounts only for the fraction that was able to dissolve and pass through the PTFE filter. The refractive index

(RI) detector was offline, hence the lack of an RI peak.
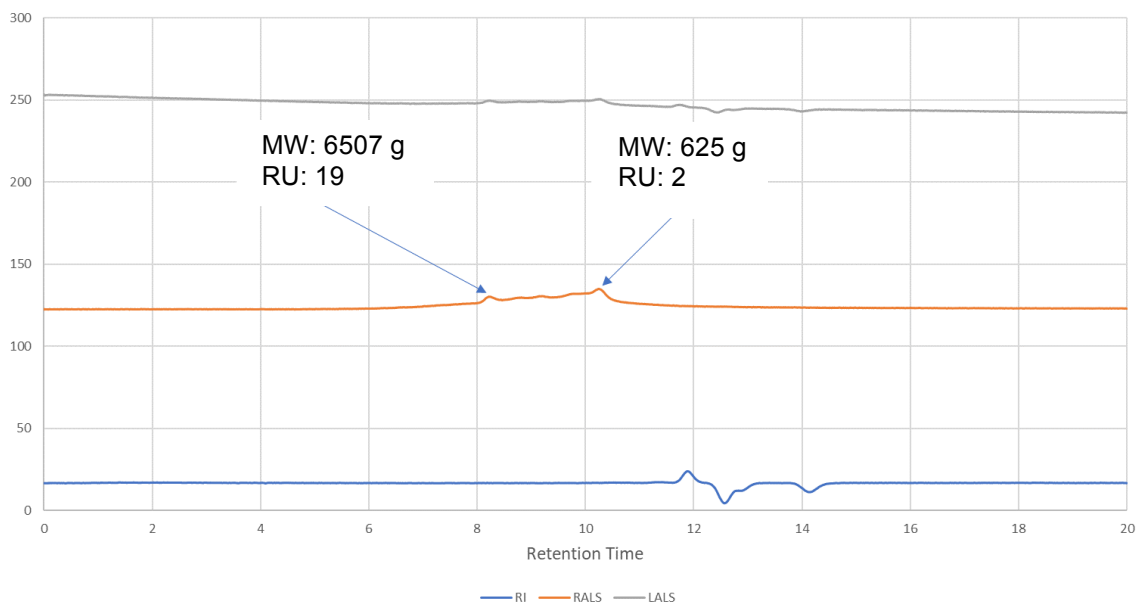
Figure 46. Gel permeation chromatography of chemically polymerized PProDOT-Br$_2$ in chloroform

Due to the reactivity of the ProDOT-Br$_2$ bromine groups, infrared spectroscopy was performed on the chemical oxidation solutions to determine if any side reactions occurred (Figure 47). An IR of the monomer was also conducted for comparison purposes. As expected, all of the solutions appeared slightly different in the spectrum, with the fingerprint region showing the highest variability. Once again, there are no significant peaks in the $500 - 600$ cm^{-1} region which would pertain to the C-Br stretch in any of the solutions.
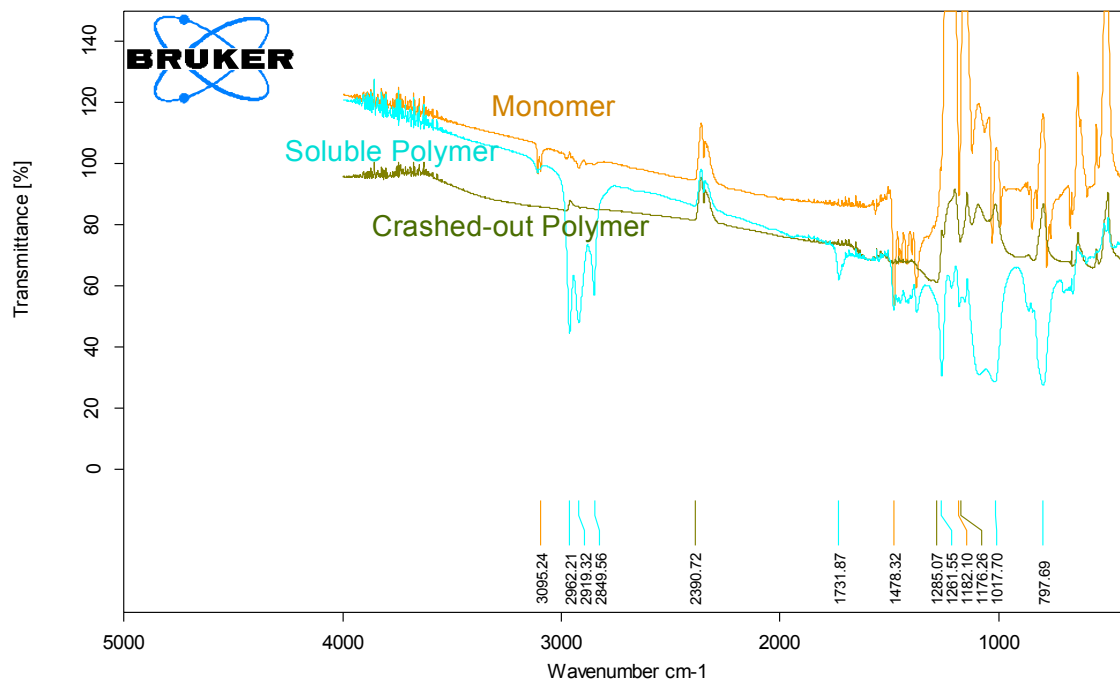
Figure 47. Infrared spectroscopy of chemical oxidation solutions of ProDOT-Br_2

3.3.2 EDOT-C_{12}

3.3.2.1 EDOT-C_{12} Monomer and Polymer Electrochemistry

To study the electrochemistry of the monomer EDOT-C_{12}, a 0.01 M monomer in 0.1 M TBAP/CH_3CN electrolyte solution was prepared. Electrochemical polymerization was then accomplished using a 0.01 M monomer solution in 0.1 M TBAP in CH_3CN at 100 mV/s. The monomer was cycled from -1.45 to +1.3 V vs Ag/Ag^+ on a platinum button working electrode. As shown on Figure 48, onset of monomer oxidation ($E_{on,m}$) was observed at 1.0 V with a peak ($E_{p,m}$) at 1.1 V. With each subsequent scan the current response increased, indicating the amount of polymer on the electrode was increasing.
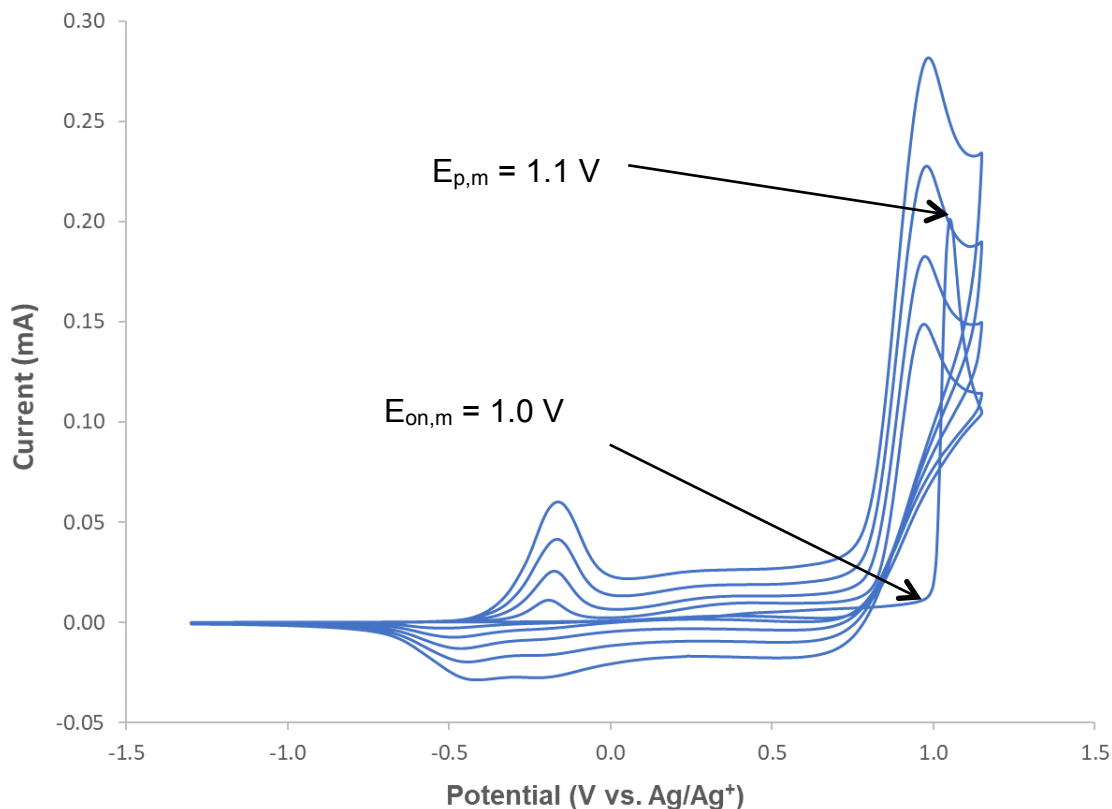
Figure 48. Electrochemical polymerization of 0.01 M EDOT-C$_{12}$ in 0.1 M TBAP in CH$_3$CN at 100 mV/s for 5 cycles from -1.45 to +1.3 V. WE: Pt button.

The polymer was then rinsed with electrolyte solution and transferred to a monomer-free solution of 0.1 M TBAP in CH$_3$CN to study its electrochemistry as a function of scan rate. The polymer was first cycled four times to ensure that there was only polymer left on the WE. It was then cycled at 50, 100, 200, 300, 400, and 500 mV/s from -1.45 to +1.2 V (Figure 49). The linear dependence of peak current on scan rate (Figure 50) indicates that the polymer was electroactive. The small deviance in the anodic peaks may be due to the polymer's mild solubility in the solvent.
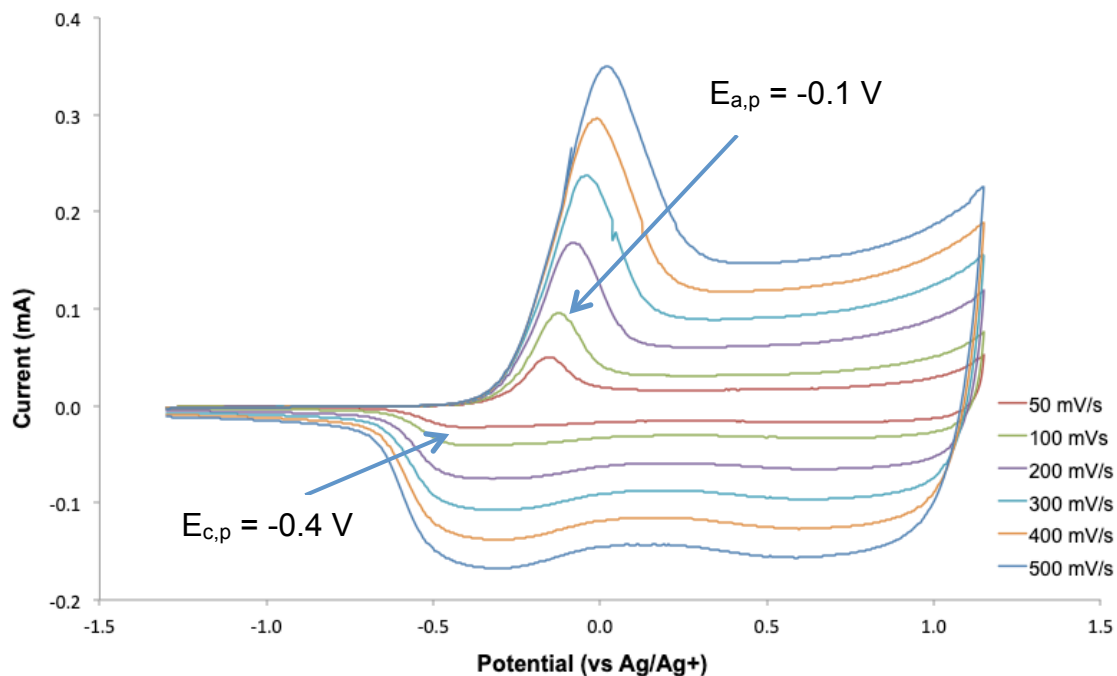
Figure 49. Cyclic voltammetry of 0.01 M PEDOT-C$_{12}$ in 0.1 M TBAP in CH$_3$CN at 50, 100, 200, 300, 400, 500 mV/s from -1.0 to +1.55 V. WE: Pt button.
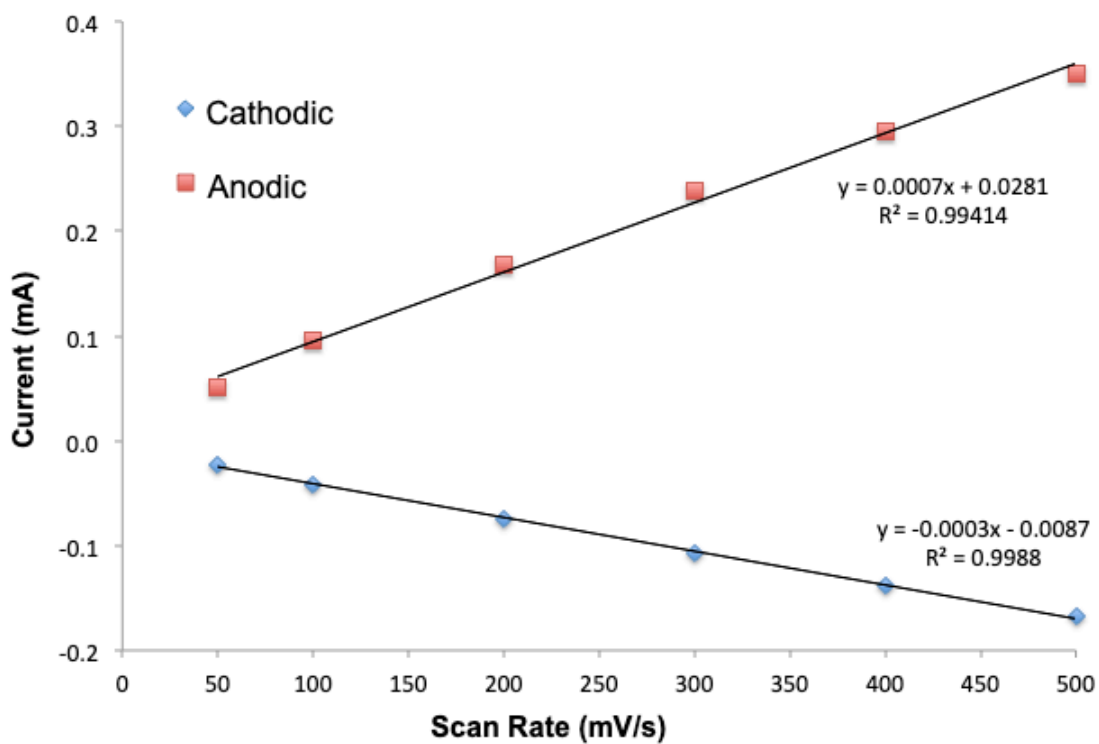
Figure 50. Peak current versus scan rate dependence of 0.01 M EDOT-C_{12} in 0.1 M

TBAP in CH_3CN

3.3.2.2 PEDOT-C_{12} Spectroelectrochemistry

PEDOT-C_{12}, like the PBEB derivatives, also undergoes a color change (from dark

blue to light blue) when changing between the reduced to the oxidized states.

Spectroelectrochemistry can be used to determine the exact potential at which the

polymer undergoes a redox change. However, the setup used with PBEB-$(OHex)_2$

requires the polymer to be in the electrolyte solution for a significant amount of time,

which is a problem since the polymer is mildly soluble in the electrolyte solvent.

Therefore, the polymer was grown at constant potential using chronocoulometry (Figure

51) as described in section 3.3.1.3.
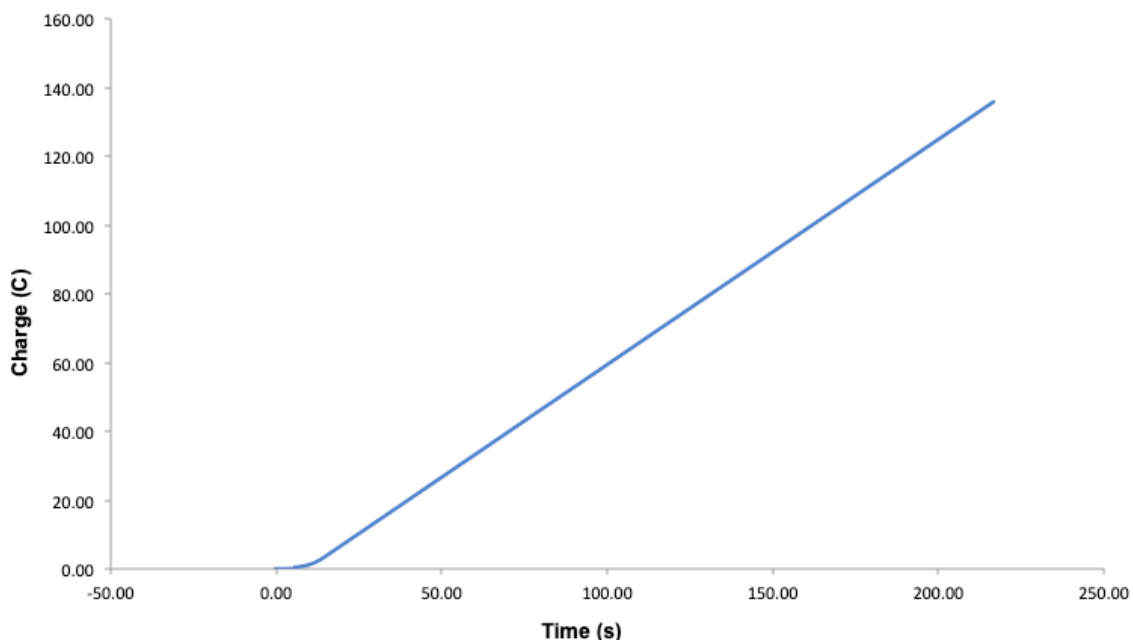
Figure 51. Cottrell plot for PEDOT-C_{12}. Parameters: induction period: 0 V for 5 seconds,

forward step period: 1.15 V for 215 seconds

A UV-vis spectrum was taken (Figure 52) after which the deep blue PEDOT-C_{12} polymer was placed into a vial containing CH_3CN and 3 drops of hydrazine. Despite the hydrogen evolution observed, indicating that the hydrazine was indeed reacting, there was no appreciable color change of the polymer film (Figure 53). A UV-Vis spectrum (Figure 45) confirmed that the polymer had not been reduced, as indicated by the rather high wavelength (low energy) at which the polymer absorbed. Since chemical reduction seemed to have failed, electrochemical reduction was then attempted by performing chronocoulometry, holding the potential at the reducing voltage (-1.35 V). Once again, no color change or change in wavelength absorbance was observed (Figure 55). The difficulties in reducing the PEDOT-C_{12} may be attributed to phase separation due to the alkyl chains, which extend from the PEDOT backbone.
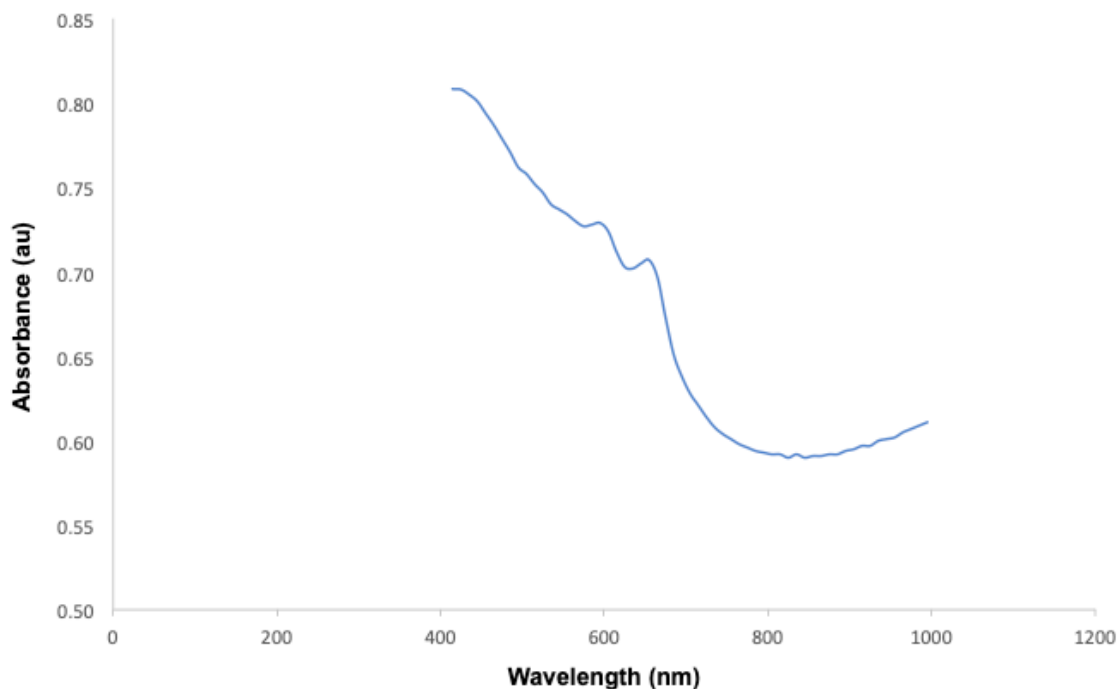
Figure 52. UV-vis spectrum of oxidatively deposited PEDOT-C_{12}
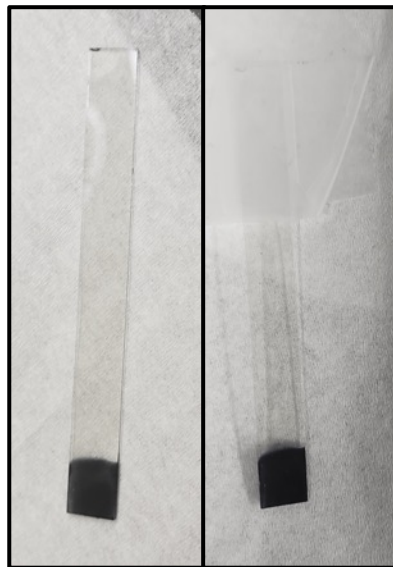
Figure 53. Oxidatively deposited polymer (left) and polymer post hydrazine (right)
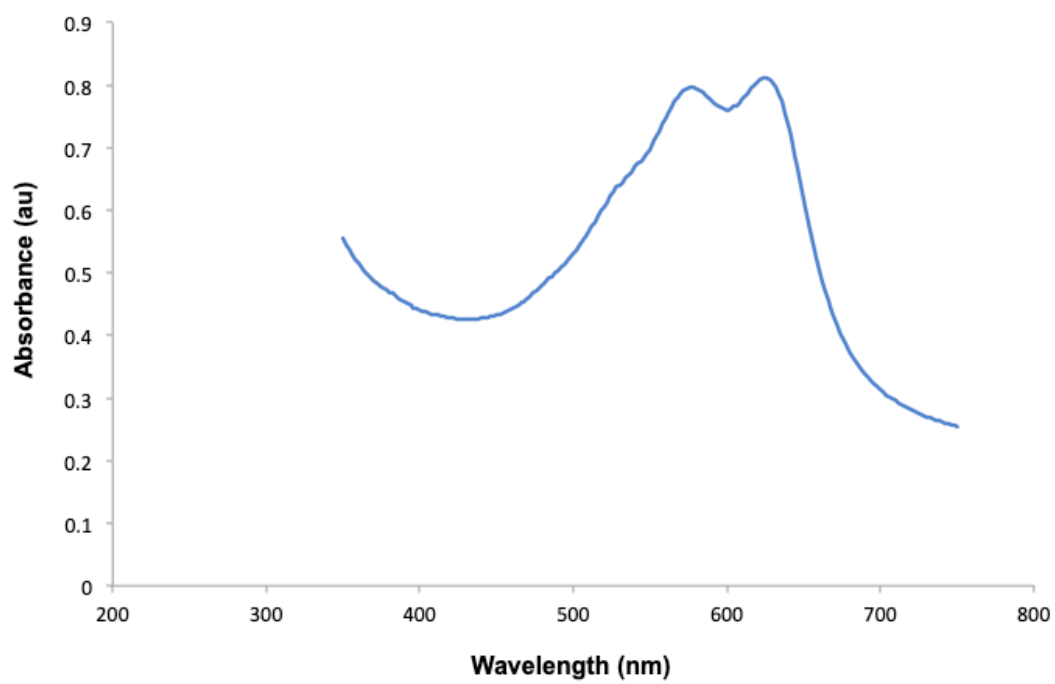
Figure 54. UV-vis spectrum of PEDOT-C$_{12}$ after attempted reduction with hydrazine
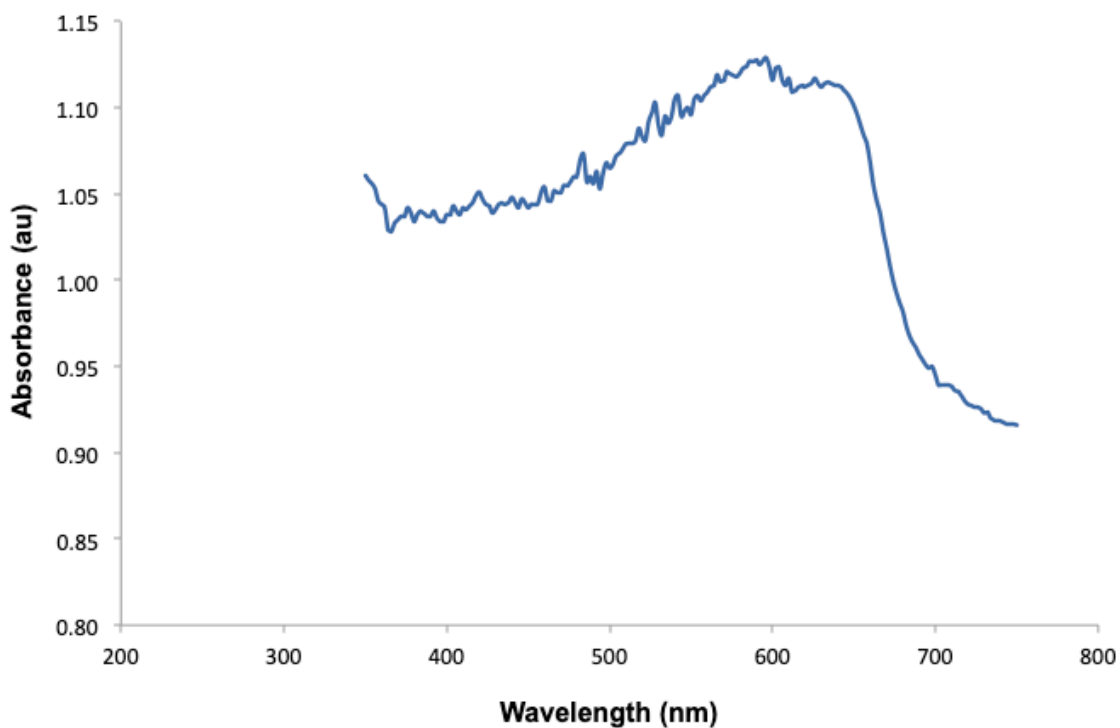
Figure 55. UV-vis spectrum of PEDOT-C$_{12}$ after attempted reduction via

chronocoulometry

Due to issues reducing the electrochemically prepared PEDOT-C$_{12}$, a sample of

chemically prepared PEDOT-C$_{12}$ was dissolved in chlorobenzene, and its UV-Vis

spectrum was acquired (Figure 56 and 57 – for nm and eV). From Figure 57, it can be

seen that this polymer has a band gap of 1.6 eV.
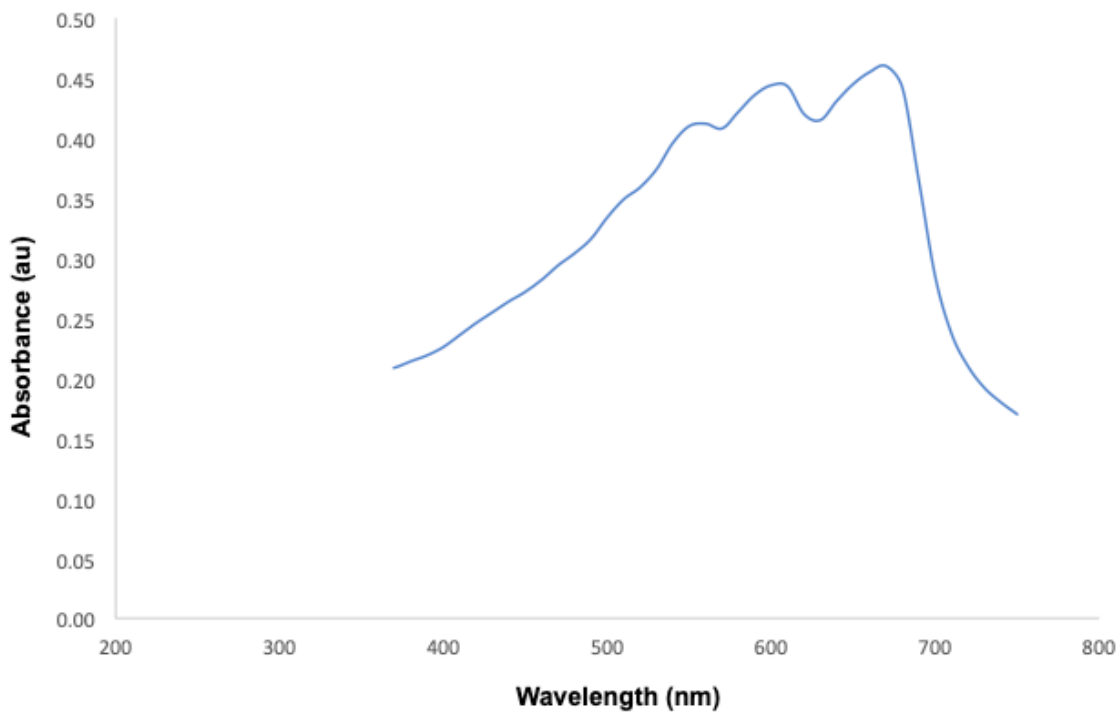
Figure 56. UV-vis spectrum of reduced PEDOT-C$_{12}$

$E_g = 1.6$ V
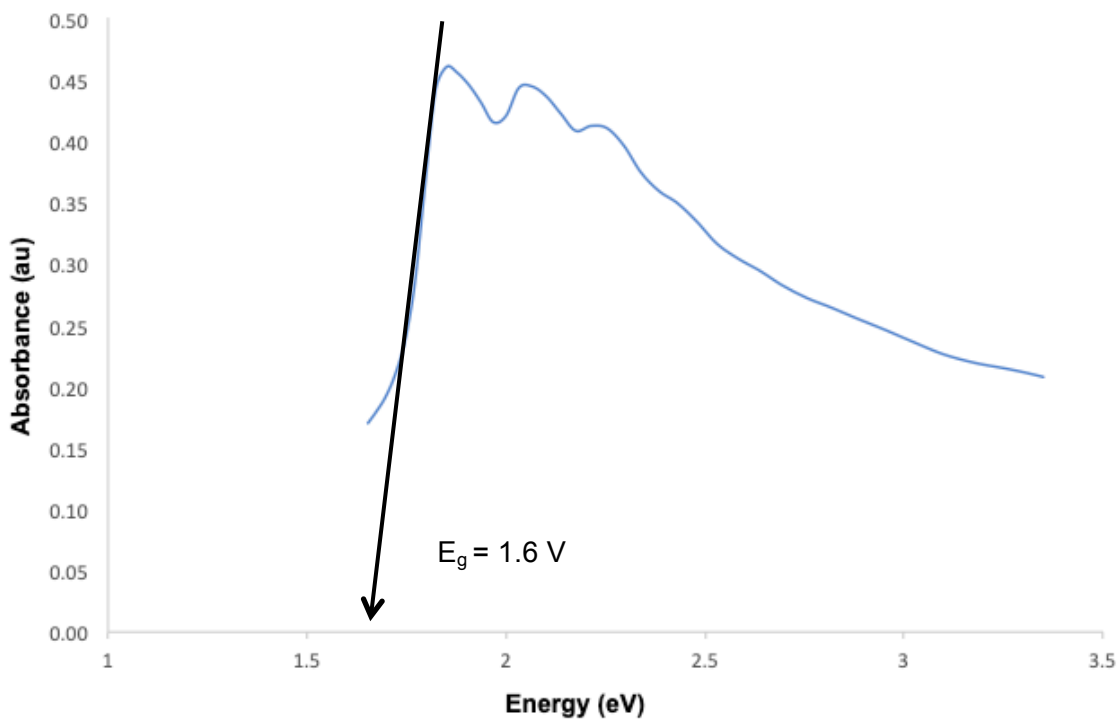
Figure 57. UV-vis spectrum of chemically prepared and reduced dropcast PEDOT-C$_{12}$

3.3.2.3 Chemical Oxidative Polymerization of PEDOT-C$_{12}$

The average molecular weight of PEDOT-C$_{12}$ was investigated using GPC. EDOT-C$_{12}$ was chemically polymerized in chloroform using iron (III) chloride as the oxidant. The precipitated polymer was then re-suspended in solution and reduced with hydrazine to yield an opaque deep blue solution. An aliquot was taken from the solution and filtered through a 0.2 μm PTFE filter prior to injection into the GPC. As shown below in Figure 56, the polymer eluted around minute 8. The calibration curve was then calibrated with respect to the Right-Angle Light Scattering (RALS) detector, which provided an average molecular weight of 4572 g/mol, which is about 15 repeat units. As with the other polymers studied, these data accounts only for the chloroform-soluble fraction that was able to pass through the PTFE filter. The refractive index (RI) detector was offline, hence the lack of an RI peak.
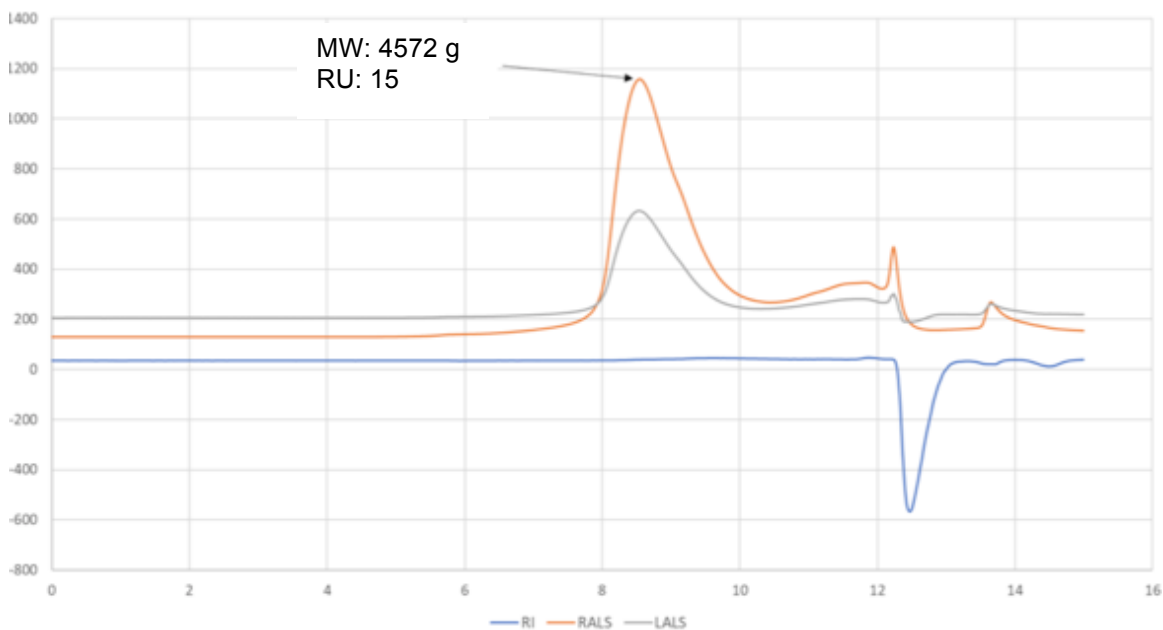
Figure 58. Gel permeation chromatography of chemically polymerized PBEB-C$_{12}$ in

chloroform

3.4 Conclusions

While ProDOT-Br$_2$ was polymerized using chemical and electrochemical means, its high solubility in organic solvents proved problematic. The polymer was soluble even in the oxidized state, making even chronocoulometry an ineffective method for growing a PProDOT-Br$_2$ film. Aqueous electrochemistry, on the other hand, provided too small a window to affect polymerization. While initially promising, creating a well-adhered electroactive polymer film of PProDOT-Br$_2$ was not possible.

The electrochemistry of EDOT-C$_{12}$ occurred as expected, albeit with minor solubility issues. However, the spectroelectrochemistry proved significantly trickier. The lack of color change after addition of hydrazine was surprising, as were the absorbance measurements, which showed no shift in the absorbance wavelength. Band gap measurements were then taken on a chemically prepared and reduced polymer, giving a band gap of 1.6 eV.

4. CONCLUSIONS

BEB-(OHex)$_2$, BEB-(OEs)$_2$, ProDOT-Br$_2$ and EDOT-C$_{12}$ were all successfully synthesized and chemically and electrochemically polymerized. Electrochemistry showed all polymers remained electroactive but only PBEB-(OHex)$_2$ and PBEB-(OEs)$_2$ were well-adhered to the electrode. PEDOT-C$_{12}$ showed minor solubility in the electrolyte while PProDOT-Br$_2$ was significantly soluble in the organic electrolyte. Attempts to create a PProDOT-Br$_2$ film using aqueous electrochemistry was impossible due to the narrow window available in the aqueous solvent. The inability to create a well-adhered, electroactive PProDOT-Br$_2$ film precludes any of the post-polymerization modification experiments. Spectroelectrochemistry was performed on BEB-(OHex)$_2$, BEB-(OEs)$_2$, and EDOT-C$_{12}$ to determine their band gaps. While all had band gaps comparable to other similar polymers, spectroelectrochemistry of PEDOT-C$_{12}$ proved significantly more complicated than expected, as the reduction of the oxidized polymer took multiple attempts and several days to accomplish.

Attempts were made to electrochemically polymerize PyVEDOT with no success. Solubility issues were a major problem, as was the limited quantity available for experimentation and the lack of an inert environment.

Future Work

Due to the success seen with the BEB-(OEs)$_2$, other monomers with esters at varying distances from the benzene should be synthesized and studied to determine at what distance the ester moiety begins to affect the electrochemistry.

Further attempts at elucidating the nature of PyVEDOT would involve electrochemistry in an inert environment for potentially an extended period of time. Alternatively, small amounts of PyVEDOT could be electrochemically polymerized in an EDOT monomer solution, such that most of the polymer is PEDOT, with some PPyVEDOT sections interspersed. n-Doping experiments should also be conducted using a carbon working electrode in an inert environment.

It would prove beneficial to further study the reduction of PEDOT-C_{12}. The problems with reduction could be attributed to either over oxidation of the polymer or exposure to air. Performing electrochemistry in an inert environment such as a glove box may provide the answers needed.

APPENDIX SECTION

NUCLEAR MAGNETIC RESONANCE SPECTRA

A.1 ^{1}H NMR of BEB-(OHex)$_2$

A.2 ^{13}C NMR of BEB-(OHex)$_2$
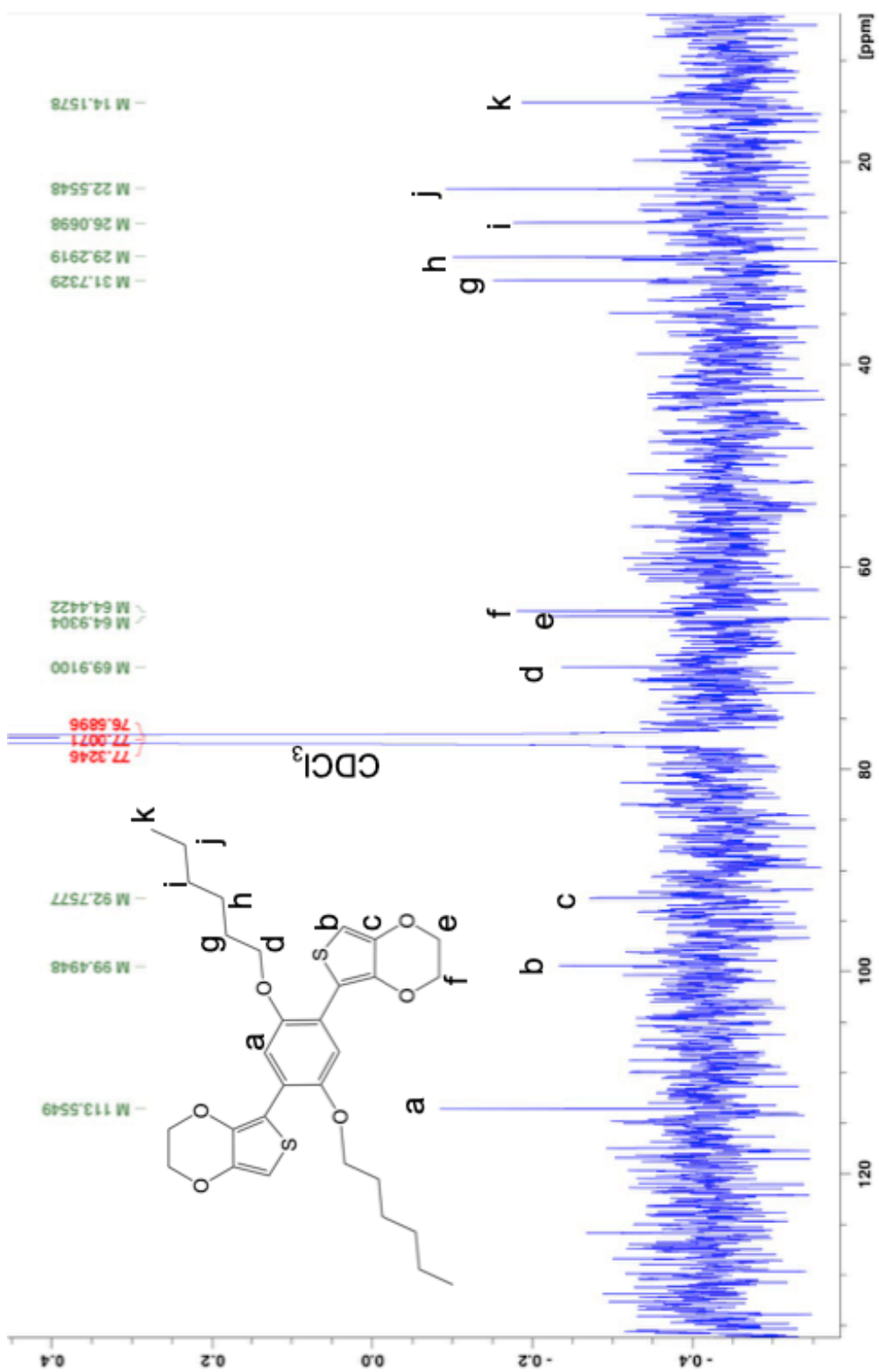
A.3 ^{1}H NMR of EDOT-C$_{12}$

A.4 ^{13}C NMR of EDOT-C$_{12}$

A.1 ^{1}H NMR of BEB-(OHex)$_2$
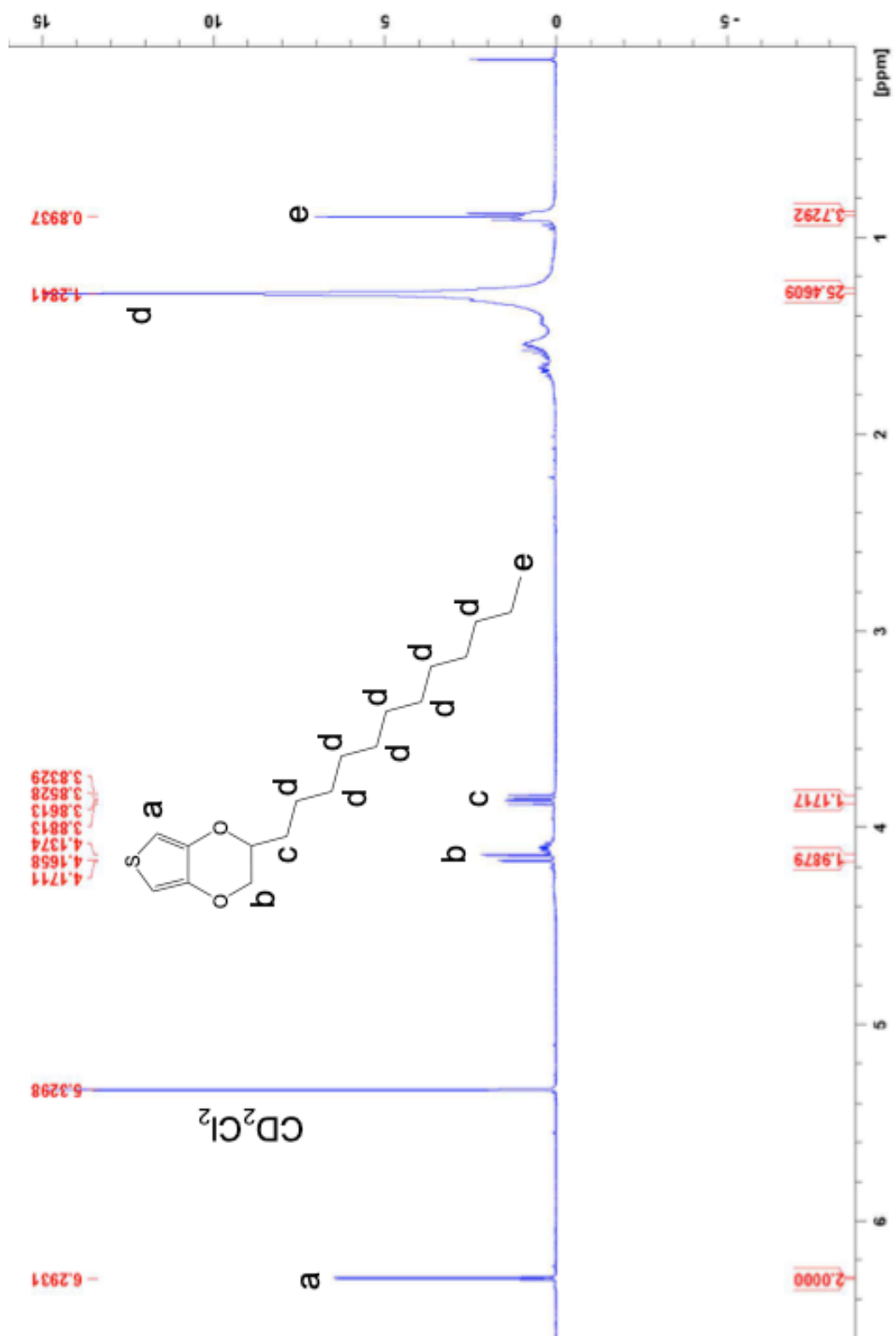
A.4 ^{13}C NMR of EDOT-C$_{12}$
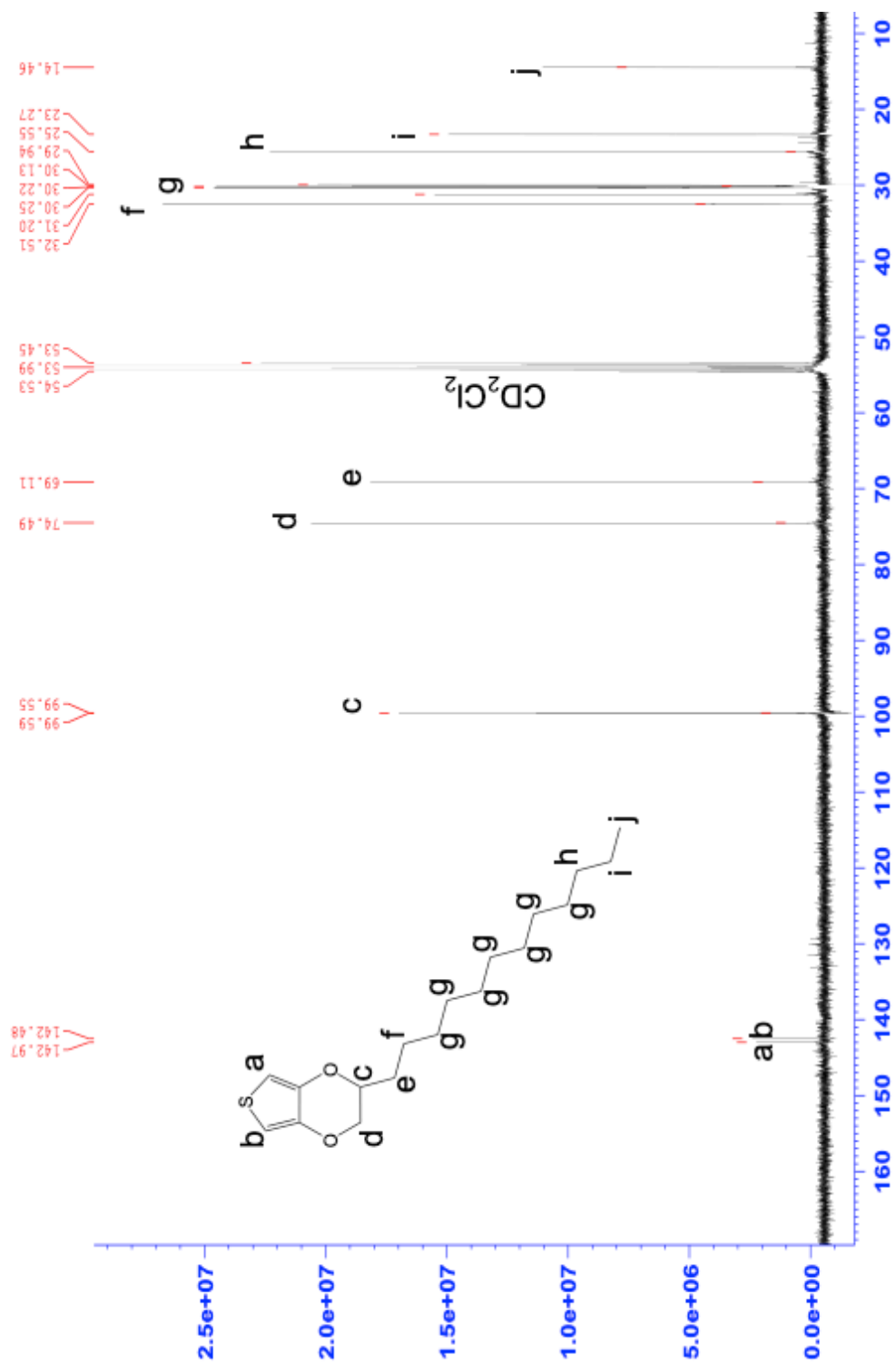
REFERENCES

1.   Rasmussen, S. C., The Early HIstory of Polyaniline: Discovery and Origins. *Substantia* 2017, *1* (2).

2.   Shirakawa, H.; Louis, E. J.; MacDiarmid, A. G.; Chiang, C. K.; Heeger, A. J., Synthesis of electrically conducting organic polymers: halogen derivatives of polyacetylene, (CH). *Journal of the Chemical Society, Chemical Communications* 1977, (16), 578-580.

3.   Press Release: The 2000 Noble Prize in Chemistry. nobelprize.org: 2000.

4.   Shirakawa, H.; Louis, E. J.; MacDiarmid, A. G.; Chiang, C. K.; Heeger, A. J., Synthesis of electrically conducting organic polymers: halogen derivatives of polyacetylene,(CH) x. *Journal of the Chemical Society, Chemical Communications* 1977, (16), 578-580.

5.   Awuzie, C., Conducting Polymers. *Materials Today: Proceedings* 2017, *4* (4), 5721-5726.

6.   Irvin, J. A.; Reynolds, J. R., Low-oxidation-potential conducting polymers: alternating substituted para-phenylene and 3, 4-ethylenedioxythiophene repeat units. *Polymer* 1998, *39* (11), 2339-2347.

7.   Lee, Y. S.; Kertesz, M., The effect of heteroatomic substitutions on the band gap of polyacetylene and polyparaphenylene derivatives. *The Journal of Chemical Physics* 1988, *88* (4), 2609-2617.

8.   Bundgaard, E.; Krebs, F. C., Low band gap polymers for organic photovoltaics. *Solar Energy Materials and Solar Cells* 2007, *91* (11), 954-985.

9.   Le, T.-H.; Kim, Y.; Yoon, H., Electrical and electrochemical properties of conducting polymers. *Polymers* 2017, *9* (4), 150.

10.   Zarras, P.; Irvin, J., Electrically Active Polymers. In *Encyclopedia of Polymer Science and Technology*, 2009.

11.   Mooney, J.; Kambhampati, P., Get the Basics Right: Jacobian Conversion of Wavelength and Energy Scales for Quantitative Analysis of Emission Spectra. *The Journal of Physical Chemistry Letters* 2013, *4* (19), 3316-3318.

12.   Ahonen, H. J.; Lukkari, J.; Kankare, J., n- and p-Doped Poly(3,4-ethylenedioxythiophene): Two Electronically Conducting States of the Polymer. *Macromolecules* 2000, *33* (18), 6787-6793.

13.   Wallace, G. G.; Teasdale, P. R.; Spinks, G. M.; Kane-Maguire, L. A., *Conductive electroactive polymers: intelligent polymer systems*. CRC press: 2008.

14.   Brédas, J. E.; Chance, R. R.; Silbey, R., Theoretical Studies of Charged Defect States in Doped Polyacetylene and Polyparaphenylene. *Molecular Crystals and Liquid Crystals* 1981, *77* (1-4), 319-332.

15.   Bishop, A.; Campbell, D.; Fesser, K., Polyacetylene and relativistic field theory models. *Molecular Crystals and Liquid Crystals* 1981, *77* (1-4), 253-264.

16.   Bredas, J. L.; Street, G. B., Polarons, bipolarons, and solitons in conducting polymers. *Accounts of Chemical Research* 1985, *18* (10), 309-315.

17.   Chiechi, R. C.; Sonmez, G.; Wudl, F., A Robust Electroactive n-Dopable Aromatic Polyketone. *Advanced Functional Materials* 2005, *15* (3), 427-432.

18.   Cieplak, A. S., Stereochemistry of nucleophilic addition to cyclohexanone. The importance of two-electron stabilizing interactions. *Journal of the American Chemical Society* 1981, *103* (15), 4540-4552.

19.   Abu-Thabit, N. Y., Chemical Oxidative Polymerization of Polyaniline: A Practical Approach for Preparation of Smart Conductive Textiles. *Journal of Chemical Education* 2016, *93* (9), 1606-1611.

20.   Okada, T.; Ogata, T.; Ueda, M., Synthesis and Characterization of Regiocontrolled Poly(2,5-di-n-butoxy-1,4-phenylene) by Oxovanadium-Catalyzed Oxidative Coupling Polymerization. *Macromolecules* 1996, *29* (24), 7645-7650.

21.   Albagli, D.; Bazan, G.; Wrighton, M.; Schrock, R., Well-defined redox-active polymers and block copolymers prepared by living ring-opening metathesis polymerization. *Journal of the American Chemical Society* 1992, *114* (11), 4150-4158.

22.   Lewis, T. W.; Wallace, G. G.; Kim, C. Y.; Kim, D. Y., Studies of the overoxidation of polypyrrole. *Synthetic Metals* 1997, *84* (1), 403-404.

23.   Sawyer, D. T.; Sobkowiak, A.; Roberts, J. L., *Electrochemistry for chemists*. Wiley: 1995.

24.   Audebert, P.; Miomandre, F., Electrochemistry of conducting polymers. *Handbook of conducting polymers* 2007, *3*.

25.   Gau, V.; Ma, S.-C.; Wang, H.; Tsukuda, J.; Kibler, J.; Haake, D. A., Electrochemical molecular analysis without nucleic acid amplification. *Methods* 2005, *37* (1), 73-83.

26.   Tanaka, K.; Shichiri, T.; Wang, S.; Yamabe, T., A study of the electropolymerization of thiophene. *Synthetic metals* 1988, *24* (3), 203-215.

27.   Inzelt, G., Pseudo-reference electrodes. In *Handbook of Reference Electrodes*, Springer: 2013; pp 331-332.

28.   Frazer, J. Impact of Processing Parameters on Conductive Polymer Electroactivity. Texas State University, San Marcos, TX, 2018.

29.   Miehe, C.; Welschinger, F.; Hofacker, M., Thermodynamically consistent phase-field models of fracture: Variational principles and multi-field FE implementations. *International Journal for Numerical Methods in Engineering* 2010, *83* (10), 1273-1311.

30.   Gurunathan, K.; Murugan, A. V.; Marimuthu, R.; Mulik, U. P.; Amalnerkar, D. P., Electrochemically synthesised conducting polymeric materials for applications towards technology in electronics, optoelectronics and energy storage devices. *Materials Chemistry and Physics* 1999, *61* (3), 173-191.

31.   Bar-Cohen, Y., 8 - Electroactive polymers as actuators. In *Advanced Piezoelectric Materials*, Uchino, K., Ed. Woodhead Publishing: 2010; pp 287-317.

32.   Council, N. R., *Expanding the vision of sensor materials*. National Academies Press: 1995.

33.   Hulanicki, A.; Glab, S.; Ingman, F., Chemical sensors: definitions and classification. *Pure and Applied Chemistry* 1991, *63* (9), 1247-1250.

34.   Knoll, W.; Advincula, R. C., *Functional Polymer Films, 2 Volume Set*. John Wiley & Sons: 2013.

35.   Schröter, S.; Stock, C.; Bach, T., *Regioselective Cross-Coupling Reactions of Multiple Halogenated Nitrogen-, Oxygen-, and Sulfur-Containing Heterocycles*. 2005; Vol. 61, p 2245-2267.

36.   Stille, J. K., The palladium-catalyzed cross-coupling reactions of organotin reagents with organic electrophiles [new synthetic methods (58)]. *Angewandte Chemie International Edition in English* 1986, *25* (6), 508-524.

37.   Buchwald, S. L.; Fugami, K.; Hiyama, T.; Kosugi, M.; Miura, M.; Miyaura, N.; Muci, A.; Nomura, M.; Shirakawa, E.; Tamao, K., *Cross-coupling reactions: a practical guide*. Springer: 2003; Vol. 219.

38.   Negishi, E.-i.; Hu, Q.; Huang, Z.; Qian, M.; Wang, G., Palladium-catalyzed alkenylation by the Negishi coupling. *Aldrichim. Acta* 2005, *38*, 71-87.

39.   Xi, Z.; Liu, B.; Chen, W., Room-Temperature Kumada Cross-Coupling of Unactivated Aryl Chlorides Catalyzed by N-Heterocylic Carbene-Based Nickel(II) Complexes. *The Journal of Organic Chemistry* 2008, *73* (10), 3954-3957.

40.   Bellina, F.; Carpita, A.; Rossi, R., Palladium catalysts for the Suzuki cross-coupling reaction: an overview of recent advances. *Synthesis* 2004, *2004* (15), 2419-2440.

41.   Dubbaka, S. R.; Vogel, P., Palladium-catalyzed stille cross-couplings of sulfonyl chlorides and organostannanes. *Journal of the American Chemical Society* 2003, *125* (50), 15292-15293.

42.   Mosquera, Á.; Riveiros, R.; Sestelo, J. P.; Sarandeses, L. A., Cross-Coupling Reactions of Indium Organometallics with 2,5-Dihalopyrimidines: Synthesis of Hyrtinadine A. *Organic Letters* 2008, *10* (17), 3745-3748.

43.   Pérez, I.; Sestelo, J. P.; Sarandeses, L. A., Palladium-Catalyzed Cross-Coupling Reactions of Triorganoindium Compounds with Vinyl and Aryl Triflates or Iodides. *Organic Letters* 1999, *1* (8), 1267-1269.

44.   Roncali, J.; Garreau, R.; Yassar, A.; Marque, P.; Garnier, F.; Lemaire, M., Effects of steric factors on the electrosynthesis and properties of conducting poly (3-alkylthiophenes). *Journal of Physical Chemistry* 1987, *91* (27), 6706-6714.

45.   Varghese, S.; Das, S., Role of molecular packing in determining solid-state optical properties of π-conjugated materials. *The journal of physical chemistry letters* 2011, *2* (8), 863-873.

46.   Elsenbaumer, R. L.; Jen, K. Y.; Miller, G. G.; Shacklette, L. W., Processible, environmentally stable, highly conductive forms of polythiophene. *Synthetic Metals* 1987, *18* (1), 277-282.

47.   Irvin, D. J. Modification of the Electronic Properties of Conjugated Polymers. University of Florida, Florida, 1998.

48.   Cantu, T.; Walsh, K.; Pattani, V. P.; Moy, A. J.; Tunnell, J. W.; Irvin, J. A.; Betancourt, T., Conductive polymer-based nanoparticles for laser-mediated photothermal ablation of cancer: synthesis, characterization, and in vitro evaluation. *International journal of nanomedicine* 2017, *12*, 615.

49.   Cantu, T.; Rodier, B.; Iszard, Z.; Kilian, A.; Pattani, V.; Walsh, K.; Weber, K.; Tunnell, J.; Betancourt, T.; Irvin, J., Electroactive polymer nanoparticles exhibiting photothermal properties. *Journal of visualized experiments: JoVE* 2016, (107).

50.   Wang, X. Polyaromatic Cores for Enhanced Conductivity in Inherently Conductive Polymers. Texas State University, San Marcos, TX, 2017.

51.   Hoye, T. R.; Eklov, B. M.; Voloshin, M., No-D NMR Spectroscopy as a Convenient Method for Titering Organolithium (RLi), RMgX, and LDA Solutions. *Organic Letters* 2004, *6* (15), 2567-2570.

52.   Cantu, T. Synthesis, Characterization, and In Vitro Evaluation of Near-Infrared Absorbing Conductive Polymer Nanoparticles as Agents for Photothermal Ablation of Breast Cancer Cells. Texas State University, San Marcos, TX, 2015.

53.   Ko, S.-B.; Cho, A.-N.; Kim, M.-J.; Lee, C.-R.; Park, N.-G., Alkyloxy substituted organic dyes for high voltage dye-sensitized solar cell: Effect of alkyloxy chain length on open-circuit voltage. *Dyes and Pigments* 2012, *94* (1), 88-98.

54.   Umezawa, K.; Oshima, T.; Yoshizawa-Fujita, M.; Takeoka, Y.; Rikukawa, M., Synthesis of Hydrophilic–Hydrophobic Block Copolymer Ionomers Based on Polyphenylenes. *ACS Macro Letters* 2012, *1* (8), 969-972.

55.   Wang, F.; Wilson, M. S.; Rauh, R. D.; Schottland, P.; Thompson, B. C.; Reynolds, J. R., Electrochromic Linear and Star Branched Poly(3,4-ethylenedioxythiophene−didodecyloxybenzene) Polymers. *Macromolecules* 2000, *33* (6), 2083-2091.

56.   Irvin, J. A. Low Oxidation Potential Electroactive Polymers. University of Florida, Gainesville, FL, 1998.

57.   Electrically Active Polymers. In *Encyclopedia of Polymer Science and Technology*.

58.   Senthilkumar, V.; Vickraman, P.; Jayachandran, M.; Sanjeeviraja, C., Structural and optical properties of indium tin oxide (ITO) thin films with different compositions prepared by electron beam evaporation. *Vacuum* 2010, *84* (6), 864-869.

59.   Reynolds, J. R.; Ruiz, J. P.; Child, A. D.; Nayak, K.; Marynick, D. S., Electrically conducting polymers containing alternating substituted phenylenes and bithiophene repeat units. *Macromolecules* 1991, *24* (3), 678-687.

60. Sotzing, G. A.; Reddinger, J. L.; Reynolds, J. R.; Steel, P. J., Redox active electrochromic polymers from low oxidation monomers containing 3,4-ethylenedioxythiophene (EDOT). *Synthetic Metals* 1997, *84* (1), 199-201.

61. Godeau, G.; N'Na, J.; Darmanin, T.; Guittard, F., Poly(3,4-propylenedioxythiophene) mono-azide and di-azide as platforms for surface post-functionalization. *European Polymer Journal* 2016, *78*, 38-45.

62. Reeves, B. D.; Grenier, C. R.; Argun, A. A.; Cirpan, A.; McCarley, T. D.; Reynolds, J. R., Spray coatable electrochromic dioxythiophene polymers with high coloration efficiencies. *Macromolecules* 2004, *37* (20), 7559-7569.

63. Anson, F. C., Innovations in the Study of Adsorbed Reactants by Chronocoulometry. *Analytical Chemistry* 1966, *38* (1), 54-57.

64. Bott, A.; Heineman, W., Chronocoulometry. *Current Separations* 2004, *20* (4), 121-126.